Deep Learning for Improved Myoelectric Control

By

Muhammad Zia ur Rehman

NUST201590295PSMME2715S

Supervised By

Dr. Syed Omer Gilani

School of Mechanical and Manufacturing Engineering

National University of Sciences and Technology

Islamabad, Pakistan

December 2018

Deep Learning for Improved Myoelectric Control

Author

Muhammad Zia ur Rehman

NUST201590295PSMME2715S

A thesis submitted in partial fulfillment of the requirements for the degree of

PhD Robotics and Intelligent Machine Engineering

Thesis Supervisor:

DR. Syed Omer Gilani

Thesis Supervisor's Signature: _____

School of Mechanical and Manufacturing Engineering

National University of Sciences and Technology

December 2018

National University of Sciences & Technology, Islamabad
REPORT OF DOCTORAL THESIS DEFENCE

Name _____ MUHAMMAD ZIA UR REHMAN _____ Regn No NUST201590295PSMME2715S

School/College/Center: School of Mechanical and Manufacturing Engineering (SMME)

DOCTORAL DEFENCE COMMITTEE

Doctoral Defence Held on _____ 7th December 2018 _____

	QUALIFIED	NOT QUALIFIED	SIGNATURE
GEC Member 1: Dr. Mohsin Jamil	☐	☐	_____
GEC Member 2: Dr. Shahid Ikramulllah Butt	☐	☐	_____
GEC Member 3: Dr. Syed Irtiza Ali Shah (External)	☐	☐	_____
Supervisor: Dr. Syed Omer Gilani	☐	☐	_____
Co-Supervisor: Not Applicable	☐	☐	____N.A____
External Evaluator 1: Dr. Faraz Akram (Local Expert)	☐	☐	_____
External Evaluator 2: Dr. Muhammad Asif (Local Expert)	☐	☐	_____
External Evaluator 3: Dr. Sylvain Cremoux (Foreign Expert*)	☐	☐	
External Evaluator 4: Dr. Nikola Kasabov (Foreign Expert*)	☐	☐	

FINAL RESULT OF THE DOCTORAL DEFENCE
(Appropriate box to be signed by HOD)

☐ PASS ☐ FAIL

- -

The student Muhammad Zia ur rehman Reg No NUST201590295PSMME2715S is / is NOT accepted for Doctor of Philosophy Degree.

Dated: _____

_____
Dean/Commandant/Principal/DG

Approval

It is certified that the contents and form of the thesis entitled "Deep Learning for Improved Myoelectric Control" submitted by Muhammad Zia ur rehman have been found satisfactory for the requirement of the Doctor of Philosophy degree.

Advisor: Dr. Syed Omer Gilani

Signature:_____

Date: _____

Committee Member 1: Dr. Mohsin Jamil

Signature: _____

Date: _____

Committee Member 2: Dr. Shahid Ikramullah Butt

Signature: _____

Date: _____

Committee Member 3 (External): Dr. Syed Irtiza Ali Shah

Signature: _____

Date: _____

Thesis Acceptance Certificate

Certified that final copy of PhD thesis written by <u>Mr. Muhammad Zia ur rehman</u>   Registration No. <u>NUST201590295PSMME2715S</u> of __**SMME**___ has been vetted by undersigned, found complete in all aspects as per NUST Statutes/Regulations/PhD Policy, is free of plagiarism, errors, and mistakes and is accepted as partial fulfillment for award of PhD degree. It is further certified that necessary amendments as pointed out by GEC members and foreign/local evaluators of the scholar have also been incorporated in the said thesis.

Signature: _____

Name of Supervisor: <u>Dr. Syed Omer Gilani .</u>

Date: _____

Signature (HOD): _____

Date: _____

<u>Countersign by</u>

Signature (Dean/Principal): _____

Date: _____

CERTIFICATE OF APPROVAL

This is to certify that the research work presented in this thesis entitled "**Deep Learning for Improved Myoelectric Control**" was conducted by **Mr. Muhammad Zia ur rehman** under the supervision of **Dr. Syed Omer Gilani**.

No part of this thesis has been submitted anywhere else for any degree. This thesis is submitted to the **School of Mechanical and Manufacturing Engineering** in partial fulfillment of the requirements for the degree of Doctor of Philosophy in Field of **Robotics and Intelligent Machine Engineering** Department of **Robotics and Artificial Intelligence, School of Mechanical and Manufacturing Engineering (SMME)** University of **National University of Sciences and Technology, Islamabad, Pakistan.**

Student Name:**Muhammad Zia ur rehman**　　　　Signature: _____

Examination Committee:

a)	**External Examiner 1:**		
	Name	Dr.Sylvain Cremoux	
	Designation	Associate Professor	Signature
	Official Address	University of Valenciennes and Hainaut-Cambresis, Faculty of Science and Sports Professions, Le Mont Houy ; F-59313 Valenciennes Cedex 09, France.	

b)	**External Examiner 2:**		
	Name	Dr. Nikola Kasabov	Signature
	Designation	Professor	

	Official Address	KEDRI, Auckland University of Technology AUT Tower, Level 7, Corner Rutland and Wakefield Street, Auckland, New Zealand.	

c)	**Internal Examiner 1:**		
	Name	Dr. Faraz Akram	
	Designation	Assistant Professor	
	Official Address	Office no. B202, Department of Biomedical Engineering, Faculty of Engineering and Applied Sciences,Riphah International University Sector I-14, Islamabad, Pakistan	Signature

d)	**Internal Examiner 2:**		
	Name	Dr. Muhammad Asif	
	Designation	Professor	
	Official Address	Chairperson office, Electrical Engineering Department, Faculty of Engineering Science and Technology, Ziauddin University, Karachi, Pakistan.	Signature

Supervisor Name:**Dr. Syed Omer Gilani**   Signature: _____

Name of Dean/HoD:**Dr. Shahid Ikramullah Butt**   Signature: _____

Author's Declaration

I Muhammad Zia ur rehman hereby state that my PhD thesis titled "Deep Learning for Improved Myoelectric Control" is my own work and has not been submitted previously by me for taking any degree from "National University of Sciences and Technology (NUST)" Or anywhere else in the country/world.

At any time if my statement is found to be incorrect even after my Graduate the university has the right to withdraw my PhD degree.

Name of Student: Muhammad Zia ur rehman

Date:

_____

Plagiarism Undertaking

I solemnly declare that research work presented in the thesis titled "Deep Learning for Improved Myoelectric Control" is solely my research work with no significant contribution from any other person. Small contribution/help wherever taken has been duly acknowledged and that complete thesis has been written by me. I understand the zero tolerance policy of the HEC and National University of Sciences and Technology (NUST) towards plagiarism. Therefore, I as an Author of the above titled thesis declare that no portion of my thesis has been plagiarized and any material used as reference is properly referred/cited. I undertake that if I found guilty of any formal plagiarism in the above titled thesis even after award of PhD degree, the University reserves the rights to withdraw/revoke my PhD degree and that HEC and the University has the right to publish my name on the HEC

/University Website on which names of students are placed who submitted plagiarized thesis.

Student /Author Signature:

_____

Name: <u>Muhammad Zia ur rehman</u>

Acknowledgment

It is foremost to thank Allah almighty, no other than Him bestow strength, an aptitude, patience and concentration required to achieve this remarkable milestone of my life.

I am grateful to my supervisor Dr. Syed Omer Gilani on his mentoring and guidance throughout my PhD candidacy at NUST. He remained helpful and humble over my mistakes and motivational throughout this period. His critique acted as catalyst to refine and improve the quality of my research. It is an honor working under his guidance and supervision.

I am also thankful to rest of my thesis committee members for a continuous mentoring and guidance. Dr. Syed Irtiza Ali Shah, Dr. Mohsin Jamil and Dr. Shahid Ikramullah Butt has been fostering innovative ideas for my thesis work that resulted in a mature research work.

I share my deepest gratitude to my foreign research collaborators

- Prof. Ernest Nlandu Kamavuako, Kings College, London U.K

- Dr. Imran Khan Niazi, college of Chiropractic, New Zealand

- Prof. Dario Farina, Imperial College, London U.K

- Dr. Mads Jochumsen, Aalborg University, Denmark

for their persistent valuable input, correction of my mistakes and dedicated guidance to narrow down my research problem.

I also extend my deepest appreciations to all of thesis evaluators, faculty, fellow researchers, lab members and staff of SMME for their valuable comments and support.

I am extremely grateful to Principal SMME Dr. Shahid Ikramullah Butt and HoD Dr. Yasir Ayaz. They have facilitated with all available resources during my whole PhD candidacy. I extend my thanks to all others who contributed in any way for a successful accomplishment of my degree.

My family has supported and encouraged me unconditionally to pursue my studies with complete devotion and peace of mind. I dedicate this thesis to my beloved family.

Muhammad Zia ur Rehman

List of publications

1. Zia ur Rehman, Muhammad, et al. "**Multiday EMG based classification of hand motions with deep learning techniques**" *Sensors 2018,* 18 (8), 2494 <u>**I. F=2.475**</u>

2. Zia ur Rehman, Muhammad, et al. "**Stacked sparse autoencoders for EMG based classification of hand motions: A comparative multi day analyses between surface and intramuscular EMG.**" *Applied Sciences (Special Issue "Deep Learning and Big Data in Healthcare"). 2018; 8(7):1126.* <u>**I.F=1.689**</u>

3. Zia ur Rehman, Muhammad, et al. " **Performance of combined surface and intramuscular EMG for classification of hand movements**." *40th IEEE International conference of the Engineering in medicine and biology society*, 17-21 July 2018- Honolulu, Hawaii USA.

4. Zia ur Rehman, Muhammad, et al. "**A Novel Approach for Classification of Hand Movements Using Surface EMG Signals**." *17th IEEE International Symposium on Signal Processing and Information Technology(ISSPIT)2017*, At December 18-20, 2017 - Bilbao – Spain.

Dedicated ….

To a Person who is "The Rehmat" for all the universe,

And

To our Parents and to whom we love and respect

List of abbreviation

AE: Autoencoders

ANOVA: Analysis of variance

cEMG: Combined EMG

CH: Close hand

CNN: Convolutional neural networks

DoF: Degree of freedom

EMG: Electromyography

HCI: Human computer interface

iEMG: intramuscular EMG

L2R: L2 regularization

LDA: Linear discriminant analysis

MAV: Mean absolute value

MES: Myoelectric signal

OH: Open hand

PCA: Principal component analysis

POV: Percent of variance

PR: Pattern recognition

PRO: Pronation

RMS: Root mean square

RT: Rest

sEMG: Surface EMG

SP: Sparsity proportion

SR: Sparsity regularization

SSAE: stacked sparse autoencoders

SSC: Slope sign change

SUP: supination

WE: Wrist extension

WF: Wrist flexion

WL: Waveform length

ZC: Zero crossing

Abstract

Advancement in the myoelectric interfaces have increased the use of myoelectric controlled robotic arms for partial-hand amputees as compared to body-powered arms. Current clinical approaches based on conventional (on/off and direct) control are limited to few degree of freedom (DoF) movements which are being better addressed with pattern recognition (PR) based control schemes. Performance of any PR based scheme heavily relies on optimal features set. Although, such schemes have shown to be very effective in short-term laboratory recordings, but they are limited by unsatisfactory robustness to non-stationarities (e.g. changes in electrode positions and skin-electrode interface). Moreover, electromyographic (EMG) signals are stochastic in nature and recent studies have shown that their classification accuracies vary significantly over time. Hence, the key challenge is not the laboratory short-term conditions but the daily use.

Thus, this work makes use of the longitudinal approaches with deep learning in comparison to classical machine learning techniques to myoelectric control and explores the real potential of both surface and intramuscular EMG in classifying different hand movements recorded over multiple days. To the best of our knowledge, for the first time, it also explores the feasibility of using raw (bipolar) EMG as input to deep networks. Task are completed with two different studies that were performed with different datasets.

In the first study, surface and intramuscular EMG data of eleven wrist movements were recorded concurrently over six channels (each) from ten able-bodied and six amputee subjects for consecutive seven days. Performance of stacked sparse autoencoders (SSAE), an emerging deep learning technique, was evaluated in comparison with state of art LDA using offline

classification error as performance matric. Further, performance of surface and intramuscular EMG was also compared with respect to time. Results of different analyses showed that SSAE outperformed LDA. Although there was no significant difference found between surface and intramuscular EMG in within day analysis but surface EMG significantly outperformed intramuscular EMG in long-term assessment.

In the second study, surface EMG data of seven able-bodied were recorded over eight channels using Myo armband (wearable EMG sensors). The protocol was set such that each subject performed seven movements with ten repetitions per session. Data was recorded for consecutive fifteen days with two sessions per day. Performance of convolutional neural network (CNN with raw EMG), SSAE (both with raw data and features) and LDA were evaluated offline using classification error as performance matric. Results of both the short and long-term analyses showed that CNN and SSAE-f outperformed the others while there was no difference found between the two.

Overall, this dissertation concludes that deep learning techniques are promising approaches in improving myoelectric control schemes. SSAE generalizes well with hand-crafted features but fails to generalize with raw data. CNN based approach is more promising as it achieved optimal performance without the need to select features.

List of figures

List of tables

Chapter 1.   Introduction

1.1.Motivation

The advancement in myoelectric interfaces and artificial intelligence algorithms has revolutionized the use of wearable prosthetic devices which are used as an artificial substitute to the missing part of a human body. One of such devices is the prosthetic hand that substitute a missing arm below the elbow. A myoelectric prosthetic hand is controlled by electrical activity that is produced with in the reminant muscles and the technique for recording this electrical activity is called Electromyography (EMG). An accurate control of prosthetic hand strongly relies on accurate recording and processing of EMG signals that are stochastic in nature. Researchers have proposed lot of techniques for control of prosthetic hands and promising results have been achieved. However, limitations still exist [1] in control robustness due to randomness of EMG patterns, complex movements and lack of perfect data representation for machine learning algorithms that makes them insufficient in many real-time applications. Data representations for machine learning algorithms are also called features that are designed and selected manually. Therefore, it is very difficult task to decide the best combination of features for particular applications [2].

In recent years, Deep learning as branch of machine learning, showed promising results in computer vision and natural language processing [3, 4]. The power of parallel and distributed computing and sophisticated algorithms of deep learning has revolutionized the way in which more complex and powerful features have been extracted. This overcome the issues of feature designing and selection (Engineered features) and hence research interests increased in deep learning.

Literature on deep learning also show its application in biomedical signal processing[5]. Biomedical signals are usually noisy and include many artifacts. They are first decomposed into wavelets or frequency components before using them as input to deep learning algorithms. In addition, human designed features like normalized decay and peak variation are also used to improve results. Therefore, challenges exist in this domain that needs to be explored in order to find possible breakthroughs and improvements. The purpose of this project is to investigate and propose deep learning algorithms that could accurately classify EMG patterns and could improve control robustness for a prosthetic hand. To achieve this goal, multiple studies are being performed to evaluate the performance of deep learning techniques with both the surface, intramuscular and combined EMG as well and with the data of both abled-bodied and amputee subjects.

1.2. Background

The main source for controlling a myoelectric prosthetic hand is the EMG signal. An EMG signal is basically an electrical activity that is produced due to neuromuscular activation associated with contraction of a muscle. These signals represent the physiological variations in the muscle fiber membrane that may be due to stimulated, voluntary or involuntary muscle contraction. They have several applications in clinical and biomedical studies [6]. Obtaining EMG signals from human body involve several processing steps including recording, data acquisition, signal condition and processing. Recording of EMG signals in performed using electrodes. Three different types of electrodes used in EMG recording are wire, needle and surface electrode. The later one is the only non-invasive technique that is most commonly used. In EMG recording, electrodes are placed either over the skin(sEMG) or within muscles (iEMG) and contraction strength is recorded in the form of electrical energy using computer interface.

Along with important information, it also includes [7] a noise factor that may be due to electrode-skin interface (in sEMG), electromagnetics and other different sources. Hence the raw EMG is filtered in order to remove noise from it.

Different myoelectric control schemes have been developed to efficiently utilized the cues in EMG signals and they are discussed below.

1.2.1.   Conventional myoelectric control schemes

Myoelectric signals had been introduced in actuation of prosthetic hand since 1948 [8, 9]. The first clinically significant prosthetic hand using myoelectric signals (MES) was developed at Central Prosthetic Research Institute, Moscow in 1957 that used stepper motor [10] that was later modified with permanent DC motor.

Later, different control schemes were analyzed in order to translate the EMG signals to capture useful information. These schemes are classified based on the control strategy that is either sequential or simultaneous control [11]. Most of the commercially available prosthetic hand utilize the sequential control while research is being conducted to employ the simultaneous control. The sequential control schemes include on-off control, proportional control, direct control, finite state machine control, pattern recognition-based control, regression control and posture control etc. Steps taken in each of the sequential schemes are shown in figure 1-1 below.
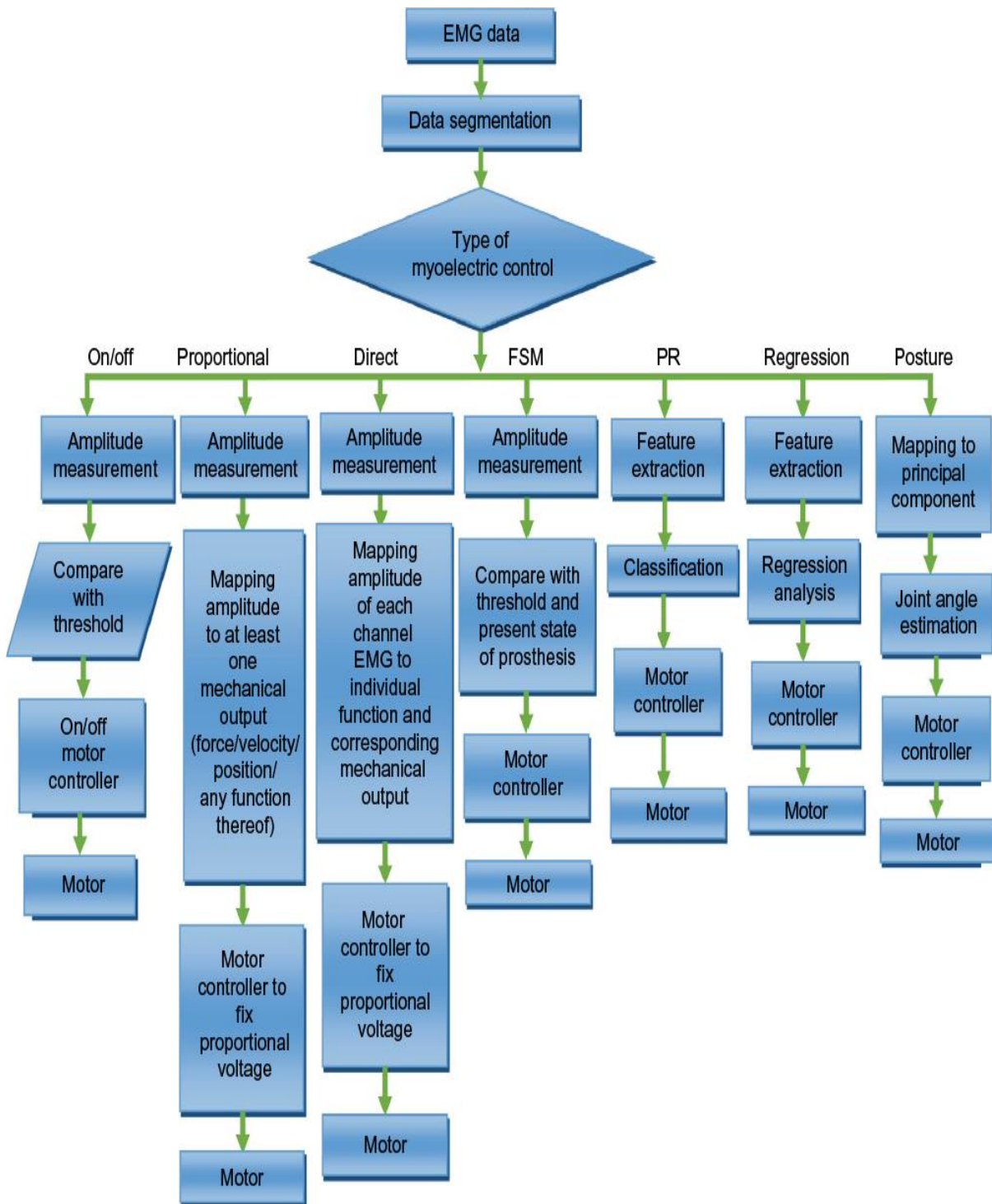
Figure 1-1: Conventional myoelectric control schemes (Geethanjali, 2016)

ON-OFF control: In this control scheme, prosthetic hand is operated in clock and counter clock wise direction with a stop. Basically, the amplitude of EMG signal is measured either average value or root mean square (RMS) value and threshold is set to operate the hand in one direction at a constant speed and independent of the level of contraction. The simultaneous control is also possible in this strategy [11].

Proportional Control: In this control strategy, the voltage applied to motor is directly proportional to the amplitude or intensity level of a signal. This helps in grasping for gross movements. It is still under study for upper limb prosthetic control. Researchers have been focusing on simultaneous proportional control schemes.

Finite State Machine control: in this control strategy, fixed number of hand postures are declared as states and based on the EMG signals, it is varied from one fixed state to other. No of states are limited and hence this scheme has limitations in multifunctionality of prosthetic hand.

Direct Control: in this control scheme, based on the amplitude level, voltage is applied to the motor and EMG is captured from independent sites to control the individual finger movements. Due to cross talk in surface EMG signals, it is considered as a difficult approach but it may be possible with intramuscular EMG.

Posture Control: In this control scheme, EMG signals are mapped to control parameters in the principal component domain that coordinates in the linear transformation of joint angles to present target postures [12]. This provides simultaneous control of prosthetic hand.

Regression Control: This control scheme is a newly developed scheme that overcomes the limitation of other control strategy. It is capable of simultaneously controlling the prosthetic

hand [13]. i.e it can simultaneous detect the hand pronation/supination with the hand open/close positions, which is itself a new class for classification. Researchers are using nonnegative matric factorization [14, 15], neural networks [16] and other techniques to achieve it.

1.2.2. Pattern recognition based myoelectric control schemes

In the past few decades, myoelectric control systems have attracted more and more attention for its application in rehabilitation and human-computer interface (HCI). In such systems, hand movements are often used to control peripheral equipment. Studies on pattern recognition based myoelectric control schemes have started in early 70's. Both the surface and intramuscular EMG date is being used as control source. However, studies showed that there was no significant difference found between the two (details of comparison studies have been discussed in appendix B). Moreover, Surface EMG is non-invasive and is therefore most commonly used in literature on myoelectric control.

Pattern recognition-based scheme includes the following steps; preprocessing of signals, windowing, features extraction, classification and post processing.
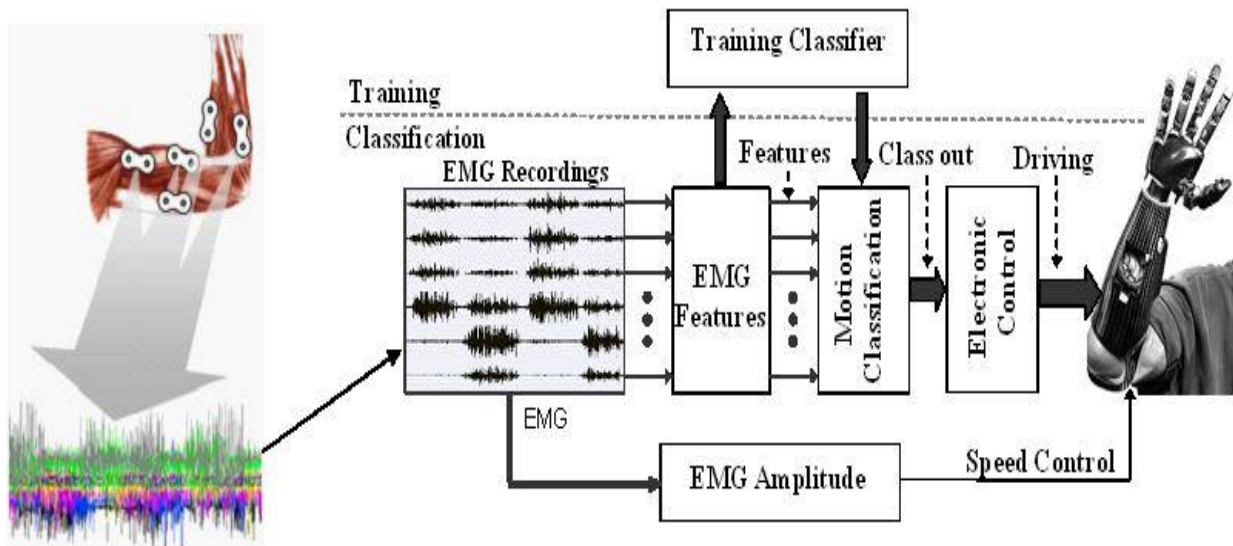
Figure 1-2: Real-time pattern recognition based myoelectric control interface.

Such schemes work on the principal that patterns for individual movements should be repeatable and differentiable from each other. However, EMG signals are stochastic in nature and may include various sources of noise like movement artifacts and hum etc. Therefore, selection of optimal features for classification is very important. Furthermore, features are extracted from windows and hence selection of optimal window length is also necessary as lengthy windows may introduce delays in recognition time (generally window length should be up to 300 msec).

Different studies explored feature sets in order to increase the classification accuracy which is one of the performance matric in pattern recognition-based scheme. Both the time and frequency domain features are used separately and in combined with machine learning algorithms. These features included integral of absolute value (IVA), Wilson amplitude, zero crossing, the number of turns, mean of amplitude, wavelength, mean frequency, histogram, autoregressive coefficient, cepstral coefficient and energy of wavelength coefficients etc. [17]. Different linear and non-linear machine learning algorithms including Artificial neural networks [18-20], Backpropagation neural networks [21], log linearized Gaussian mixture

networks (LLGMN) [22], Recurrent LLGMN, LLGMN based probabilistic neural network [23], Fuzzy mean max neural network [24], Radial basis function ANN [25], Hidden Markov model [26] and Bayes network [27], SVM and LDA are utilized. Many classifiers showed promising results and achieved classification of up to 95 %. However, due to stochastic nature of EMG signals, fatigue or some other factors, classification accuracies vary largely even in within sessions and hence it can degrade the performance of classifier in long term.

1.2.3. Deep learning based myoelectric control schemes

As discussed in the previous section, the efficient performance of any machine learning algorithm heavily relies on data representation (features). Features are mostly designed by human Engineers and selection of proper features for any particular task is difficult step. Therefore, limitations exist that makes the control robustness a very challenging task and hence limits the use of myoelectric prosthetic hands in various real-time applications.

To advance from these hand design features to data driven features, deep learning algorithms has shown successful stories in recent years, especially in the field of computer vision and natural language processing. Basically, Deep learning architectures are combination of many nonlinear layers of artificial neural networks that has the capability to extract data dependent features and other complex features from simple data driven features. Such features represent an important aspect of the raw data that makes the learning algorithms robust enough to classify different complex labels. Literature on Convolutional neural networks (CNN) also show its application in biomedical signal processing and promising results have been achieved with it. The pioneer work [28] of deep learning application in myoelectric, show promising results and sensitivity of more than 90% is achieved using convolutional neural network. In this study, it was investigated whether deep feature learning can improve performances in the inter-user

variability. To achieve this goal, convolutional neural network was trained and results were compared with traditional Support vector machine (SVM) classifier. Although author has not mentioned about the detailed architecture of CNN but it was observed that CNN outperformed the SVM.

Manfredo Atzori [1] proposed a multi-block convolutional neural network for classification of hand movements using sEMG. They used publically available datasets from Ninapro database [29] that includes EMG data related to 50 different hand movements of 78 subjects (67 intact and 11 transradial amputee subjects). Their proposed CNN consisted of a modified version of well-known network called LeNet [30] and its performance was compared with Random forest, KNN, SVM and LDA. It was observed that there was no significant difference found between the deep learning and other machine learning algorithms. Some other studies have also evaluated the performance of CNN in myoelectric control and their details are provided in chapter 5 section 5.3. However, most of these studies were performed with the data recorded in single session and used RMS of EMG signal as input to CNN. Therefore, nothing can be said about performance of CNN over multiple sessions/days and with raw data as input.

Apart from CNN, Autoencoders (AE) also showed promising results in biomedical signal processing field but till date, it is never utilized for myoelectric control.

Currently, some of the commercially available prosthetic hands offers extreme robustness from mechanical point of view with many different movements, but most of the controlling algorithms are still inefficient to offer the required robustness (due to hand made feature) with sufficient controlling speed. But state of art deep learning algorithms may contribute well to help the transradial amputees in recovering their missing or limited capabilities by filling gap between the prosthetic market and the scientific research in rehabilitation robotics.

1.3. Objectives of work

Although pattern recognition based myoelectric control schemes have shown promising results. These schemes work on the principle that individual movements should be repeatable and differentiable from each other. However, the random nature of EMG signals, fatigue, poster change, and some other factors may limit the performance of classifiers in long term assessment. Furthermore, feature Engineering and optimal feature selection is also challenging. Therefore, recent approaches now focused towards the data driven features and hence research interest increased in deep learning.

This project has been taken up to explore the deep learning techniques both with the surface and intramuscular data of both able-bodied and amputee subjects. This dissertation included two main studies.

The objectives of first study are as follows

➢ Explore stacked sparse autoencoders (an emerging deep learning technique) for improved myoelectric control and compare its performance with classical machine learning algorithms

➢ Performance comparison of surface and intramuscular EMG recorded over multiple sessions for both able bodied and amputee subjects

➢ Evaluate performance of combined EMG for both the able bodied and amputee subjects

The objectives of second study are as follows

➢ Explore convolutional neural network for improved myoelectric control

➢ Compare the performance of both the engineered and data driven features for long term assessment

1.4. Thesis structure

Chapter 01 highlights the motivation for the selection of this dissertation topic and overviews the different control schemes including both conventional and pattern recognition based. It also introduces the application of deep learning to myoelectric control and finally objectives of this study are discussed.

Chapter 02 provides the detailed methodology of study one. It introduces the protocol used and the recording technique for both able-bodied and amputee subjects. The mathematics and specific block diagram of Autoencoders in discussed.

Chapter 03 is the journal paper with title "Stacked Sparse Autoencoders for EMG-Based Classification of Hand Motions: A Comparative Multi Day Analyses between Surface and Intramuscular EMG" [31] and is published in the "Applied Sciences" journal with impact factor 1.689. In this chapter, comparison of SSAE is performed with state of art LDA using surface and intramuscular EMG data of both able-bodied and amputee subjects. Furthermore, statistical comparison of both kinds of data is also provided.

Chapter 04 is the conference paper with title "Performance of Combined Surface and Intramuscular EMG for Classification of Hand Movements" [32] accepted in the 40th IEEE international conference of Engineering in medicine and biology (IEEE EMBC'18). It analyzes the strength of combined EMG data using both the deep learning and classical machine learning techniques.

Chapter 05 is based on study two. It is the research paper with title "Multiday EMG-Based Classification of Hand Motions with Deep Learning Techniques" [33] and is published in the "Sensors" journal with impact factor 2.475. It highlights the long-term data collection protocol

and investigate the hand movement classification with both engineered and data driven features using both SSAE and CNN.

Chapter 2.   Materials and Methods

2.1. Introduction

As discussed in the previous chapter, two different types of studies are conducted. This chapter presents the material and methodology adopted for study one and hence it is applicable to only chapter 3, 4 and appendix A. The material and methodology for study two is quite different and hence presented separately in section 5.4 (chapter 5).

More precisely, this chapter presents

- Subjects participated for data collection

- Experimental procedures for data collection

- Signal processing

- Introduction to SSAE

- Statistical test (Friedmann's test)

Note: Details regarding datasets are given in Appendix D

2.2.Subjects

Ten healthy (male, 18 to 38 years, mean age 24.5 yrs) and six transradial amputee subjects (male, three left and three right transradial amputation, 23 to 56 years, mean 34.8 yrs) took part in the experiments. One amputee regularly used a body-powered prosthesis while the others did not use any prostheses. The experimental procedures were in conformity with the Declaration of Helsinki and validated by ethical committee of Riphah International University

(approval no: ref# Riphah/RCRS/REC/000121/20012016). Subjects assisted voluntarily and supplied written informed agreement prior to the experimental procedures.

2.3.Experimental procedures

Surface EMG and iEMG signals from both able-bodied and amputee subjects were collected successively. For data collection from healthy subjects, six sEMG and six iEMG electrodes were used. Three of each sEMG and iEMG electrodes were mounted on flexor and same on extensor muscles. Same setup of electrodes was used for three of the amputees. The other three amputees were able to place only three to six iEMG electrodes and five sEMG electrodes. Intramuscular signals were filtered with analog bandpass filter of 100-900 kHz and sampled at 8 kHz. Surface signals were filtered at 10-500 Hz and sampled at 8 kHz.

11 hand motions were conducted by each subject in each experimental session (figure 2-1).

Figure 2-1: Types of hand movements

hand open (HO), hand close (CH), flex hand (WF), extend hand (WE), pronation (PRO), supination (SUP), side grip (SG), fine grip (FG), agree (AG) and pointer (PO) and rest (RT)

Each subject performed seven experimental sessions with a gap of 24 h. Each hand movement was repeated four times for each session with a contraction and relaxation time of 5 s as shown in figure 2-2 and hence total time taken by a single session was 400 s. For each session, the sequence of movements was randomized.
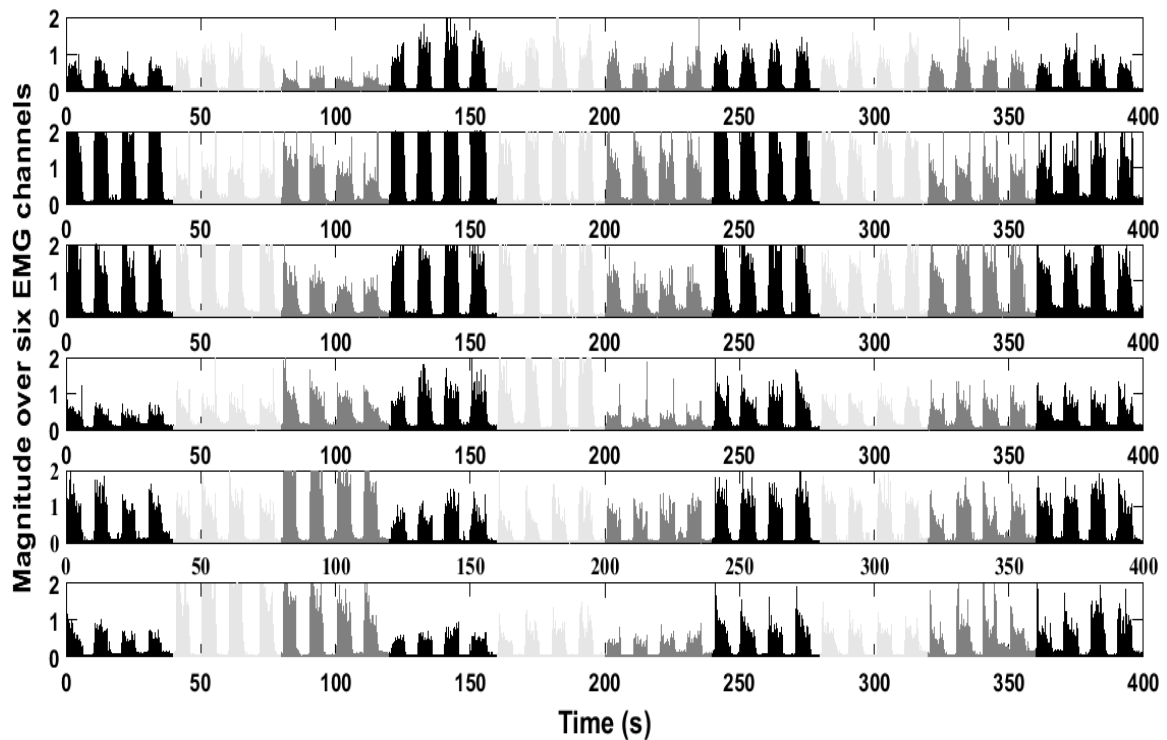
Figure 2-2: Rectified EMG recorded from the six surface electrode systems in a trial of an intact-limb subject.

Six iEMG channels were also recorded concurrently (not shown). Eleven movements (including rest) were repeated four times with a contraction and relaxation time of 5 s. Group of four with the same gray level represents the four repetitions of same movement.

2.4. Signal processing

The data were manually labelled for EMG onset and offset. The sEMG and iEMG signals were digitally filtered using a 3rd order Butterworth bandpass filter with bandwidth 20 – 500 Hz and 0.06 – 1.5 kHz, respectively, and a 3rd order Butterworth band-stop filter to suppress the 50-Hz powerline noise.

Four time domain features, mean absolute value (MAV), waveform length (WL), zero crossing (ZC) and slope-sign change (SSC) [34] were extracted from surface EMG and intramuscular EMG signals with a window length of 200 ms and increments of 28.5 ms.

The SSAE [35] and LDA [36] were used to classify the signals, as elaborated below. For the within-day analysis, testing was performed with a five-fold cross validation data. For the between-days analysis, an eight-fold cross validation technique was used to compare data of all the pairs of days (by randomly dividing data into eight equal folds). Furthermore, the classifiers were used for training and testing of data on different days using a two-fold validation. Additionally, a seven-fold cross validation was used to test the data of seven days, with six days being used as training data and one day used as testing data.

2.5. Stacked Sparse Autoencoders

AEs are deep neural networks that replicate the input at the output when trained in an unsupervised manner [29]. They are comprised of an encoder which depicts an input x to a new representation z, and a decoder which decodes z back to obtain the input x' at the output.

$$z = h(Wx + b) \tag{1}$$

$$x' = g(W'z + b') \tag{2}$$

Where h, g are activation functions, W, W' are weight matrices and b, b' represent bias vectors for the encoder and decoder respectively [37]. The optimization of error between x and x' is done as follows:

$$\min_{(W,b,W',b')} = \sum_{i=1}^{n}\|x_i - x'_i\|^2$$

(3)

Input   **Features 1**   **Features 2**   **Softmax classifier**
(unsupervised learning)   (unsupervised learning)   (supervised learning)
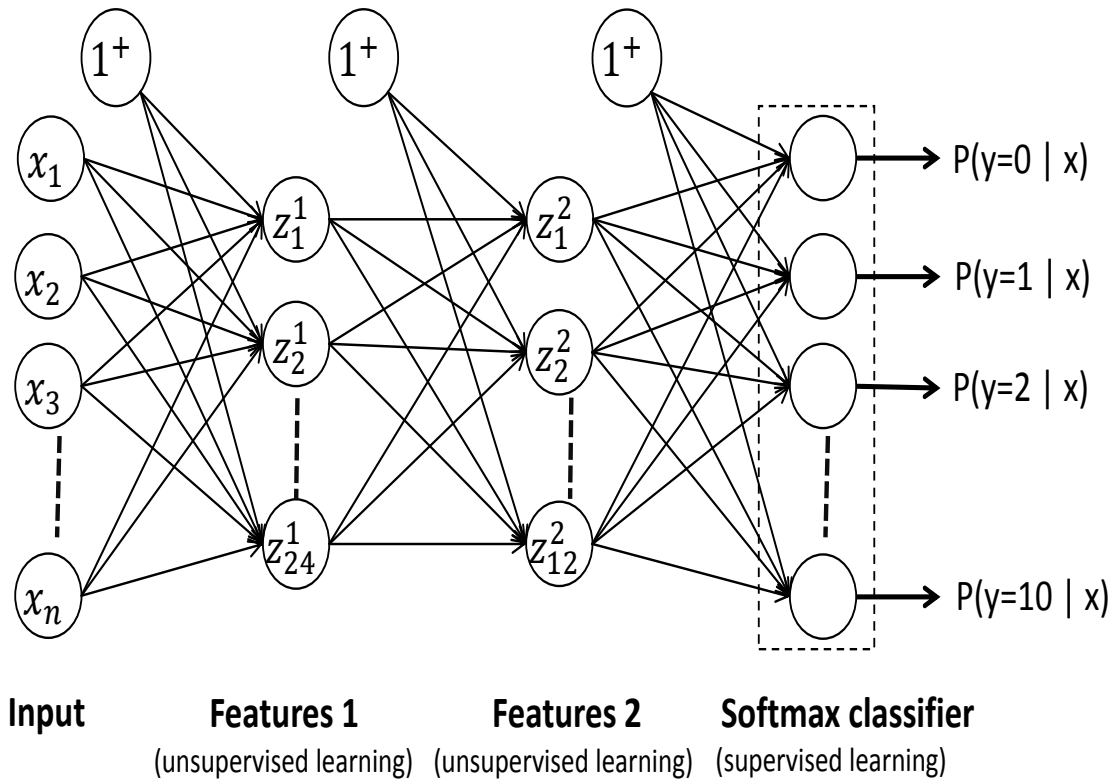
Figure 2-3: Block diagram of SSAE

Block diagram of SSAE used in this work. Features at layer 1 are improved by minimizing the error through equation 3. These improved features are then fed as input to the next AE and again, improved features at layer 2 are fed to the softmax classifier where labels are obtained.

All the layers were trained independently from each other and were stacked together. Hence, features were learned in an unsupervised fashion while classification was supervised.

This work is based on stacked sparse autoencoders (SSAE) [38] which consist of two hidden layers with 24 and 12 hidden units respectively (Figure 2-3). For both layers, logistic sigmoid function was used for the encoders and linear functions for the decoders. In SSAE, the output of one AE acts as the input of another AE [39] and regularization is applied to the cost function to enhance sparsity [40], which represents the average output activation of a neuron. An average output activation for a neuron i can be represented as:

$$\hat{p}_i = \frac{1}{n} \sum_{j=1}^{n} z_i(x_j)$$

(4)

Where i represents ith neuron, n is the total number of training examples and j denotes the jth training example. This regularization term is added to the cost function using the Kullback-Leibler divergence [41]:

$$\Omega_{sparsity} = \sum_{i=1}^{d} p \log(\frac{p}{\hat{p}_i}) + (1-p) \log(\frac{1-p}{1-\hat{p}_i})$$

(5)

Where d is the total number of neurons in a layer [29] and p is the required activation value, called sparsity proportion (SP). An L_2 regularization term (L2R) is further applied to the cost function to adjust the weights:

$$\Omega_{weights} = \frac{1}{2} \sum_{l}^{L} \sum_{j}^{N} \sum_{i}^{K} (w_{ji}^{(l)})^2$$

(6)

Where L indicates the number of hidden layers, N the total number of observations and K the number of features within an observation.

Hence the cost function with the regularization terms (Equation 5, 6) added to the reconstruction error (equation 3) can be represented as follows:

$$E = \underbrace{\frac{1}{N} \sum_{n=1}^{N} \sum_{k=1}^{K} (x_{kn} - \hat{x}_{kn})^2}_{mean\ square\ error} + \lambda * \underbrace{\Omega_{weights}}_{\substack{L2 \\ Regularization}} + \beta * \underbrace{\Omega_{sparsity}}_{\substack{Sparsity \\ Regularization\ (SR)}}$$

(7)

The three regularization parameters are λ (coefficient for L2R) that prevents overfitting, β (coefficient for sparsity regularization SR) that oversees the sparsity penalty term, and p (SP) that specifies the preferred level of sparsity [42, 43]. Parameter optimization for the two hidden layers is denoted in Figures 3 and 4.

Scale conjugate gradient descent function [44] was applied to train both the AEs by using greedy layer wise training [45]. Eventually, the training of a softmax layer was performed in a supervised manner which was then stacked with the sparse AEs (as shown in Figure 2-3). In this way, the network was finely adjusted for final classification.

2.6. Statistical tests

The performance of two classifiers, SSAE and LDA, and surface vs intramuscular EMG based control scheme were compared by applying Friedman's tests with a two-way layout. The

performance and results of classification are determined as mean error with standard deviation.

The statistical P- values below 0.05 were considered significant.

Chapter 3. Deep learning with stacked sparse autoencoders for multiday analysis between surface and intramuscular EMG

3.1.Introduction

This chapter thoroughly presents the evaluation of stacked sparse autoencoders (SSAE) in comparison with classical machine learning technique. Both the surface and intramuscular EMG data of able-bodied and amputee subjects are used. Apart from that, surface EMG and intramuscular EMG have also been compared.

Material and methodology for this study is discussed in chapter 2.

3.2.ABSTRACT

Advances in EMG pattern recognition show promising results for improving the control of active prostheses. However, the poor robustness of control still limits user acceptance. In this study, we propose the use of stacked sparse autoencoders (SSAE), a rising deep learning approach, for myoelectric control and we compare its performance for sEMG and iEMG recordings over multiple sessions. Ten healthy subjects and six amputees were tested over seven days. The performance of classification of 11 hand motions (classification error, CE) from sEMG and iEMG was analyzed offline when using SSAE and linear discriminant analysis (LDA). Within each day, SSAE (CE 1.38 $\pm$ 1.38%) substantially outperformed LDA (8.09 $\pm$ 4.53%) using surface EMG and intramuscular EMG in both healthy and amputee subjects (P<0.001). SSAE surpassed LDA also in the between pair of days' analysis for able-bodied and amputee subjects using both sEMG and iEMG (7.19 $\pm$ 9.55% vs 22.25 $\pm$ 11.09%). In conclusion, SSAE was superior for myocontrol regarding the state of the art classification approach.

3.3.Background

The proficiency in myoelectric articulation has the ability to facilitate the individuals with missing or disabled limbs to use wearable prosthetic devices as replacement. Upper limb prosthesis use EMG signals for on-off control. Electrodes which may be invasive or non-invasive are used to record these signals from the disabled muscles. EMG signals help to control mobile hand prosthesis which enables the bidirectional movement of limbs with a constant velocity [11]. If proportional control of a prosthetic function is added, velocity is proportional to the intensity of the electromyography signals [46]. The influence of EMG signals control determines the degree of freedom (DoF) for limb actuation in these clinical control methods [11]. So each DoF may be operated by using at least two separate EMG channels. In order to avoid this restriction, pattern recognition [34, 47-49] based control schemes have been used with the purpose of decoding various prosthesis functions by supervised learning.

Different algorithms have been evaluated for the classification of EMG, including Artificial neural networks (ANN) [7, 18-21], log linearized Gaussian mixture networks (LLGMN) [22, 23, 50, 51], Fuzzy mean max NN [24], Bayesian network [24], Radial basis function [25], Hidden Markov model [26], linear discriminant analysis (LDA) [36], Random forest [52], k-nearest neighbors (KNN) [53] and support vector machine (SVM) [54]. When these algorithms were applied to temporal and frequency EMG features, some of them attained classification accuracies >95% for up to 10 classes [55].

The sophisticated algorithms of deep learning has an impact in different applied fields, such as speech recognition [3] and computer vision [4]. Besides classical machine learning approaches,

several deep learning algorithms, such as convolutional neural networks (CNN) and autoencoders (AEs) have also a remarkable role in biomedical signal applications [56], specifically in electrocardiography (ECG) [57-59] and electroencephalography (EEG) [43, 57, 60]. However, despite some applications in EMG processing [39, 61], deep learning methods have not been extensively applied in EMG control. Park and Lee [28] investigated that CNN performed decoding of movement intention better than an SVM classifier using EMG. Atzori et al. [1] suggested a multi-block CNN for publicly available Ninapro database, consisting of sEMG data of amputee and intact-limb subjects, for the classification of several hand movements [29]. This CNN performed commensurable with respect to LDA, KNN, random forest and SVM.

As surface electromyography is most frequently used for myoelectric control, intramuscular EMG has also been proved as a useful approach that may overcome some of the drawbacks related to non-invasive systems [62]. For instance, Kamavuako et al. [47] proved that the combined use of sEMG and iEMG gave outstanding classification accuracy of a myoelectric control system as compared to sEMG alone. Other studies [63-66] obtained similar results from the comparison of the individual performance of surface and intramuscular EMG for the classification of wrist and upper limb movements. Nevertheless, all these previous research studies have shown results on healthy subjects and in a single recording session.

In this study, we applied for the first time SSAE (deep networks) in a myoelectric control application. Furthermore, we performed comparison of sEMG and iEMG classification for both amputee and healthy subjects over multiple sessions in separate days.

3.4. RESULTS

3.4.1. Parameter optimization

Both layers were applied with different combinations of optimization parameters (L2R, SR, SP) to find the best suitable parameter values for these layers which reduce their mean squared error (MSE). The parameter values selected for the layers were same (L2R=0.0001, SR=0.01 and SP= 0.5). Figure 3-1 and 3-2 indicate the three parameters with different combinations and MSE for the two layers (maximum Epochs of 500).
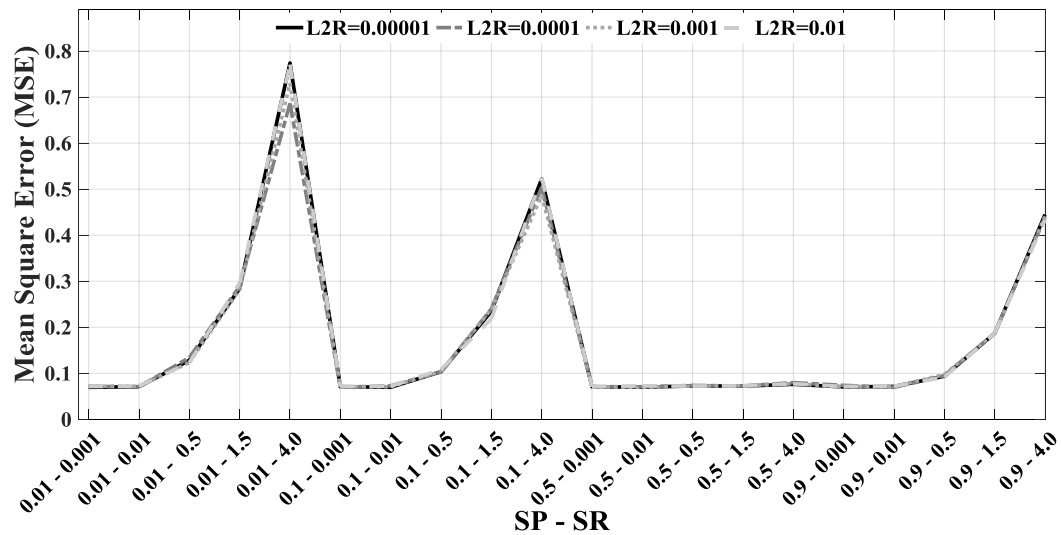
Figure 3-1: Parameters selection for layer one

Parameters selection for layer one. It shows the MSE graph for layer one. Parameters L2R, SP and SR were varied as 0.00001 - 0.1, 0.01 - 0.9 and 0.001 - 4.0 respectively and best values were chosen that optimized the MSE.
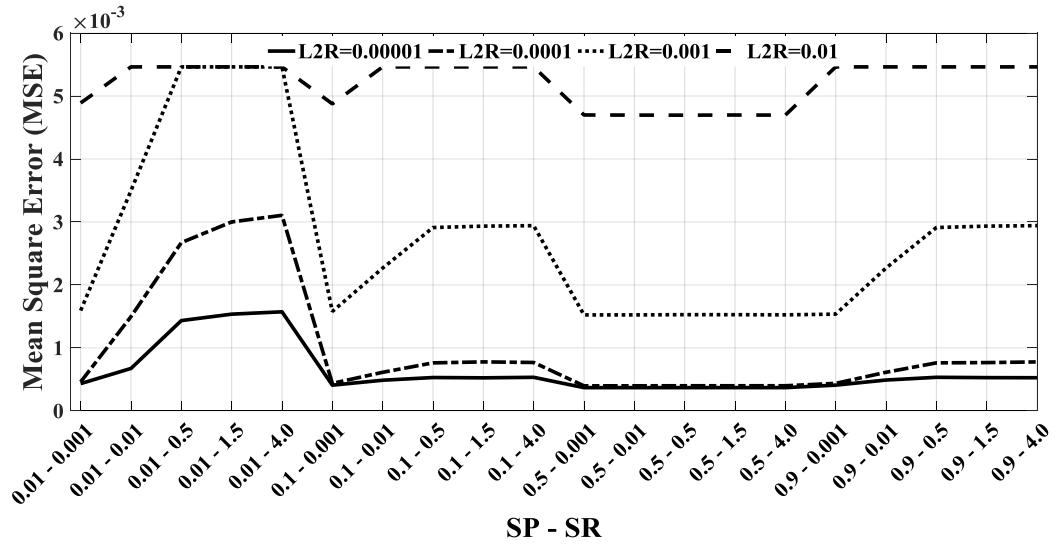
Figure 3-2: Parameters selection for layer two

Parameters selection for layer two. It shows the MSE graph for layer two. As greedy layer-wise training strategy was adopted and hence, this layer was trained independent of layer one. Same parameters values were also varied for layer two and best values were chosen that optimized the error at layer two.

3.4.2. SSAE vs LDA

Five-fold cross validation was used to determine the classification errors for each day which were averaged over seven days for each subject.

During this analysis, whole data was distributed in four sets comprising surface and intramuscular EMG data of able-bodied and amputee subjects. SSAE and LDA were then used to classify all sets of EMG data. The classification results are indicated in Figure 3-3.
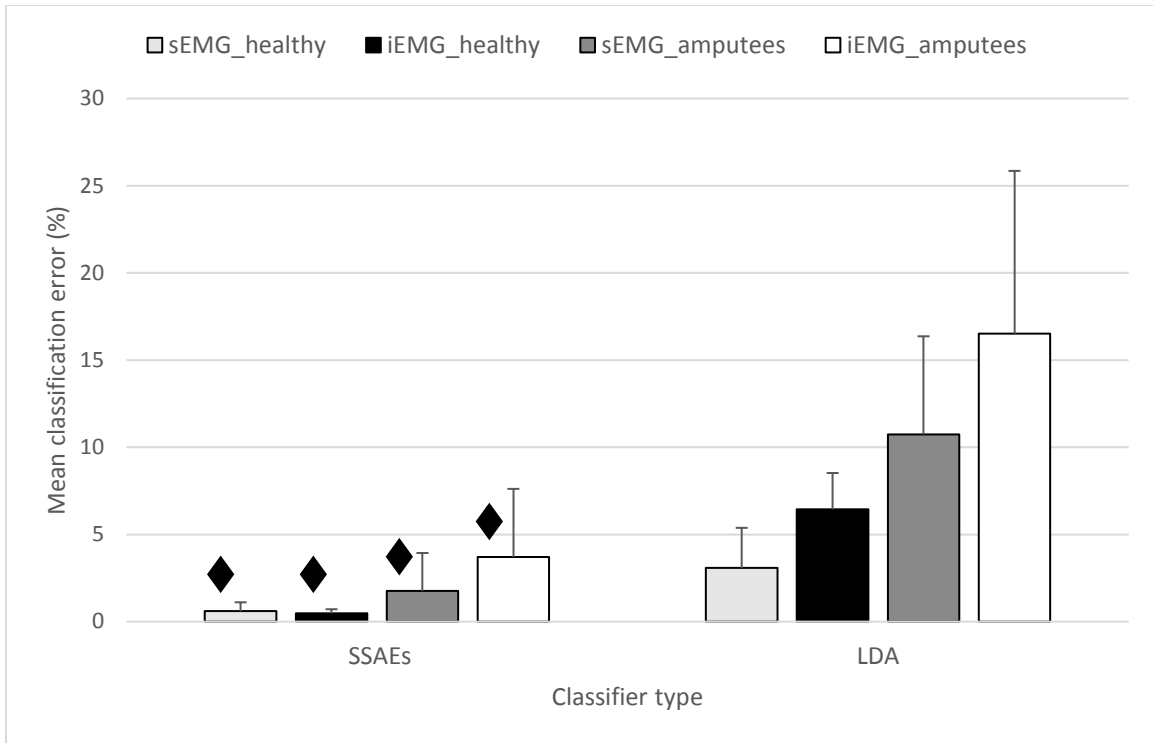
Figure 3-3: classification errors for within day analysis using both SSAE vs LDA.

Mean (and SD) classification error for SSAE and LDA classifiers for the four sets of EMG data. The diamond symbol indicates the best classifier, with statistical significance (P < 0.001).

Table 3-1: performance comparison of SSAE vs LDA in within day analysis using Friedman's test.

Data	Mean accuracy		P value	Conclusion (better classifier)
	SSAE	LDA		
sEMG healthy	99.40	96.92	3.1447e-15	SSAE
imEMG healthy	99.51	93.56	3.8346e-23	SSAE
sEMG amputees	98.24	89.25	8.5094e-14	SSAE
ImEMG amputees	96.29	83.48	5.8398e-14	SSAE

Less statistical error rates were observed for SSAE as compared to LDA for each case (P < 0.001) (Table 3-1).

3.4.3.   sEMG vs iEMG

The classification results of SSAE and LDA for the four combinations of sEMG and iEMG datasets of able-bodied and amputee subjects were compared and are demonstrated in Figure 3-4.
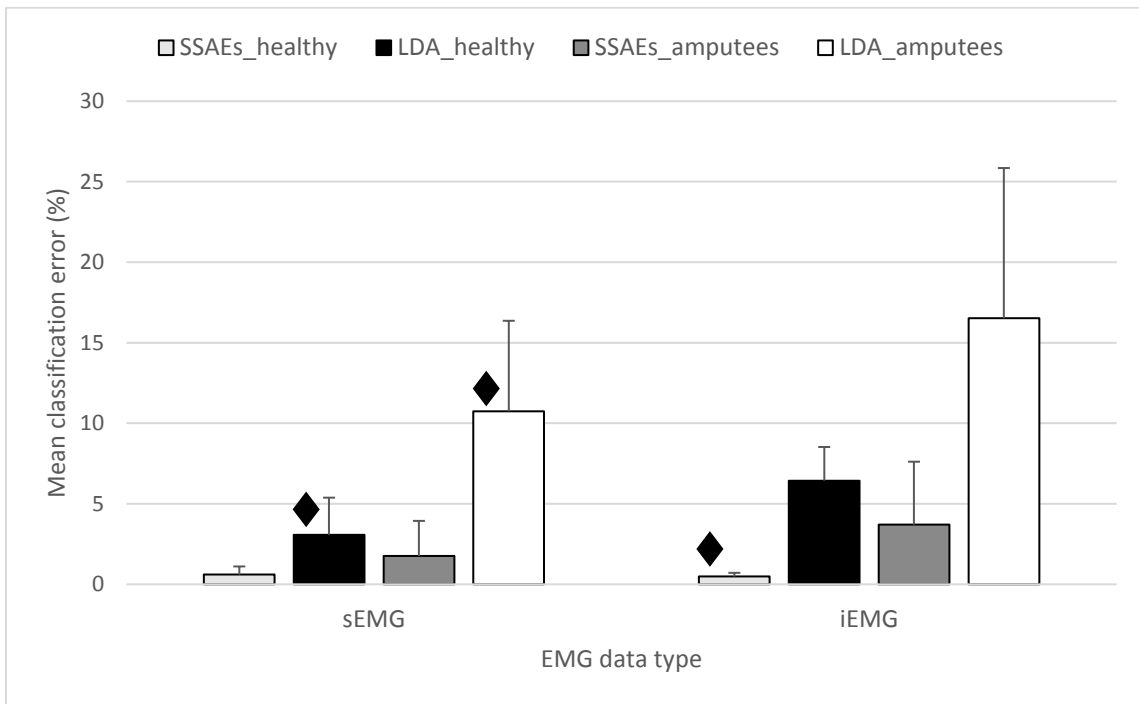
Figure 3-4: Classification errors of sEMG vs iEMG data in within day analysis

Mean (and SD) classification error obtained with two different classifiers for both kinds data of healthy and amputee subjects. Diamond symbol indicates the best EMG data type, with statistical significance.

Table 3-2: performance comparison of sEMG vs iEMG in within day analysis using Friedman's test.

Classifier	Mean accuracy		P value	Conclusion (Better Data)
	sEMG	imEMG		
SSAEs (healthy)	99.40	99.51	0.0186	imEMG
LDA (healthy)	96.92	93.56	9.5636e-12	sEMG
SSAEs (amputee)	98.24	96.29	0.1585	No significant difference
LDA (amputee)	89.25	84.48	0.0324	sEMG

It can be seen from table 3-2, SSAE (P > 0.05) indicated no considerable difference between iEMG and sEMG while sEMG surpassed iEMG while using LDA (P < 0.05).

3.4.4. Analysis between pairs of days

Data of seven days was categorized into twenty-one unique pairs. Eight-fold cross validation was used to compute the classification errors for each pair which were then averaged over all pairs of data for each subject.
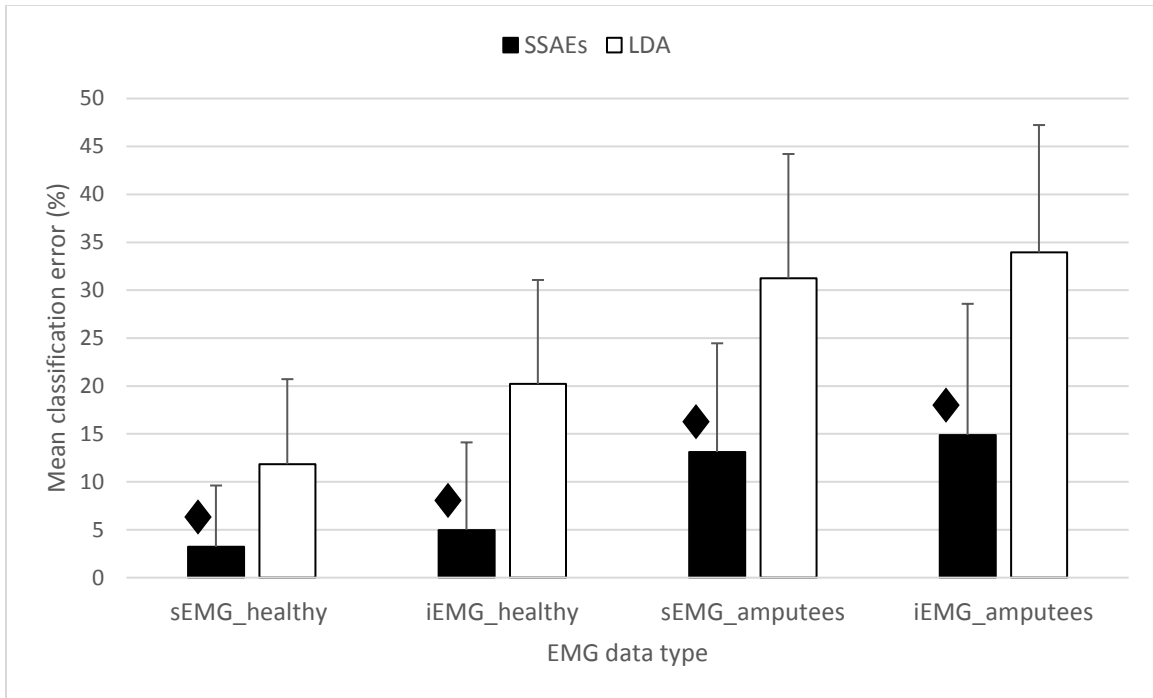
Figure 3-5: classification errors of SSAE vs LDA (between pair of days analysis)

Mean (and SD) classification error obtained with SSAE and LDA for both EMG data types of healthy and amputee subjects. The diamond symbol indicates the best classifier with statistical significance ($P < 0.001$) for each EMG data type of both healthy and amputee subjects.

Table 3-3: SSAE vs LDA performance comparison (between pair of days analysis)

Data	avg accuracy with standard deviation		P value	Conclusion (better classifier)
	SSAEs	LDA		
Healthy Surface	96.78 ± 6.40	88.15 ± 8.87	1.4981e-65	SSAEs
Healthy intramuscular	95.02 ± 9.14	79.78 ± 10.85	3.5372e-66	SSAEs
Amputee Surface	86.89 ± 11.35	68.76 ± 12.98	1.1829e-39	SSAEs
Amputee Intramuscular	85.11 ± 13.69	66.06 ± 13.30	1.1955e-39	SSAEs

29

SSAE beat LDA for both able-bodied and transradial amputee subjects by 11.93 and 21.59 percentage points respectively (Figure 3-5 and table 3-3). Further, in the within day analysis, SSAE acquired same error rates as those of the corresponding data, attaining percentage points difference of 3.55 and 11.26 for able-bodied and amputee subjects respectively. Contrarily, LDA showed considerable worst performance between days as compared to the within day analysis by 11.28 and 18.95 percentage points for able-bodied and amputee subjects respectively. Tables 3-4 and 3-5 indicate the mean classification errors computed for each pair of days for the data of ten healthy and six disabled subjects where upper diagonal shows the results with SSAE and lower with LDA .

Table 3-4: sEMG vs iEMG data comparison for healthy subjects (between pair of days analysis).

Healthy sEMG Data							
Days	**D1**	**D2**	**D3**	**D4**	**D5**	**D6**	**D7**
D1		2.29	3.06	2.23	3.09	2.74	3.88
D2	10.28		3.8	3.15	3.23	2.95	3.65
D3	10.4	9.96		3.74	4.08	3.57	4.31
D4	11.22	11.37	11.02		3.02	2.61	3.45
D5	13.16	12.78	12.68	11.43		2.53	3.46
D6	12.74	12.94	12.66	12	11.11		2.69
D7	13.54	13.56	13	11.62	11.31	9.95	
Healthy iEMG Data							
Days	**D1**	**D2**	**D3**	**D4**	**D5**	**D6**	**D7**
D1		5.68	6.63	6.03	5.7	5.15	6.25
D2	21.69		5.36	4.75	4.79	3.93	4.54
D3	23.42	17.93		5.19	5.03	4.78	5.24
D4	21.96	19.5	18.16		5.16	5.2	5.33
D5	24.68	21.03	20.52	18.98		3.05	3.58
D6	23.59	20.19	20.96	18.73	17.66		3.12
D7	23.85	20.53	19.03	19.65	16.55	15.9	

Table 3-5: sEMG vs iEMG data comparison for amputee subjects (between pair of days analysis).

Amputees sEMG Data							
Days	**D1**	**D2**	**D3**	**D4**	**D5**	**D6**	**D7**
D1		14.56	16.23	14.4	15.47	13.21	12.18
D2	34.75		14.32	13.51	12.96	11.54	11.48
D3	38.19	34.03		16.4	15.84	12.73	13.31
D4	32.27	31.77	34.36		13.49	11.83	12.11
D5	36.1	33.21	34.79	30.56		10.34	10.78
D6	31.45	30.42	30.76	27.42	24.18		8.57
D7	34.12	31.01	32.27	27.92	25.38	20.91	
Amputees iEMG Data							
Days	**D1**	**D2**	**D3**	**D4**	**D5**	**D6**	**D7**
D1		15.84	17.41	18.64	16	16.46	15.32
D2	36.15		14.96	16.99	13.39	13.76	13.53
D3	39.66	34.25		16.54	13.76	13.83	13.74
D4	38.16	33.58	33.91		15.11	15.2	14.43
D5	38	34.23	35.01	32.42		11.79	12.78
D6	36.07	33.56	34.9	32.55	29.47		13.16
D7	36.75	31.99	34.11	31.18	28.97	27.72	

From Table 3-4, it was observed that classification of sEMG and iEMG with SSAE derived similar results (percentage point difference of 1.76) while it showed remarkable difference by using LDA (sEMG better than iEMG with difference of 8.37 in percentage points).

Nevertheless, for trans-radial amputees, sEMG and iEMG classified with both SSAE and LDA obtained similar accuracy (table 3-5).

3.4.5. Between days' analysis

In this study, two-fold and eight-fold validation methods were used for EMG analysis. For two-fold validation, twenty-one pairs of days were tested, with alternate days used for training and testing of data. For seven-fold data validation, six days were reserved for training and one day for testing, performing seven repetitions. Mean classification errors are shown in figure 3-6 and 3-7 and the corresponding Friedmann test observations are shown in table 3-6 and 3-7. Additionally, table 3-8 and 3-9 shows the comparison of SSAE vs LDA (day to day performance) for both healthy and amputee subjects respectively for between days analysis with two-fold validation.
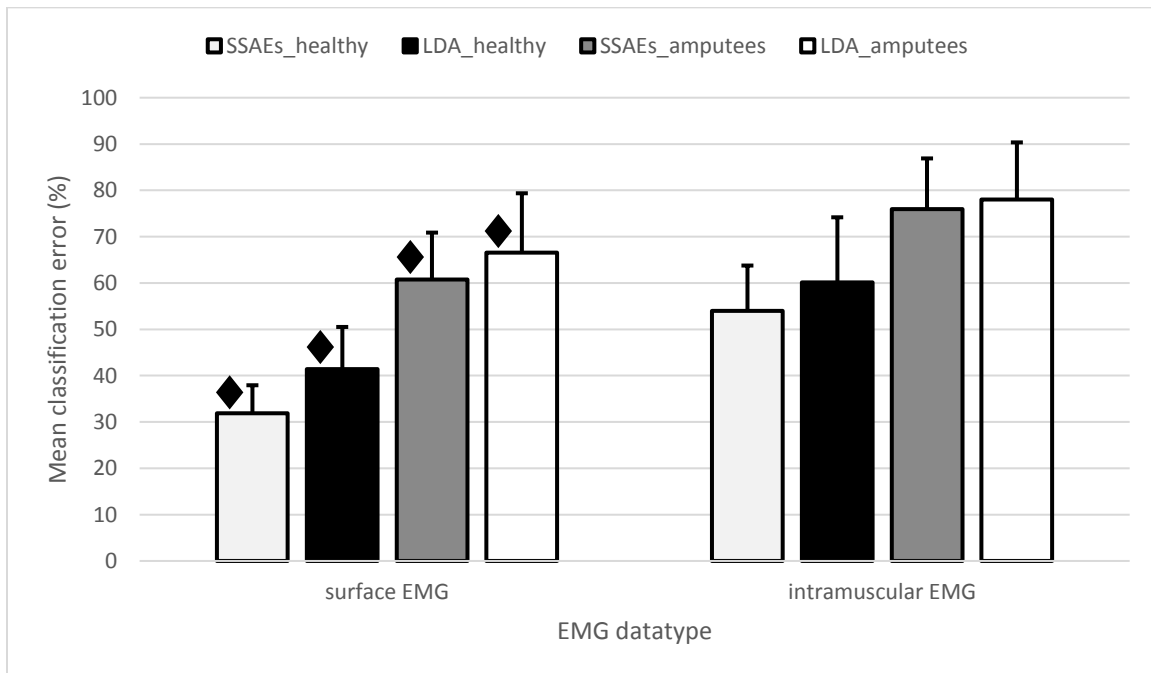
Figure 3-6: Between days analysis with two-fold validation.

Two-fold validation. Mean (and SD) classification error obtained with two different classifiers for both kinds data of healthy and amputee subjects. Diamond symbol indicates the best EMG data type, with statistical significance (P < 0.001).
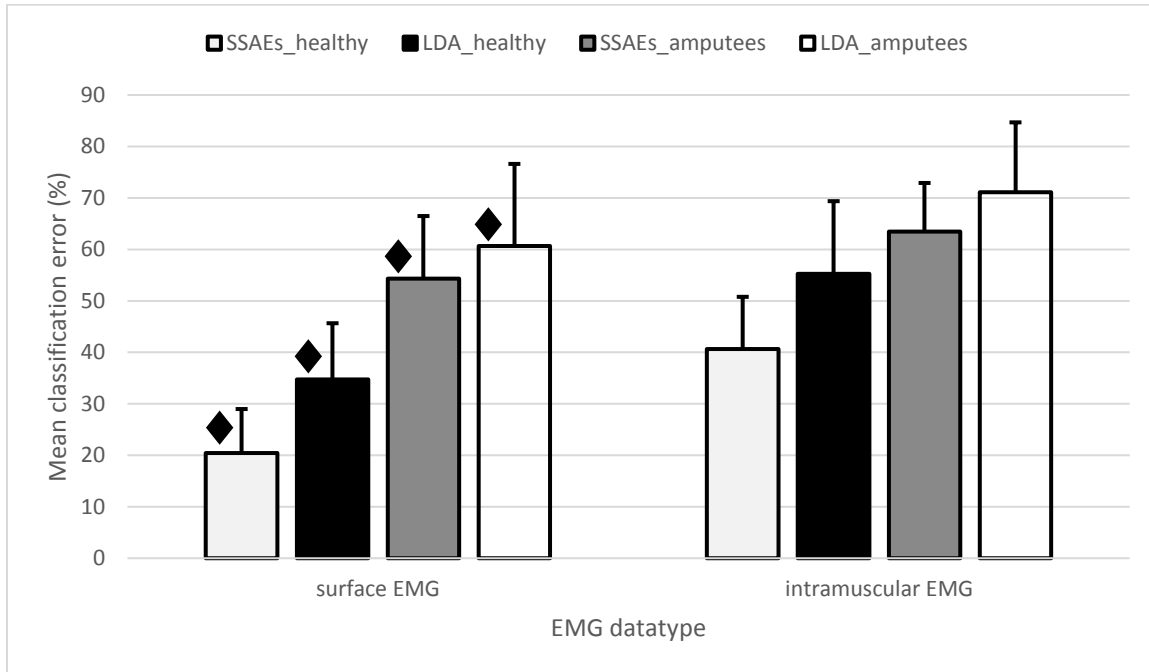
Figure 3-7: Between days analysis with seven-fold validation

Seven-fold validation. Mean (and SD) classification error obtained with two different classifiers for both kinds data of healthy and amputee subjects. Diamond symbol indicates the best EMG data type, with statistical significance (P < 0.01).

Table 3-6: Between days performance comparison of sEMG vs iEMG with two-fold validation.

Classifier	Mean accuracy ± standard deviation		P value
	sEMG	imEMG	
SSAEs (healthy)	68.13 ± 6.07	46.01 ± 9.78	1.5985e-19
LDA (healthy)	58.60 ± 9.12	39.86 ± 14.05	5.6279e-14
SSAEs (amputee)	39.22 ± 10.11	24.11 ± 10.91	3.5655e-14
LDA (amputee)	33.41 ± 12.79	21.97 ± 12.33	3.7117e-10

Table 3-7: Between days performance comparison of sEMG vs iEMG with seven-fold validation.

Classifier	Mean accuracy ± standard deviation		P value
	sEMG	imEMG	
SSAEs (healthy)	79.57 ± 8.56	54.34 ± 10.15	3.2700e-16
LDA (healthy)	70.29 ± 10.95	44.73 ± 14.10	1.0705e-17
SSAEs (amputee)	43.67 ± 12.15	36.57 ± 9.48	0.0123
LDA (amputee)	41.35 ± 15.96	28.88 ± 13.56	5.9036e-05

SSAE acquired better performance with lower error rates than LDA in case of both the two-fold and seven-fold cross validation. Moreover, error rates were lower when classifying sEMG than iEMG ($P < 0.01$). Increase in the training data from one to six days caused a decrease in the error rate of SSAE by 13.03 and 9.50 percentage points for iEMG and sEMG, respectively. For LDA, this reduction in error rate with increasing training data was minor (6.39 and 5.16).

Table 3-8: sEMG vs iEMG data comparison for healthy subjects (between days with two-fold validation).

Healthy sEMG Data (SSAE vs LDA)						
Days	**D1**	**D2**	**D3**	**D4**	**D5**	**D6**	**D7**
D1		36.71	35.24	38.25	33.64	33.87	36.61
D2	48.42		29.87	26.37	26.66	31.21	34.33
D3	49.6	44.38		28.42	27.97	27.9	36.06
D4	49.99	33.67	36.97		25.56	30.93	32.22
D5	47.88	38.36	42.56	32.81		26.14	33.91
D6	43.64	40.34	38.55	36.13	35.35		37.34
D7	45.28	43.98	45.44	36.69	41.93	44.63	

Healthy imEMG Data (SSAE vs LDA)						
Days	**D1**	**D2**	**D3**	**D4**	**D5**	**D6**	**D7**
D1		59.23	56.74	54.82	58.47	51.82	51.80
D2	67.72		57.72	48.74	56.50	55.86	59.08
D3	66.59	59.81		48.21	57.46	50.93	58.45
D4	68.58	52.46	51.19		48.01	45.72	48.82
D5	68.84	59.92	59.84	52.96		49.11	58.39
D6	62.51	61.08	53.11	55.4	56.36		57.91
D7	64.95	63.64	61.54	55.42	63.06	64.91	

Table 3-9: sEMG vs iEMG data comparison for amputee subjects (between days with two-fold validation).

Amputees sEMG Data (SSAE vs LDA)

Days	D1	D2	D3	D4	D5	D6	D7
D1		56.31	62.90	53.62	62.64	59.89	55.79
D2	63.69		56.64	65.38	64.22	63.4	55.15
D3	71.27	65.74		63.81	65.75	62.94	59.17
D4	64.96	73.59	69.7		65.92	57.66	65.2
D5	68.53	73.03	67.82	69.78		57.92	58.45
D6	66.71	71.67	66.28	61.41	58.96		63.56
D7	63.12	66.23	60.93	71.32	60.07	67.22	

Amputees imEMG Data (SSAE vs LDA)

Days	D1	D2	D3	D4	D5	D6	D7
D1		75.92	80.52	76.88	80.97	77.79	75.74
D2	73.8		71.12	83.90	75.85	73.56	68.69
D3	84.36	76.83		82.18	77.99	75.15	70.51
D4	78.76	83.84	82.94		81.80	74.33	81.18
D5	81.09	84.95	80.71	84.68		69.77	68.74
D6	76.41	78.68	76.11	72.01	71.47		73.03
D7	75.02	75.84	72.19	82.6	73.19	73.31	

3.5.Discussion

For both surface EMG and intramuscular EMG data of healthy and amputee subjects, SSAE showed outstanding performance as compared to LDA. Furthermore, SSAE proved to be more robust to the between day variation of EMG features.

Performance of the two layers improved when non-linear activation functions were used for encoders and linear for decoders. Moreover, optimization of the number of hidden units minimized the error but there was no considerable reduction upon their further increment. It was observed that during training the data, error in each layer was minimized independently by some specific parameters. Training of each layer was carried out independently in a greedy layer-wise training fashion. At layer 1, the MSE performance was affected by SR but was uninfluenced by L2R. Contrarily, at layer 2, MSE was minimized with decrease in the values of L2R.

In case of within day analysis, SSAE revealed similar performance upon its application to surface and intramuscular EMG. For between days subject's data, iEMG and sEMG acquired classification errors <1% for healthy subjects, however, iEMG (σ^2=0.05) exhibited less variance than sEMG (σ^2=0.26). The classification error obtained in case of LDA was greater than SSAE and was different in sEMG and iEMG as for sEMG, LDA indicated lower error rates. These findings are in accordance with the previous work that indicated similar classification results for both iEMG and sEMG or slight improved performance for iEMG [64-66].

The results of SSAE for analysing between pairs of days were same as those attained for the within day analysis. Contrarily, LDA performed considerably worst in case of different days

analysis. Therefore unlike LDA, SSEE gave more generalized results when more data was added from other days.

SSAE surpassed ($P < 0.001$) the LDA in two-fold and seven-fold cross validation of between days' analysis and sEMG performed well as compared to iEMG. Furthermore, increase in the training set improved the results of SSAE comparatively more than those of LDA.

Previous research work related to myocontrol with deep networks application only emphasized on sEMG [1, 28]. The findings of this study for sEMG are commensurable to previous studies that revealed either similar or improved performance of deep networks as compared to classical machine learning techniques. This research work has also taken the iEMG data into account and demonstrated that classification with deep networks is way better than LDA classification for the combined use of sEMG and iEMG as it attain more robustness across days.

3.6. Conclusion

SSAE remarkably surpassed the state of the art classifier, LDA when using sEMG or iEMG data and was more robust across days. These results indicate that deep SSAE based schemes are promising approaches for improving classification accuracy and robustness of myocontrol schemes.

Chapter 4. Performance of combined surface and intramuscular EMG for classification of hand movements using stacked sparse autoencoders

4.1. Introduction

This chapter is a part of study one which evaluates the performance of combined surface and intramuscular EMG data with respect to surface EMG. Both the SSAE and LDA classifiers are utilized and their performance is also compared.

The general methodology for this study is same as described in chapter 2 (same protocol and signal processing steps). However, this study is performed with five healthy and three amputee subjects and different cross-fold validation schemes are used. This difference is briefly described in section 4.4 of this chapter.

4.2. Abstract

Previous studies proposed surface EMG and intramuscular EMG as promising control sources for upper limb prosthetics. The purpose of this study is to investigate the effect of using combined surface and intramuscular EMG (cEMG) upon myoelectric control. Data of five healthy subjects and three transradial amputees were collected and used to determine offline classification error as performance metric. Simultaneous recording of six surface and intramuscular channels from each subject was completed for seven successive days and Stacked sparse autoencoders (SSAE) and LDA classifiers were used for classification. Either sEMG channels or combined channels were utilized as a control source with reduced features with the help of PCA. In the within session analysis, cEMG ($2.21 \pm 1.19\%$) outperformed the sEMG ($4.63 \pm 2.07\%$) for both healthy and amputee subjects using SSAE. For between session

analysis, cEMG performed better than the sEMG for both healthy and amputee subjects with percentage points difference of 7.93. These results revealed the fact that myoelectric control methods for pattern recognition can perform amazingly well with the use of cEMG even in case of amputee subjects and more improvement can be achieved by using SSAE which confirmed better performance as compared to LDA.

4.3. Background

The electrical activity generated within the remnant muscles is used to control a myoelectric prosthetic hand and EMG plays key role to record this electrical activity. EMG signals are collected from a contracting muscle with the help of either a wire, needle or surface electrodes. Surface EMG (sEMG) is the non-invasive [67] scheme for myoelectric control of upper limb prosthetics and is extensively utilized in the literature for this purpose [65]. On the other hand, intramuscular EMG (iEMG) is an invasive method [64] and in comparison with sEMG, it has little crosstalk and ensure stability of the control signals obtained from deep muscles [62, 64, 68]. But unlike sEMG which contains enough information collected from the surrounding muscles, iEMG only provides data from specific muscles which is a major drawback [69].

Myoelectric control techniques have been evaluated for both the sEMG and iEMG as control sources [11, 70]. Classical methods follow simple strategies to analyze the EMG signals collected from one or few sites [66]. E.g. on-off, direct and proportional methods use the amplitude of EMG signals with some post-processing, but they have limited potential to accurately control the multiple functions performed by dexterous prosthetic hands [1, 71]. Pattern recognition (PR) based control methods [34, 72-74] could be used to overcome this limitation which have obtained satisfactory results with both the sEMG and iEMG-based techniques. The successful PR-based control requires repeated patterns which must be

differentiable from each other [75]. Two important steps of PR-based control are features extraction and classification. More useful information is obtained with the help of extracted features from EMG signals to achieve greater functional ability of a prosthetic hand. Different classifiers such as artificial neural networks, support vector machines, random forest and decision tree etc. have been investigated for myoelectric control methods, but LDA proves to be the more common, reliable and robust. Previous studies [47, 63-66] related to myoelectric control methods, propose that either sEMG did well as compared to iEMG or both gave similar results with no notable difference. Kamavuako et al. [47] conducted a real-time study to investigate the role of combined sEMG and iEMG in the improvement of myoelectric control. For this purpose, five performance metrics for real time and one as offline classification error (concern of this study) were used. In case of real-time performance metrics, combined EMG (cEMG) either surpassed sEMG or both gave almost similar results whereas in the offline work, cEMG performed remarkably better than sEMG. Nevertheless, that approach was applicable only to healthy subjects and there is no surety to achieve the same results for amputee subjects.

Therefore, the purpose of this work was to compare the offline classification errors of both combined and surface EMG signals. It is evaluated using both SSAE and LDA classifiers.

4.4. Methodology

Data collection protocol, number of movements and signal processing steps are same as described in chapter 2, except that data of only five able-bodied and three transradial amputee subjects was used. The difference exists only in the processing of cEMG and different validation schemes which are described below.

For experimentation, right hand of all subjects was used except for two amputee subjects where their left hand was used. In case of amputees, two subjects had only five surface electrodes while the number of intramuscular electrodes varied from three to six due to limited space.

The electric noise was removed with a 3rd order configurable Butterworth filter and features were extracted from a 200 msec time window with an increment of 28.5 msec. Features included mean absolute value (MAV), waveform length (WL), zero crossing (ZC) and slope-sign change (SSC) [34]. Classification was performed with both SSAE [35] and LDA [36]. Optimization of SSAE's parameters is explained in chapter 3.

In sEMG based control, all six surface channels were used while for combined EMG based control, features vector from all channels were reduced by using principal component analysis (PCA) and were equalized to that of surface features. For features reduction using PCA, percent of variance (POV) was calculated for each subject of both healthies and amputee's data and are shown in figure 4-1 and 4-2.
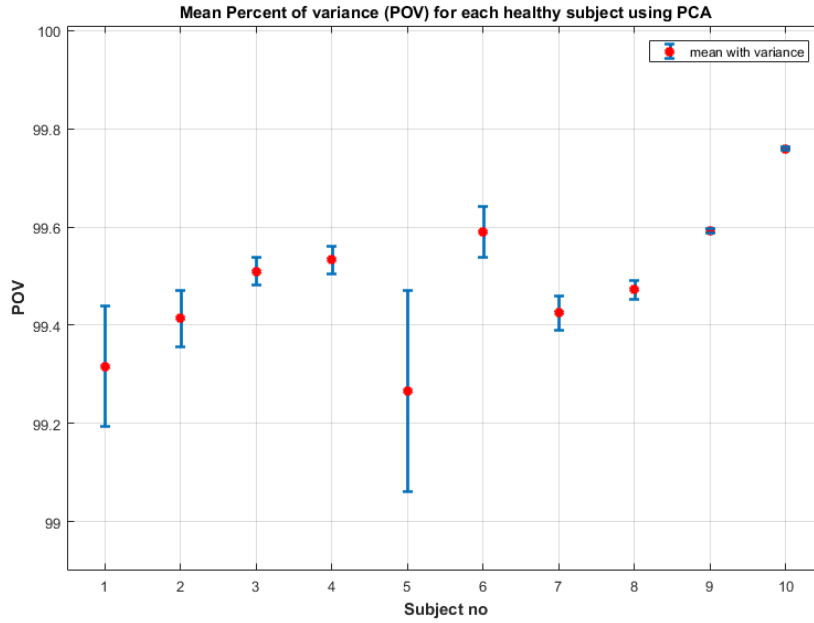
Figure 4-1: Percent of variance for each healthy subject.
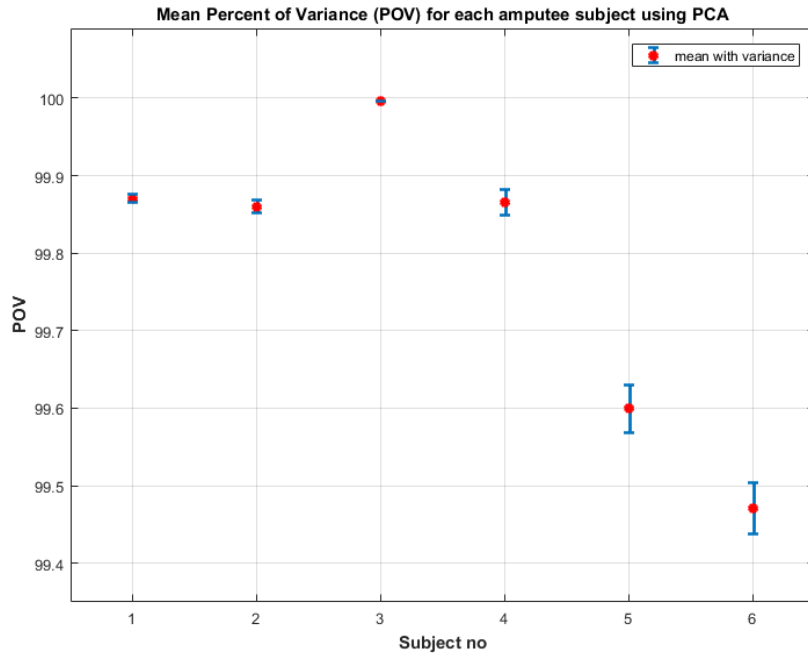
Figure 4-2: Percent of variance for each amputee subject

For within session analysis, four-fold cross validation scheme was used while eight-fold cross validation was used in the between session analysis. All these steps were performed in exactly the same way for both healthy and amputee subjects. The same folds were used for classification using LDA and SSAEs to make a fair comparison.

In order to quantify the difference of sEMG vs combined EMG and SSAE vs LDA, Friedman's statistical test was used and P values less than 0.05 were considered significant.

4.5. Results

4.5.1.   Within session analysis

In this analysis, for an individual subject, data of a single day were randomly divided into four-folds. three folds were used for training and one for testing. This was repeated four times and each time; a new fold was used for testing. Classification errors of seven sessions were averaged for each subject and results are presented as mean of all healthy and amputee subjects separately as shown in figure 4-3.
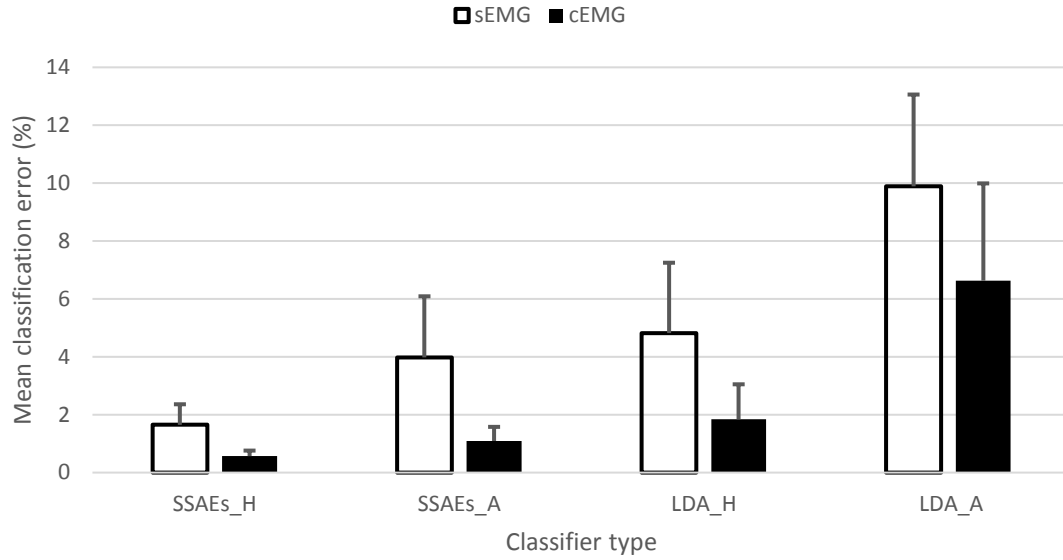
Figure 4-3: classification errors of sEMG vs cEMG for within session analysis

Table 4-1: performance comparison of sEMG vs cEMG for within session analysis

Classifier	Mean accuracy ± standard deviation		P value
	sEMG	*Combined EMG*	
SSAE_H	98.35 ± 0.71	99.43 ± 0.19	0.0021
LDA_H	95.18 ± 2.43	98.16 ± 1.21	0.0019
SSAE_A	96.02 ± 2.11	98.91 ± 0.49	0.0001
LDA_A	90.11 ± 3.17	93.37 ± 3.36	0.0001

To compare the performance of both kinds of data, statistical tests were conducted, and P-values are tabulated in table 4-1.

From table 4-1, it can be verified that cEMG outperformed the sEMG data for both healthy and amputee subjects. Further, comparing performance of SSAEs and LDA, it was found that

SSAEs achieved comparatively less classification error rates for both healthy and amputee subjects and outperformed LDA with 6.81 and 9.08 percentage points for both cEMG and sEMG, respectively.

4.5.2. Between sessions analysis

For seven sessions, we have a total of twenty-one unique pairs of sessions. Eight-fold cross validation was used for each pair and classification errors were averaged over twenty-one pairs for each subject. Results are presented as mean classification errors of healthy and amputee subjects separately (as shown in figure 4-4 and table 4-2).
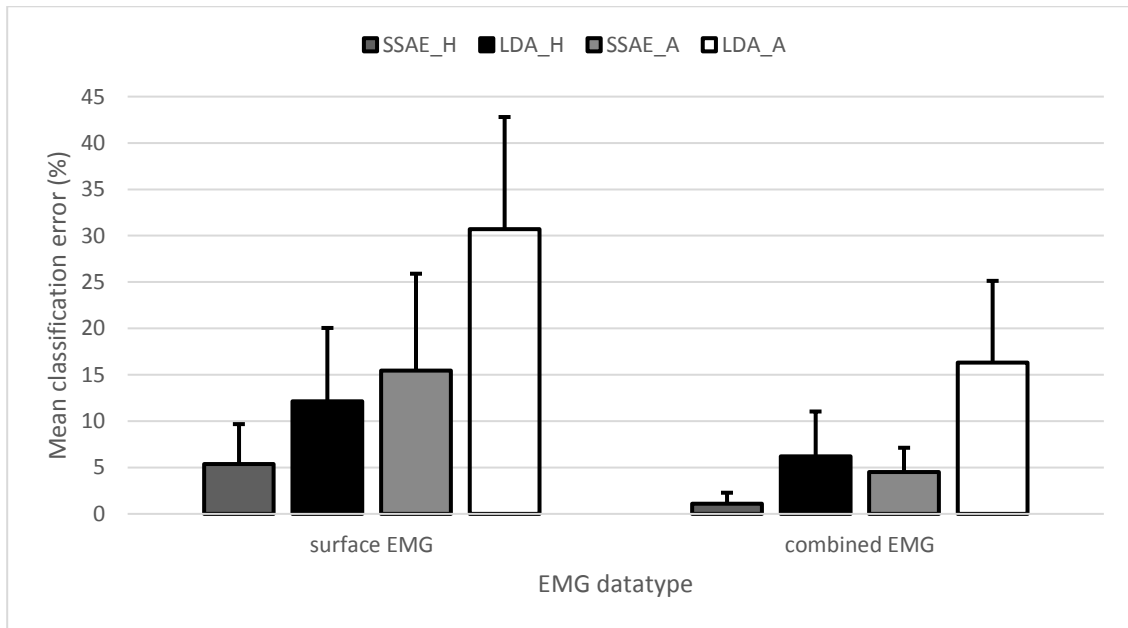
Figure 4-4: classification errors of sEMG vs cEMG for between sessions analysis

Between session analysis. Mean classification errors for both kinds of data obtained with SSAEs and LDA. _H and _A represents the data for both healthy and amputee subjects respectively. bars represent the standard deviation.

Table 4-2: Performance comparison of sEMG vs cEMG for between sessions analysis

Classifier	Mean accuracy ± standard deviation		P value
	sEMG	*Combined EMG*	
SSAE_H	94.63 ± 4.31	98.91 ± 1.19	0.0001
LDA_H	87.86 ± 7.91	93.80 ± 4.84	0.0000
SSAE_A	84.54 ± 10.44	95.48 ± 2.61	0.0000
LDA_A	69.31 ± 12.11	83.67 ± 8.80	0.0000

Table 4-3: Between pairs of sessions analysis for healthy subjects

Healthy subjects cEMG vs sEMG with SSAEs							
Days	*D1*	*D2*	*D3*	*D4*	*D5*	*D6*	*D7*
D1		0.96	1.09	0.94	0.92	0.82	1.07
D2	4.44		1.30	1.20	1.01	0.92	1.28
D3	5.21	5.95		1.32	1.27	1.12	1.63
D4	4.38	5.30	5.89		0.99	0.96	1.24
D5	5.24	5.37	6.23	5.17		0.85	1.03
D6	4.89	5.10	5.72	4.76	4.68		0.76
D7	6.03	5.80	6.46	5.60	5.61	4.84	
Healthy subjects cEMG vs sEMG with LDA							
Days	*D1*	*D2*	*D3*	*D4*	*D5*	*D6*	*D7*
D1		5.78	6.33	6.38	6.85	6.60	7.26
D2	10.57		5.51	5.88	6.30	5.89	6.58
D3	10.71	10.20		6.21	6.96	6.25	6.65
D4	11.65	11.61	11.35		5.97	6.11	6.71
D5	13.39	13.11	12.99	11.76		5.45	5.46
D6	13.02	13.23	12.88	12.24	11.54		4.78
D7	13.78	13.89	13.25	11.97	11.60	10.15	

Table 4-4: Between pairs of sessions analysis for amputee subjects

Amputee subjects cEMG vs sEMG with SSAEs							
Days	*D1*	*D2*	*D3*	*D4*	*D5*	*D6*	*D7*
D1		4.93	5.13	5.53	4.76	4.91	4.72
D2	15.89		4.61	4.31	4.08	3.98	4.11
D3	17.77	15.73		5.11	4.06	5.35	4.16
D4	15.95	15.02	17.86		4.15	4.62	4.57
D5	16.81	14.26	17.35	14.99		3.93	3.89
D6	14.60	13.18	14.09	13.35	11.85		3.60
D7	13.82	12.99	14.97	13.49	12.15	10.04	
Amputee subjects cEMG vs sEMG with LDA							
Days	*D1*	*D2*	*D3*	*D4*	*D5*	*D6*	*D7*
D1		18.69	19.25	17.54	20.25	17.07	17.27
D2	34.24		16.76	15.99	15.86	14.88	13.98
D3	37.74	33.69		16.16	16.92	14.51	14.42
D4	31.84	31.32	33.92		15.21	14.21	13.57
D5	35.62	32.84	34.24	30.03		12.94	12.13
D6	31.05	29.95	30.45	27.08	23.84		10.33
D7	33.87	30.55	31.54	27.56	25.15	20.66	

Like for within session analysis, SSAE also performed comparatively better for between sessions data and outperformed LDA with percentage points of 19.41 for both healthy and amputee subjects as can be seen from table 4-2. Table 4-3 and 4-4 (Where upper diagonal is for SSAE and lower diagonal for LDA) tabulates the confusion matric for between session analysis of all seven days. Using SSAEs, cEMG and sEMG data of both able-bodied and amputee subjects achieved close error rates for both the within and between sessions data with percentage points of 1.72 and 7.60, respectively, while this difference using LDA was 7.03 and 14.06, respectively. Unlike LDA, SSAE significantly improved the performance.

4.6.Discussion

This study compares performance of SSAE with a standard machine learning technique and investigates if the combined sEMG and iEMG obtained from deep muscles is able to considerably improve the results of myoelectric control for both healthy and transradial amputee subjects.

In the within session analysis, results confirmed that with SSAE, combined EMG performed well ($P<0.001$) than sEMG with data acquired from both healthy and amputee subjects. Same results were achieved with LDA. Nevertheless, SSAE attained comparatively low error rates than LDA in case of both combined and sEMG data as demonstrated in table 4-1. Previous discussion refers that iEMG from deep pronator and supinator muscles showed the better performance in wrist pronation, wrist supination and opening/closing of terminal device [7, 42]. However, these results were achieved only in case of healthy subjects. Data of three amputee subjects were analyzed in this study which confirmed that combined EMG enhanced the performance even for amputee subjects. This is due to the use of fine-wire and needle electrodes for recording of EMG from deep muscles which are less contaminated by crosstalk and that's why better performance was observed as compared to sEMG alone which undergo various artifacts such as electrode-skin interface and crosstalk from surrounding muscles etc.

In the between session analysis, long term performance of classifiers was retrieved. Even though, combined EMG gave better results than sEMG in case of both the classifiers, still SSAE performance was quite better than LDA and acquired close error rates to that of within day analysis with point difference of 4.65 percentage with the use of combined and sEMG data obtained from both healthy and amputee subjects. Whereas this difference for LDA was 10.05.

Thus, SSAE retained the results to the data of seven sessions collected with a gap of twenty-four hours and ensured better performance as compared to LDA.

4.7. Conclusion

The purpose of this study was to examine the effect of data collected from deep pronator and supinator muscles in improving the results of myoelectric control methods for amputee subjects. The results confirmed that combined EMG considerably improved the performance as compared to sEMG and additionally, SSAE was observed as more dependable than LDA for both the within and between sessions evaluation of classifiers.

Chapter 5. Classification of wrist movements with Convolutional neural networks and its comparison with stacked sparse autoencoders and LDA on longitudinal (15 days) surface EMG data

5.1.INTRODUCTION

This chapter is based on 2nd study and it is standalone chapter. In previous chapters, we have explored the autoencoders with engineered features. In this chapter, we have explored the deep features (data driven features) for improved myoelectric control. Data driven features are extracted using both the convolutional neural networks and autoencoders and their performance is compared with engineered features using LDA and autoencoders.

Material and methodology is separate for this study and is incorporated in this chapter.

5.2.ABSTRACT

Pattern recognition-based techniques show improved performance for myoelectric control of upper limb prosthesis. However, success of such methods strongly relies on repeatable and differentiable EMG patterns which are stochastic in nature. Thus, choosing optimal handcrafted features for classification is also a challenging task. In this work, we focus on raw electromyogram (EMG) as input to deep networks, a deep learning technique with intrinsic feature extraction capabilities. Seven able-bodied subjects participated in the experiment and recorded data for consecutive fifteen days with two sessions per day. Analyses were performed using four classifiers including Convolutional neural network (CNN) with raw data, Linear Discriminant Analysis (LDA), stacked sparse autoencoders with features (SSAE-f) and with raw data (SSAE-r) with classification error (CE) as performance metric. CNN surpassed both

LDA and SSAE-r in all cases i.e. in the within session ($p < 0.001$), between sessions on same day ($p < 0.001$), between pair of days ($p < 0.001$) and 15 days evaluation ($p < 0.001$) analysis. Nevertheless, there was no considerable difference between CNN and SSAE-f. Results imply that using raw EMG as input performed well with CNN but not with SSAE. CNN remarkably improved performance and enhanced robustness over long term compared to standard LDA with related handcrafted features and it could potentially be a solution to overcome the problem of features calibration.

5.3.BACKGROUND

Myoelectric control of upper limb prosthesis is considered as one of prominent field in Rehabilitation Engineering [76]. Prosthetic devices are controlled using electrical activity generated in remnant muscles called electromyographic (EMG) signals. The use of EMG signals in actuation of prosthetic hand dates back to 1948 [77]. These signals are recorded either non-invasively called surface (sEMG) or invasively (Intramuscular EMG). Surface EMG is the most studied signal modality for myoelectric control and it is commonly used in clinics [65]; thus it is the focus of this study.

Most of the commercially available prosthetic hands use standard myoelectric control methods (including on/off, direct and proportional control) that utilizes amplitude of EMG signals with some post processing [11] and are limited to one degree of freedom (DoF) [78]. Some of currently available prosthetic hands offer many different movements and hence multi DoF is desirable but conventional myoelectric control schemes are rudimentary enough to provide with desired robustness. Pattern recognition (PR) based control methods have emerged as a replacement to standard myoelectric control techniques with multi DoF functionality [75].

These systems have been extensively investigated to upgrade the multi-functional ability of dexterous prosthetic hands [47, 79-81].

Feature extraction and classification are two principal steps in PR based approaches. The selection of optimal features for classification is a challenging job. In many studies [34, 55, 82-84] new features and feature spaces have been proposed for optimal classification. Hudgins et al. [34] suggested four-time domain features called Hudgins set. Their feature set is most commonly used in many studies on PR based myoelectric control schemes and hence made a benchmark. Phinyomark performed multiple studies [55, 85, 86] and compared different time and frequency domain features separately and in groups in order to find a better representation of the feature space. After selecting the optimal set of features, they are being classified with different classifiers including Bayesian network [24], Hidden Markov model [26], linear discriminant analysis (LDA) [87], Artificial neural networks (ANN) [88], support vector machine (SVM) [89], Decision tree [90], K nearest neighbor (KNN) and Random forest [91]. PR based systems work on the assumption that individual movements should be repeatable and will be differentiable from each other [79]. However, EMG signals are stochastic in nature and they may change their statistic attributes even within same recording session due to posture change, fatigue or some other factors [79]. This change can be significant on day-by-day recording and hence it can significantly degrade the performance of classifier in long term [92]. Furthermore, selection of handcrafted features for any task is challenging which can also limit the use of prosthesis in amputees. Therefore, research focus is now changing from handmade features to data driven features consisting of automatically driving features from raw data and hence could improve the robustness of the system.

Studies related to deep learning algorithms in the last decade have revealed encouraging results in several fields for instance, computer vision [4], bioinformatics [5], natural language processing [93], and speech recognition [3]. These algorithms are basically the combination of non-linear layers of ANN that has the capacity to drive features from the raw data. These data dependent features are important for classification schemes. Convolutional neural networks (CNN), along with other fields of biomedical signal processing [94-96], are now being researched for sEMG based myoelectric control with the center of attention on inter-sessions/subjects and intra-session behavior. For inter-sessions/ subjects, some researchers conducted discrete sessions for training and testing data whereas others utilized data from previous sessions by using adaptation procedure. These methods are applied to easily available databases including Ninapro [1, 97], Capgmyo and csl-hdemg [98]. The formal database is recorded in single session while the later one is recorded in five sessions.

In the preliminary study of CNN based myoelectric control technique, Park and Lee [28] used Ninapro database and designed a user-adaptive multilayer CNN algorithm for the classification of sEMG patterns. They concluded that CNN surpassed the SVM in the non-adaptation as well as adaptation procedures and user-adaptation significant increased the classification accuracy as compared to non-adaptation. Geng et al. [98] developed a deep convolutional network and applied on all the three above mentioned databases for high density sEMG images. They confirmed that deep networks performed better than classical classifiers such as KNN, LDA, SVM, and Random Forests. Atzori et al. [1] used a transformed version of renowned CNN network called LeNet [30] and classify all the three Ninapro datasets including data of both healthy and amputee subjects. The input signals were RMS rectified and from results, it was found that CNN results were commensurable to other classical classifiers such as SVM, KNN

and LDA but was lower than the best classical classifier Random Forest. Du et al. [99] demonstrated a conventional HD sEMG database and proposed a deep domain adaptation configuration based multilayer CNN. They conducted both the intra and inter-session/subject analysis to show the outperformed behavior of adaptation based deep domain configuration over all other classical classifiers. Zhai et al. [92] proposed a CNN based self-resetting classifier that could update over-time with the previously used testing data. They evaluated the performance of the proposed algorithm over 40 intact and 11 amputee subjects from Ninapro database and concluded that it remarkably surpassed the SVM classifier. Du et al. [99] developed a CNN based semi-supervised learning algorithm for unlabeled data. Further information about hand postures and temporal orders of sEMG framework was learnt using data glove. They demonstrated considerable improvement in the classification accuracy for all three databases. Wei et al. [99] designed a multi-stream CNN which was able to learn interconnection between different muscles. This network had the disintegration and fusion levels and was analyzed with three standard databases. They demonstrated results of this model using divide and conquer strategy which revealed that multi-stream CNN performed better than the simple CNN and Random forests classifier. Xia et al. [100] developed a hybrid CNN-RNN architecture for the first time to deliver the signals variability with time. Time frequency frames from sEMG signals were used as the input to this network. Data of eight subjects collected in six sessions were used for the evaluation of this architecture. Results showed that this architecture outperformed both the CNN and support vector regression (SVR). Allard et al. [101] conducted a real-time work on CNN based transfer learning. They recorded two different datasets of 18 and 17 subjects respectively using 8-channels Myo armband (Thalmic

Labs) to control a 6 DoF robotic arm. Their developed CNN acquired 97.8% accuracy for the classification of seven hand movements.

Up to now, deep learning-based algorithms for myoelectric control have shown promising results in comparison with classical machine learning algorithms. However, nothing can be said about their robustness in long-term assessment as all the above studies employed data recorded in limited time span with few sessions only and most of the above studied make use of hand-crafted features such as RMS and spectrograms. Furthermore, some of the above-mentioned networks are extended version from state of art CNN architectures and most of them consisted of multiple layers which increases their computational cost [98].

In this work, we aim to investigate the use of a single layer computationally efficient CNN that takes raw sEMG of eight channels as input data collected for 15 successive days with two sessions per day. Further, the performance of stacked sparse autoencoders (SSAE), an unsupervised deep learning technique, is evaluated with both custom-built features and raw EMG data. Intra-session, inter-session and inter-days analysis are conducted and results of both the CNN and SSAE are compared with conventional LDA.

5.4. MATERIALS AND METHODS

5.4.1. Subjects

Seven healthy subjects (4m, 3f age range 24 to 30 years, mean age 27.5 years) took part in the experiments. They had no previous record of suffering from musculoskeletal disorder or upper extremity. Right hands of the subjects were used for data recording. The experimental procedures were in conformity with the Declaration of Helsinki and validated by local ethical committee of Aalborg University (approval no: N-20160021). Subjects assisted voluntarily and supplied written informed agreement prior to the experimental procedures.

5.4.2. Recording hardware

Data was captured using the commercial Myo Armband (MYB) as shown in figure 5-1. MYB is developed by Thalamic Lab and has eight channels of dry electrodes with sampling frequency of 200 Hz. It is cheap, consumer-grade device with nine-axis inertial measurement unit (IMU) [101] and communicates wirelessly to PCs via Bluetooth. It is a non-invasive, more user friendly and time-saving device as compared to Ag-AgCl electrodes which requires skin preparation and careful electrode placement and hence consume much time [102, 103]. The low sampling frequency may be a disadvantage as it may have low signal to noise ratio (SNR) as compared to conventional system. However, a recent study [104] showed that there was no significant difference found between the classification accuracies of MYB and conventional Ag-AgCl electrodes system.

Figure 5-1: Myo Armband for EMG recording.

5.4.3. Experimental procedure

The protocol was designed such that each subject performed seven different movements (including rest). Ten repetitions of each movement were recorded in a single session. Data was

collected for successive fifteen days with two sessions per day with a gap of one hour. The position of MYB was marked to confirm its correct position for each session. Hand movements considered were close hand (CH), open hand (OH), wrist flexion (WF), wrist extension (WE), pronation (PRO), supination (SUP) and rest (RT). Movements are indicated in figure 5-2.
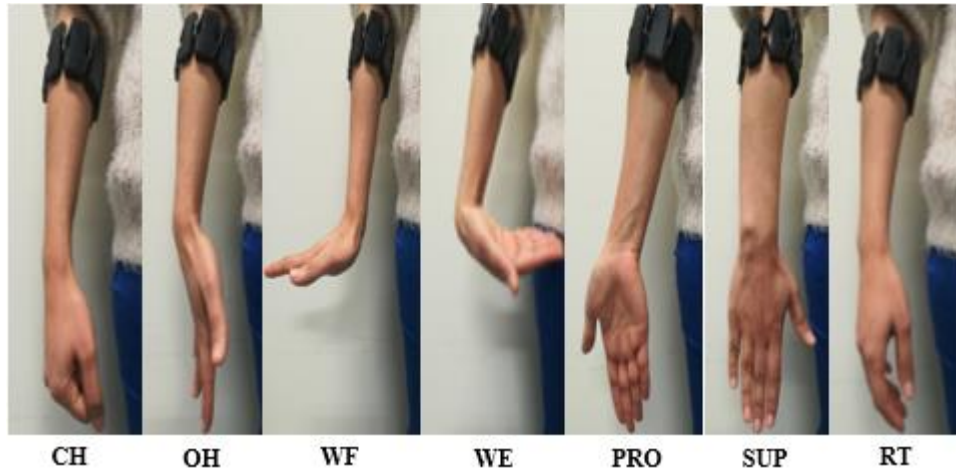
Figure 5-2: Seven types of hand movements using in this study

 Duration of contraction and relaxation of each movement repetition was 4 seconds each. The sequence of movements was kept random for each session. Figure 5-3 below shows six individual movements over eight channels of MYO.
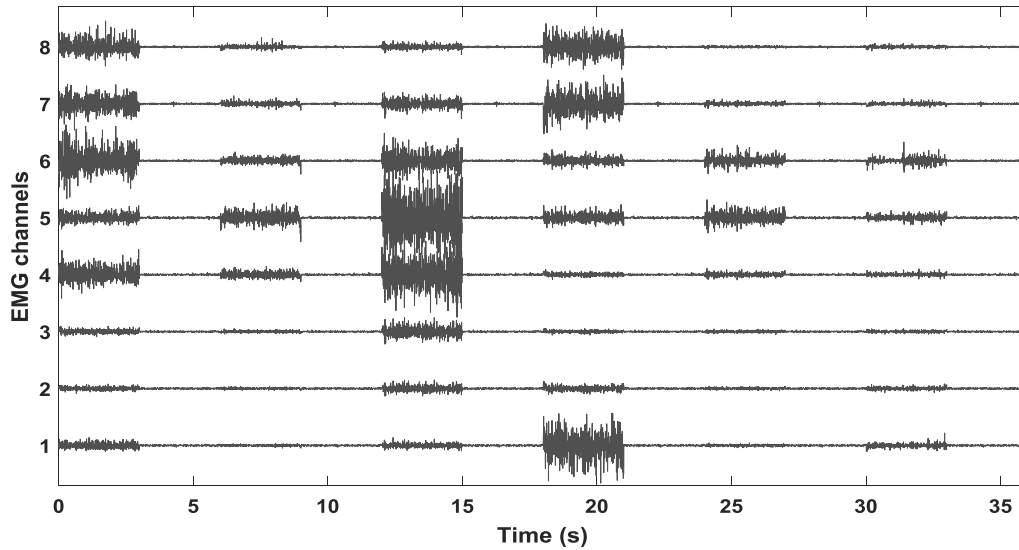
Figure 5-3: EMG data for one repetition from randomly selected session

EMG data for one repetition from randomly selected session. The first and last half second of each movement type was removed to avoid transition artifacts. Hence, it shows the 3 seconds of each movement with rest period of 3 seconds.

5.4.4. Signal processing

The movement outcomes were minimized by filtering the data with a 3rd order Butterworth high pass filter with cut-off frequency of 2 Hz. Overlapping windows of size 150 ms were used with increment step of 25ms. The inputs used for the classification by CNN and SSAE-r classifiers were raw windows whereas four time domain features i.e. mean absolute value (MAV), waveform length (WL), slope sign change (SSC), and zero crossing (ZC) [105] were used for the classification of data by using SSAE-f and LDA. The threshold value is set as zero while using SSC and ZC features [105].

Sections 2.5 and 2.6 describe SSAE and CNN in detail while for LDA, publicly available EMG library (MECLAB) [87] was used. To evaluate the short-term and long-term performance

output of classifiers, both within day and between days analysis are conducted for each subject to demonstrate results as mean of all subjects.

Within day analysis include within session with five-folds and between sessions with two-folds validation whereas between days analysis included two-fold validation (between pair of days) and k-fold cross-validations (k = 15 days). The between days analyses quantify the performance of classifiers when training data is increased to fourteen days.

5.4.5. Autoencoders

Autoencoders are unsupervised deep networks which use encoders to convert input signals to a new representation and use decoders to reconstruct them at the output. The parameters used to minimize the difference or error between the initial input and reconstructed input include L2 regularization (L2R), sparsity proportion (SP) and sparsity regularization (SR) and hence they ensure providing new optimized form of data (data driven features).
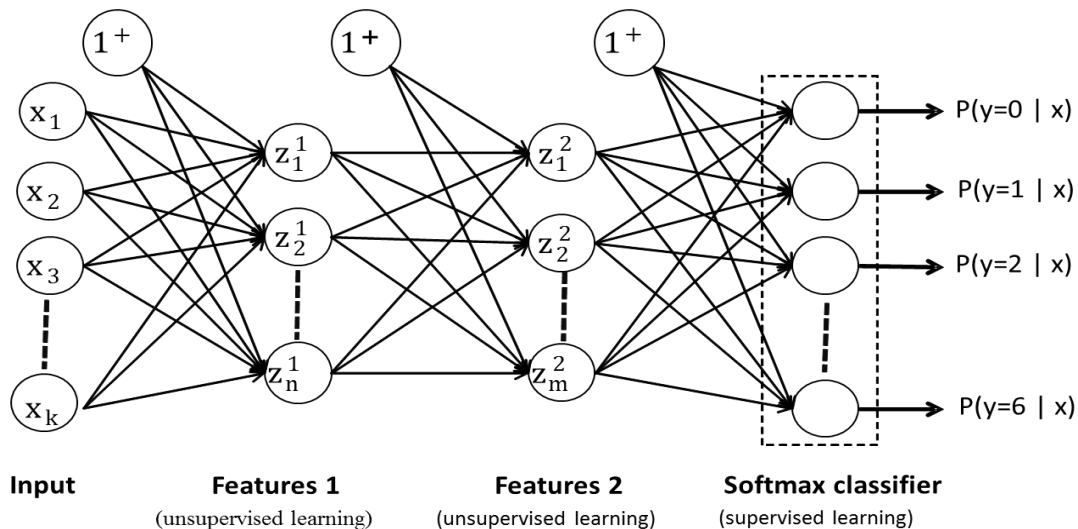
Figure 5-4: Generalized block diagram of autoencoders

Block diagram of SSAE. Features are learned un-supervisedly while classification is performed in supervised fashion. The length of both layers was adjusted accordingly to input length of SSAE-f and SSAE-r.

In this work, two-layers SSAE are used from the previous work as shown in Figure 5-4. Parameters were optimized, and the suitable size of layers for SSAE-f and SSAE-r was selected. For SSAE-f, the size of first and second layer was 32 and 16 units while for SSAE-r, it was 100 and 50 units, respectively.

5.4.6.   Convolutional neural networks

The CNN is the significant framework of deep learning and is the upgraded form of the standard neural networks. It is helpful in the analysis of data with multiple arrays such as signals, language and images. A convolutional layer uses filters which are convolved with the segments of input with specific size in such a way that a single filter contributes same leaning weights for all segments. An activation unit is applied to the dot product of filters with input segments. Pooling is used to reduce the size of the output.

This study deals with the implementation of a simple framework of CNN (as indicated in figure 5-5) using neural network toolbox in MATLAB 2017a. A bipolar raw EMG data with eight channels and 150ms size describes the input. Convolutional layer is comprised of 32 filters of size 3X3, a Relu layer and a max pooling layer of size 3X1, a fully connected layer and a softmax classification layer.

INPUT SIGNAL CONVOLUTION RELU POOLING FC SOFTMAX

30 X 8

32 @ 3 X 3

3 X 1

$P(y=0 \mid x)$

$P(y=1 \mid x)$

$P(y=2 \mid x)$

$P(y=6 \mid x)$

FEATURES LEARNING **CLASSIFICATION**
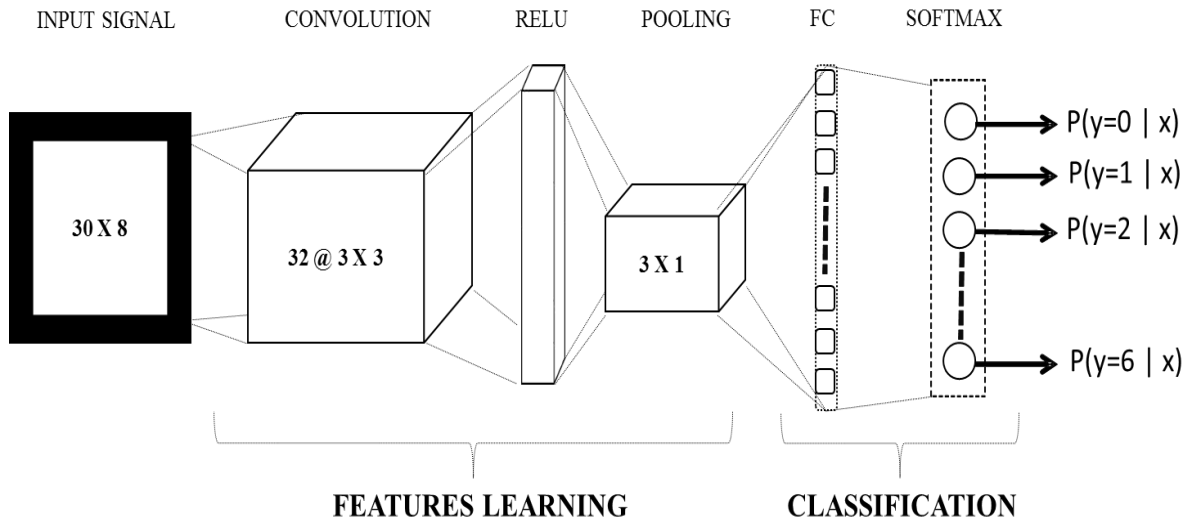
Figure 5-5: Block diagram of CNN used in this work

Block diagram of CNN used in this work. Input corresponds to 150 msec (30 samples) window of 8 channels. There were only single layers of Conv, Relu, pooling and fully connected (FC) layer. While Softmax was used for classification.

A stochastic approach, gradient descent with momentum, was used to train and test the network. After many testing trials, learning rate was fixed to 0.1, L2 regularization to 0.001, momentum to 0.95, batch size to 256 and max epochs of 25.

5.4.7. Statistical tests

Statistical tests were conducted to compare the performance of classifiers for all analyses, using two-way analysis of variance (ANOVA) with the help of two factors including the results attained from classifiers and number of days/sessions. The performance of individual classifiers was evaluated by conducting multiple comparison tests availing the stats from ANOVA and P values lower than 0.05 were estimated to be significant.

5.5.Results

5.5.1.   Within session

Five-fold cross validation was used to compute the classification errors (CE) of a single session and results of thirty sessions performed by an individual subject were averaged and final values of all seven subjects are demonstrated as mean CE. It is revealed in figure 5-6 and corresponding statistical test values are tabulated in table 5-1.
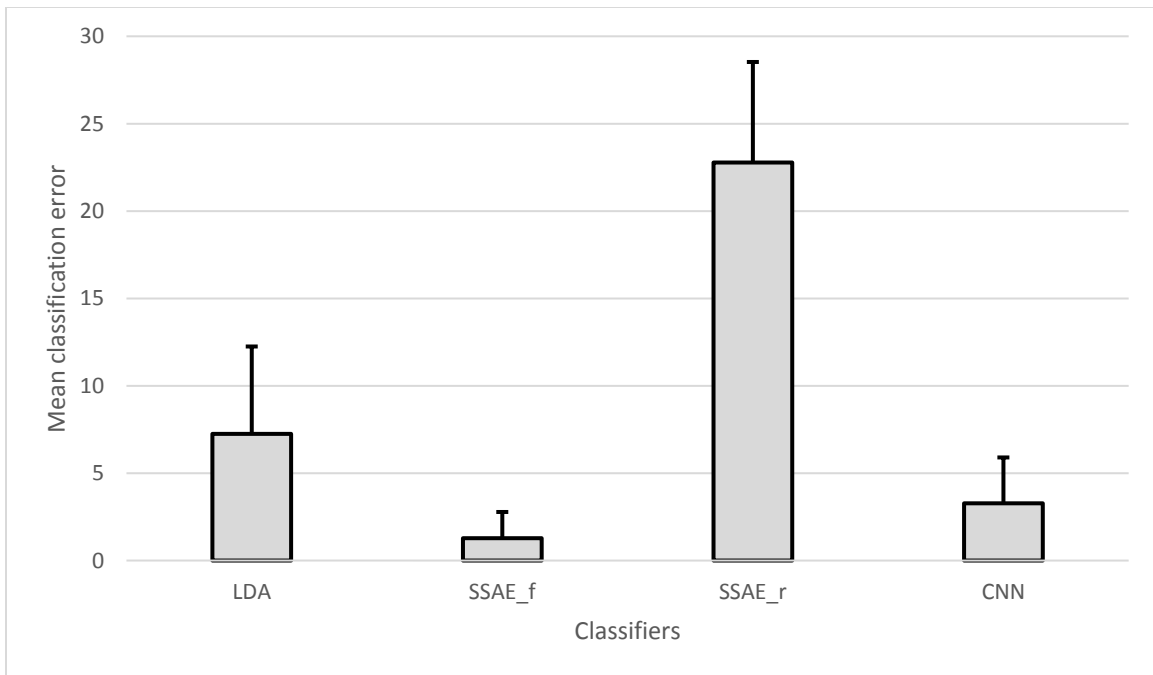
Figure 5-6: CNN, SSAE and LDA comparison for within session analysis

Mean (and SD) classification error of all classifiers for within session analysis with five-fold cross validation.

Table 5-1: statistical test for comparison of CNN, SSAE and LDA in the within session analysis

Classifier	Mean accuracy ± standard deviation		P value	Better classifier
	Classifier 1	Classifier 2		
LDA - SSAE_f	92.75 ± 5.00	98.72 ± 1.50	0.0000	SSAE_f
LDA - SSAE_r	92.75 ± 5.00	77.32 ± 5.75	0.0000	LDA
LDA - CNN	92.75 ± 5.00	96.63 ± 2.63	0.0000	CNN
SSAE_f - SSAE_r	98.72 ± 1.50	77.32 ± 5.75	0.0000	SSAE_f
SSAE_f - CNN	98.72 ± 1.50	96.63 ± 2.63	0.0000	SSAE_f
SSAE_r - CNN	77.32 ± 5.75	96.63 ± 2.63	0.0000	CNN

SSAE-f performed remarkably better (p<0.001) than all other classifiers while CNN performed remarkably better (p<0.001) than the rest of the two classifiers (LDA, SSAE-r).

5.5.2. Between session

This analysis was based on the two-fold cross-validation used between sessions which were finished on the same day. Therefore, results of fifteen days acquired from individual subjects were averaged and demonstrated as mean CE value of all seven subjects as evident from figure 5-7 and the corresponding statistical test values are tabulated in table 5-2.
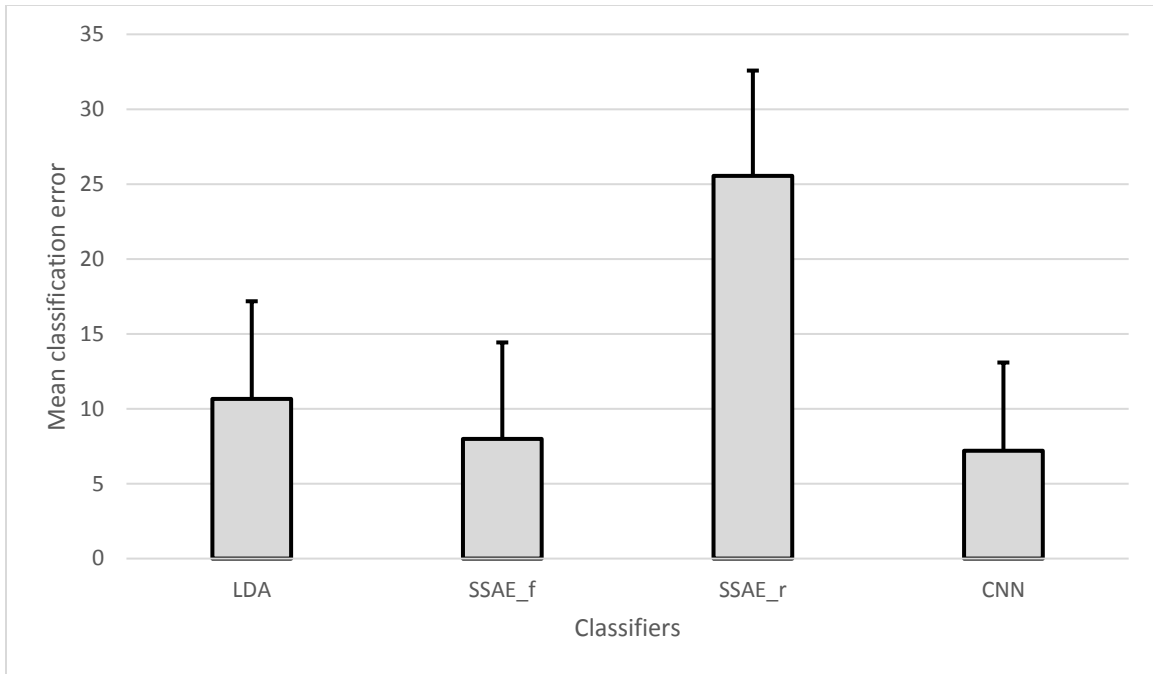
Figure 5-7: CNN, SSAE and LDA comparison for between sessions analysis

Mean (and SD) classification error of all classifiers for between sessions analysis with two-fold cross validation.

Table 5-2: statistical test for comparison of CNN, SSAE and LDA in the between sessions analysis

Classifier	Mean accuracy ± standard deviation		P value	Better classifier
	Classifier 1	Classifier 2		
LDA - SSAE_f	89.33 ± 6.51	92.00 ± 6.43	0.0000	SSAE_f
LDA - SSAE_r	89.33 ± 6.51	74.44 ± 7.02	0.0000	LDA
LDA - CNN	89.33 ± 6.51	92.80 ± 5.89	0.0000	CNN
SSAE_f - SSAE_r	92.00 ± 6.43	74.44 ± 7.02	0.0000	SSAE_f
SSAE_f - CNN	92.00 ± 6.43	92.80 ± 5.89	0.5383	No difference
SSAE_r - CNN	74.44 ± 7.02	92.80 ± 5.89	0.0000	CNN

There was no notable difference between the performance delivered by SSAE-f and CNN (p=0.538) while both of them showed remarkably better performance (p<0.001) than LDA and SSAE_r (worst).

5.5.3. Analysis between pairs of days

Fifteen day's data of an individual subject was arranged into 105 distinct pair of days. Two-fold cross validation was applied to each pair and average value for the results of all seven subjects was calculated. The results are tabulated in table 5-3 and 5-4. The averaged classification errors and corresponding statistical test values are shown in figure 5-8 and table 5-5.

Table 5-3: ANOVA test for performance comparison with raw bipolar EMG data using CNN vs SSAE-r. The upper diagonals show the CE with CNN for corresponding pair of day while the lower diagonal is for SSAE-r.

Days	01	02	03	04	05	06	07	08	09	10	11	12	13	14	15
01	-	5.8	10.25	13.41	13	11.54	12.32	11.82	13.11	11.85	12.5	12.65	12.95	12.87	14.98
02	22.71	-	8.16	11.42	9.87	8.97	9.35	8.9	9.76	9.14	9.61	10.48	11.17	10.58	12.13
03	26.17	22.89	-	8.97	7.54	8.71	8.24	7.81	9.26	9.91	9.97	11.33	11.7	12	14.33
04	29.43	25.05	23.73	-	8.03	11.44	10.59	8.48	8.12	10.88	10.55	12.07	10.47	12.51	12.75
05	27.93	23.53	21.95	22.32	-	7.9	7.63	7.33	8.4	7.26	8.1	8.83	10.73	12.54	13.46
06	29.55	24.54	24.29	25.48	21.7	-	8.92	8.62	9.12	9.44	10.08	10.47	12.93	12.71	13.65
07	29.11	24.52	24.5	25.12	21.88	23.26	-	6.12	8.84	8.79	8.92	10.08	10.51	11.77	13.07
08	27.49	22.76	22.94	23.75	20.53	22.34	20.34	-	5.6	7.23	7.73	8.66	8.33	10.5	10.77
09	33.03	25.6	27.55	24.31	25.2	25.09	24.58	20.49	-	7.52	9.09	8.29	7.75	9.84	10.11
10	30.51	26.29	27.5	28.19	23.82	24.66	24.93	20.68	22.45	-	6.22	6.4	7.33	9.5	9.01
11	28.74	24.54	25.82	26.26	22.34	25.06	23.82	20.78	23.25	20.28	-	6.89	7.02	7.77	8.97
12	29.53	25.82	27.16	27.18	23.07	24.76	24.11	21.6	22.99	20.5	20.58	-	6.92	8.66	8.6
13	30.97	27.91	29.53	27.73	27.01	29.8	27.64	23.27	23.38	21.97	21.06	21.76	-	7.69	8.25
14	31.07	27.71	28.59	27.74	26.91	27.94	25.91	22.71	24.14	22.6	21.45	22.24	19.61	-	6.19
15	34.4	30.3	32.53	30.32	29.27	30.5	29.94	25.46	25.14	23.41	23.85	23.51	21.36	19.46	-

Table 5-4: ANOVA test for performance comparison with features using SSAE-f vs LDA. The upper diagonals show the CE with SSAE-f for corresponding pair of day while the lower diagonal is for LDA.

Days	01	02	03	04	05	06	07	08	09	10	11	12	13	14	15
01	-	6.77	11.54	15.28	13.68	13.08	13.97	13.01	15.55	14.27	14.51	15.31	15.52	18.19	17.95
02	9.93	-	8.57	13.02	10.51	10.26	10.07	9.08	10.55	9.88	10.34	11.12	11.29	13.81	14.24
03	14.04	11.49	-	9.32	8.37	10.07	8.71	8.18	10.5	10.31	10.7	12.49	12.45	14.73	17.04
04	16.97	14.47	13.84	-	9.18	12.29	11.91	9.41	9.96	12.18	11.05	13.2	11.83	15.45	16.36
05	16.25	13.85	12.49	12.3	-	7.81	8.24	7.15	9.27	7.54	8.66	9.91	11.52	15.31	16.76
06	16.85	13.49	14.54	15.71	12.36	-	8.78	8.77	10.14	10.01	10.54	11.48	14.45	14.05	15.3
07	15.57	12.79	13.08	14.54	12.33	12.89	-	6.63	9.09	8.36	8.88	10.13	11.45	13.32	14.29
08	15.66	12.85	12.78	13.43	11.9	13.34	11.14	-	6.54	7.25	8.04	8.69	8.55	12.35	12.68
09	18.79	14.83	15.68	13.95	13.67	14.68	13.24	10.34	-	7.64	9.41	9.29	9.33	11.47	11.8
10	18.66	15.47	15.83	16.72	12.87	14.49	12.99	11.32	12.79	-	6.9	6.9	9.26	11.14	10.68
11	17.57	15.03	15.79	15.43	13.4	15.3	12.72	11.82	12.49	11.28	-	7.62	7.84	9.28	10.85
12	16.91	15.34	16.91	16.51	13.51	15.54	12.66	11.8	12.38	11.11	10.57	-	7.89	10.22	10.27
13	19.07	16.83	17.77	17.48	16.67	18.45	15.55	13.35	13.53	13.91	11.77	11.54	-	9.44	8.85
14	20.02	16.95	17.79	17.73	17.09	17.98	15.8	15.1	14.53	16.05	12.41	13.41	12.17	-	7.37
15	21.29	18.94	20.85	19.21	19.39	19.73	17.68	15.39	15.32	15.56	13	13.36	12.46	10.16	-
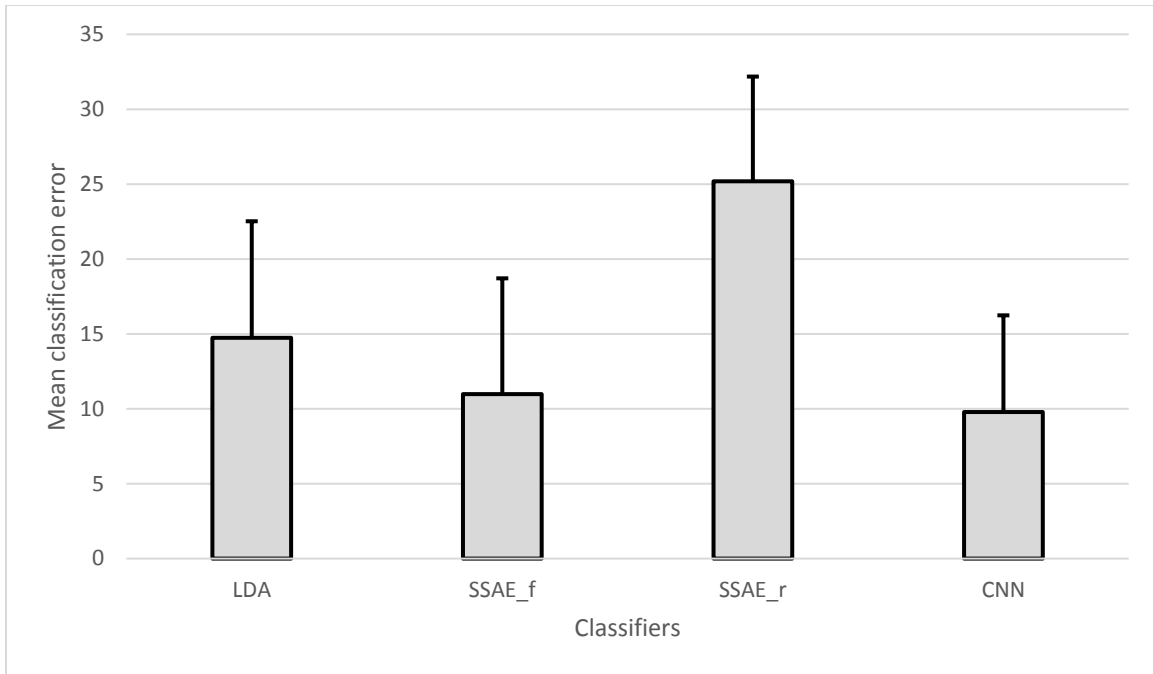
Figure 5-8: Mean (and SD) classification error of all classifiers for between pair of days analysis with two-fold cross validation

Table 5-5: Two-way ANOVA test for between pair of days analysis

Classifier	Mean accuracy ± standard deviation		P value	Better classifier
	Classifier 1	Classifier 2		
LDA - SSAE_f	85.27 ± 7.79	89.02 ± 7.73	0.0000	SSAE_f
LDA - SSAE_r	85.27 ± 7.79	74.82 ± 7.00	0.0000	SSAE_f
LDA - CNN	85.27 ± 7.79	90.21 ± 6.45	0.0000	CNN
SSAE_f - SSAE_r	89.02 ± 7.73	74.82 ± 7.00	0.0000	SSAE_f
SSAE_f - CNN	89.02 ± 7.73	90.21 ± 6.45	0.0002	CNN
SSAE_r - CNN	74.82 ± 7.00	90.21 ± 6.45	0.0000	CNN

LDA, SSAE-f, SSAE-r and CNN attained mean CE ± standard deviation of 14.73 ± 7.79, 10.98 ± 7.73, 25.18 ± 7.00 and 9.79 ± 6.45 respectively. It was evident from the statistical test results

that CNN surpassed (p<0.001) all other classifiers while SSAE-f performed better than (p<0.001) remaining two classifiers.

5.5.4.   K-fold validation between days

This analysis was based on considering a separate fold for each day for which fifteen-fold cross validation technique was applied. Results are shown as mean CE value of all seven subjects as indicated in figure 5-8 and corresponding statistical test is tabulated in table 5-6.
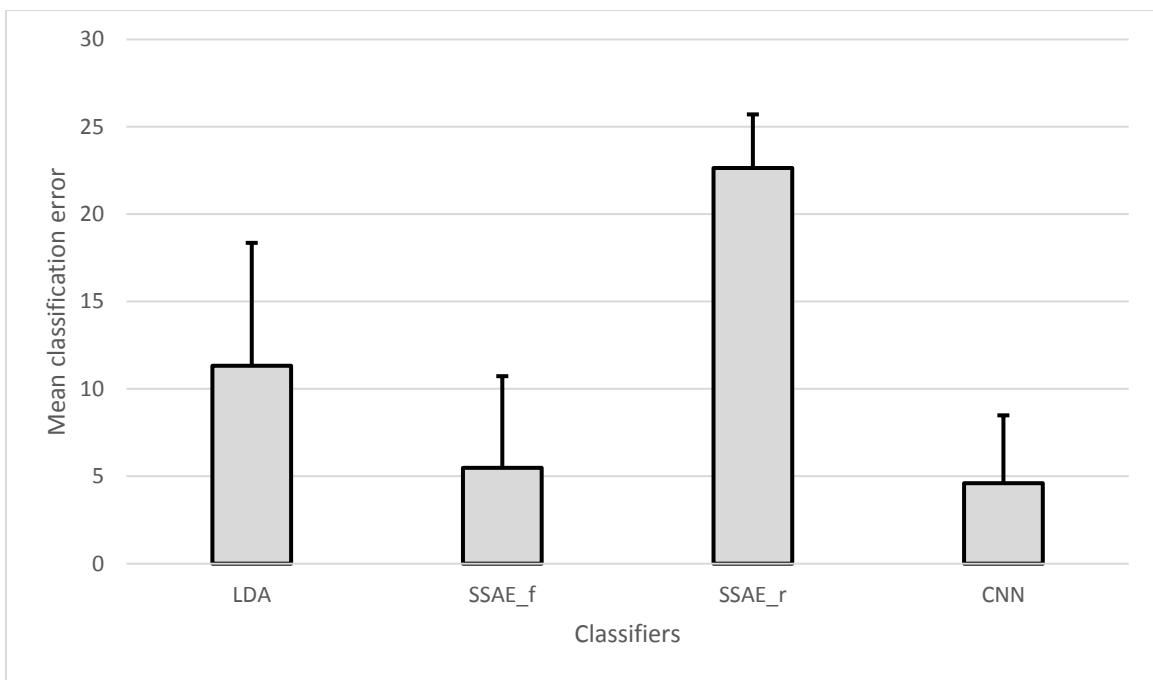
Figure 5-9: Mean (and SD) classification error of all classifiers for between days analysis with fifteen-fold cross validation

Table 5-6: Two-way ANOVA test for K-fold validation analysis

Classifier	Mean accuracy ± standard deviation		P value	Better classifier
	Classifier 1	Classifier 2		
LDA - SSAE_f	88.67 ± 7.03	94.51 ± 5.24	0.0000	SSAE_f
LDA - SSAE_r	88.67 ± 7.03	77.36 ± 3.07	0.0000	LDA
LDA - CNN	88.67 ± 7.03	95.39 ± 3.88	0.0000	CNN
SSAE_f - SSAE_r	94.51 ± 5.24	77.36 ± 3.07	0.0000	SSAE_f
SSAE_f - CNN	94.51 ± 5.24	95.39 ± 3.88	0.2199	No difference
SSAE_r - CNN	77.36 ± 3.07	95.39 ± 3.88	0.0000	CNN

In spite of the fact that CNN acquired relatively low error rate than SSAE-f, still no notable difference (p=0.219) was found between them and results of both were considerably better (p<0.001) than SSAE-r and LDA.

5.6. DISCUSSION

In recent years, several studies showed that deep learning techniques are helpful for myoelectrical control methods. Nevertheless, most of these studies are completed on datasets that were recorded in single sessions (short-term) and hence their usability remains limited. Therefore, the focus of this study was to evaluate the deep learning techniques (both with features and raw data) to find possible breakthrough in long term evaluation of myoelectric control schemes with main focus on raw EMG as input to the classifier.

The main realization for deep learning applied to CNN architecture is that raw EMG is preferable for better results. Unsatisfactory performance was achieved when computed with

SSAE without being affected by the size of the layers. For SSAE, handcrafted features are equally important as classical machine learning such as LDA.

Deep learning methods (CNN, SSAE-f) applied during different analysis declared that they showed better performance than the state-of-art LDA in both short duration and over multiple days and thus the fact was obvious from the results that deep networks improved their performance when training size was increased [106]. We believe that increasing the number of days (> 15) will converge the results of the k-fold analysis towards within sessions CE.

This study deals with both the handcrafted and data-driven features-based methods. Classical machine learning approaches with the use of handcrafted features have been extensively investigated for EMG based movement classification and several studies revealed that LDA has emerged as preferred classifier [85, 87, 107]. However, in this study, it was found that CE with LDA were comparatively higher than with autoencoders even in case of within session analysis and its performance degrades further over days. CNN, with the use of data driven features, revealed outstanding results as compared to autoencoders. In spite of the fact that autoencoders gave generalized results with handcrafted features, they failed to generalize while using raw data. It was found that results of deep learning approaches depend genuinely on network framework and suitable parameters selection.

For SSAE-f, number of units was adjusted in both layers in such a way that performance was not improved considerably with increase in the number of units but decreasing units decreased the performance. In the same way, optimal performance was observed when non-linear activation functions were used for encoders and linear for decoders. Error at layer 1 and 2 were affected by SR and L2R respectively. The size and number of filters for CNN were also increased also but no improvement was observed in the performance and it just increased the

computational cost, most probably due to small sample size and the low complexity level of the classification problem. Results were examined with different number of epochs. Initial learning rate and momentum played vital role as tuning parameters. Nevertheless, varying L2R did not disturb the performance.

Classifiers were trained on system having NVIDIA Quadro k620 GPU, 2.40 GHz processor and 256 GB of RAM. Training and testing time taken by CNN is 13.10, 15.63, 32.43 and 467 secs for within session, between sessions, pair of days and between days analysis, respectively while SSAE-f took 23.44, 26.13, 48.42 and 607.95 secs respectively. SSAE-f acquired higher accuracy than CNN only in case of within session analysis while CNN gained higher accuracies in the remaining three analyses. Hence, CNN was observed as more robust than SSAE-f and has high computational efficiency.

Previous CNN based myoelectric control studies either used spectrogram of EMG [92, 100, 101], normalized EMG [99], grayscale image [0,1] of EMG [98] or RMS rectified EMG [1] as input to models. However, the proposed CNN model used bipolar raw sEMG as input and hence the model is clinically more appealing.

Findings of current study suggests that deep learning approaches are bright for myoelectric control of upper limb prosthesis not only in short-term but long-term also. The limitation of this study is the limited number of healthy subjects without any amputee subject and it was only offline study. However, future studies will consider investigating optimizing parameters and online tests with both healthy and amputee subjects and to evaluate the robustness of deep learning techniques in real time.

5.6.1. CONCLUSION

Deep learning approaches proved to have the better results as compared to classical machine learning algorithm using both the hand-crafted features and raw EMG signals. CNN showed the ability to identify EMG patterns even from raw unprocessed data as evident from the results of intra/inter-sessions and between days and thus eliminating the fuss of feature selection.

Chapter 6.   Discussion

6.1. Introduction

As discussed in the introduction chapter, two different studies were performed in this dissertation. The main objectives of study one was 1) to evaluate the performance of stacked sparse autoencoders in comparison with classical machine learning technique 2) compare the performance of both surface and intramuscular EMG data recorded over multiples days using both healthy and amputee subjects and 3) evaluate the performance with combined surface and intramuscular EMG. The objective of study two were to explore the performance of convolutional neural networks for myoelectric control and compare the performance of data driven features (deep features) with engineered feature.

This chapter discusses the outcomes and main findings after evaluating all these objectives.

6.2. Summary of main findings

6.2.1.   Evaluation of stacked sparse autoencoders for improved myoelectric control

Autoencoders as emerging architecture of deep networks, are being successfully utilized in EEG, ECG and other medical signals related studies, but it is less utilized in EMG signals and till date it's the first study that utilized its application for myoelectric control. Its performance is being compared with state of the art LDA that was specially developed by chan and Green [87] in order to provide benchmark for comparison of classifiers in improving myoelectric control schemes. Data was collected from ten able-bodied and six amputee subjects using six surfaces and six intramuscular electrodes that were placed in pronator and supinator muscles. It was evaluated using offline performance matric.

It was found that SSAE with a simple architecture (shown in figure 2-3) significantly outperformed the LDA using both the sEMG and imEMG data of able-bodied and amputee subjects (results of chapter 3 and 4) in all the within day, between pair of days and between days analysis. During its optimization process, number of hidden units in both layers were chosen after several random trails and it was observed that increasing half the number of hidden unit did not significantly reduce the error. However, decreasing to half of the units increased the error significantly. For both of the layers, the use of non-linear activation functions for encoders and linear for decoders was helpful in achieving better performance. Apart from the framework, it was observed during training the data that error in the individual layer was minimized with the influence of some parameters of that specific layer. Greedy layer-wise training approach was used for training the layers, in which each layer is trained independent of the other layer. At layer 1, MSE was dependent on lower values of SR while almost independent of L2R and further, it was minimum at lower values of SP. At layer 2, the effect of L2R was opposite to that of layer 1 and MSE was strongly dependent on lower values of it. Along with optimal value of L2R, error was minimum with lower and middle values of SR and SP respectively.

SSAE remarkably surpassed the standard LDA classifier in all the three analyses including within day, between pair of days (training data also included data from previous day) and between days (training and testing was performed on separate days) analysis. SSAE achieved almost similar error rates for both within day and between pair of days analysis unlike LDA where classification error was significantly higher. Hence unlike classical machine learning algorithm, SSAE generalizes well with the data from previous days.

In the 2nd study (chapter 5), SSAE was trained with both the engineered (SSAE-f) and deep features extracted from raw data (SSAE-r). The main observation regarding SSAE was that it performs well with engineered features (SSAE-f) however it failed to generalize with raw data (SSAE-r). SSAE-f repeated the same performance for all analysis including within and between session, between pair of days and K-fold validation (k=15) analysis and significantly outperformed state of the art LDA classifier.

6.2.2. Evaluation of surface vs Intramuscular EMG for improved myoelectric control

Surface sEMG is most commonly used in literature on myoelectric control. Electrodes are placed over the muscles non-invasively and hence it represents the global information (information from surroundings) While intramuscular iEMG (acquired through needle electrodes) provides more specific information from targeted muscles and hence, it has been emerged as an approach that may remove some of the drawbacks associated with non-invasive systems [62]. Several studies [63-66] compared the individual performance of sEMG and iEMG for classification of hand and wrist movements and obtained almost similar results or sEMG performed better than iEMG. However, the results of all these previous studies are based on the data of healthy individuals recorded in a single session. In study one, we have compared the performance of sEMG vs iEMG for the data of both healthy and amputee subjects for multiple sessions (seven sessions recorded with a gap of one day each) and performed different analysis including within day, between pair of days and between days analysis.

Using classical machine learning algorithm (LDA), sEMG significantly outperformed iEMG in all the analyses including within session and between days. While with SSAE, no notable

was difference found between two data types for within session analysis. However, classification error reduced significantly with sEMG as compared to iEMG for between days' analyses. Hence unlike iEMG, sEMG patterns proved to be more consistent and repetitive over multiple days.

6.2.3. Evaluation of combined surface and intramuscular EMG for improved myoelectric control

In the previous objective of this study, we found that in long-term assessment, surface EMG proved to be more favorable then iEMG for myoelectric control. Furthermore, Kamavuako et al. [47] demonstrated that the classification accuracy of a myoelectric control system with combined surface and intramuscular EMG was superior to sEMG alone. However, this study was performed in single session and with only able-bodied subjects and hence nothing can be said about performance of combined EMG in long term and for amputee subjects.

In this study, we evaluated the performance of combined EMG for the data of both able-bodied and amputee subjects recorded in seven sessions with a gap of 24 hrs. In both the within session and between session analysis, it was found that combined EMG significantly outperformed the sEMG with both the SSAE and LDA. Furthermore, combined EMG achieved comparatively similar error rates in within and between session analysis while this difference was quite higher for sEMG alone. Hence combined EMG proved to be more robust and it has the strength to generalize more than sEMG. sEMG data also showed promising results when used alone but the higher performance of combined data is due to the reason that EMG recorded from deep pronator and supinator muscles through fine-wire and needle electrodes are less contaminated by crosswalks and hence could improve performance as compared to sEMG alone which

suffers from many artifacts like electrode-skin interface and crosstalk from surrounding muscles etc.

6.2.4. Demonstrating the feasibility of using raw EMG with convolutional neural networks

In recent two years, several studies have explored the application of CNN for classification of hand movement for myoelectric control. Although these studies showed promising results for improvement of myoelectric control schemes but most of these studies were performed on datasets that were collected in single session and many of the developed algorithms either used RMS value of EMG or gray scale image as input to CNN. hence its performance in long-term and feasibility of raw EMG for classification is still not explored. In chapter 5 of this dissertation, we addressed these questions. Data of seven subjects was collected for consecutive fifteen days with two sessions per day (with gap of one hour). SSAE-f and LDA were explored with engineered features while CNN and SSAE-r were explored with raw data as input. Analyses including within session, between sessions on same day, between pair of days and K-fold cross validation (k= no of days) were performed.

Results of these analyses showed that deep learning techniques (CNN, SSAE-f) revealed better performance than LDA in both short duration and for multiple days sessions and therefore it was confirmed from the results that increase in the number of training examples improves the performance of deep network.

Classical machine learning approaches with engineered (handcrafted) features have been extensively used for EMG based movement classification and several studies revealed that LDA [85, 87, 107] has emerged as optimal classifier. However, in this study, it was found that

CE with LDA was comparatively higher than with autoencoders even in within session analysis and its performance degrades further over days.

On the other hand, CNN with data-driven features obtained amazing results as compared to autoencoders. Although, autoencoders with handcrafted features gave generalized results but performed poorly to generalize while using raw data. It was found that performance of deep learning techniques was affected by the network architecture and selection of optimal parameters. For CNN, size and number of filters were increased also but performance did not improve, and it just increased the computational cost. Similarly, the number of epochs were also varied. Some tuning parameters including initial learning rate and momentum had an important role. Nevertheless, there was no effect of varying L2R on the performance.

Previous CNN based myocontrol studies either used spectrogram of EMG [92, 100, 101], normalized EMG [99], grayscale image [0,1] of EMG [98] or RMS rectified EMG [108] as input to models. However, the proposed CNN model used bipolar raw sEMG as input and hence the model is clinically more appealing.

6.3. Limitations and future direction

Although findings of chapter 3 and 4 (study one) are promising, but the analysis were performed offline and hence the generalization of autoencoders in real time needs to be investigated in future. Limited number of amputee subjects also limits the generalization of results. Moreover, database for this study included data of only seven days. Therefore, future studies will include more number of both able-bodied and amputee subjects and protocol will be made to include data collection over weeks.

Preliminary study based on exploring strength of raw EMG for classification of hand movement (chapter 5) proved that CNN could improve the field of myoelectric control and it

can eliminate some steps in conventional strategies that include the tough job of feature selection and extraction. We hypothesize in this study that training with data of fourteen days will converge error rates to that of within session analysis. Again, this study was also performed offline and with only seven able-bodied subjects which limits the generalization of results. Therefore, future studies will include data of amputee subjects also and data will be collected for a complete month with the hypothesis that cross validation with all days will surpass or equalize to that of within session analysis. CNN will also be explored in real-time application. In both the studies, analyses were limited to only intra-subject and hence inter-subjects' performance of these classifiers also needs to be explored. Further, these classifiers also need to be tested with simultaneous control strategies.

Chapter 7.　　Conclusion

In this dissertation, I have mainly explored the deep learning algorithms for possible improvement in myoelectric control schemes and evaluate the long-term performance with both the surface and intramuscular EMG data.

Performance comparison of surface and intramuscular EMG showed that there was no significant difference found between the two in short-term. However, surface EMG significantly outperformed the intramuscular in long-term and hence surface EMG patterns proved to be more consistent over days.

Deep learning algorithms are explored with both the hand-crafted and data-driven features. Using hand-crafted features, SSAE-f outperformed the LDA in both the short term and long-term analysis. However, SSAE-r failed to generalize with raw data (data-driven features). On the other hand, the proposed CNN model outperformed both the SSAE-r and LDA and showed the ability to identify EMG patterns even derived from raw bipolar EMG data (data driven features) for persisting classification regardless of the stochastic properties of the EMG signals. This is essential in alleviating the hassle of feature selection or signal modification for better classification and hence the proposed CNN model is clinically more appealing.

Chapter 8.   Appendices

8.1. Appendix A: Time Domain Features

In comparison to deep features, four-time domain features are used throughout this work. These features include, mean absolute value (MAV), waveform length (WL), zero crossing (ZC) and slope sign change (SSC). These features were proposed by Hudgins [34] and are defined below.

Mean Absolute Value:

The average computer calculated value of the absolute data of EMG signal is called mean absolute value. It is a well-known time domain feature for EMG controlled techniques and an easy method to identify the muscle contractions. This value is similar as the average rectified value denoting the area under the EMG signal after its rectification thus converting all negative values of the voltage to positive. It represents the amplitude of the EMG signal.

Mathematically, it can be defined as

$$MAV = \frac{1}{n} \sum_{I=1}^{n} |x(i)|$$

Where

n is the total number of data points in a selected window of length n

i is the ith point in the window.

Waveform Length:

Waveform length feature illustrates a measure of signal complexity. It defines the progressive length of the signal within the window selected for analysis.

Mathematically, it can be defined as

$$WL = \sum_{I=1}^{n} |x(i) - x(i-1)|$$

Where n and i are defined in MAV.

Slope Sign Change:

slope sign change feature determines the number of times the sign of the slope of signal waveform within an analysis window is changed. This feature also uses a threshold value in order to reduce counts induced by noise.

If three consecutive data points are given as X_{i-1}, X_i and X_{i+1}

Then it can be calculated as

$$(x_i - x_{i-1}) * (x_i - x_{i+1}) \geq threshold$$

In this work, threshold of zero was used as accordingly to Kamavuako et al [105] threshold value of zero seems to be good tradeoff between system performance and generalization.

Zero Crossing:

The point at which mathematical function alters its positive or negative sign in the graph of that function denoted by a zero value at the boundary of the axis is called zero crossing.

In EMG, this point shows how many times a signal passes through zero within an analysis window thus related to signal frequency. This feature uses a threshold value to minimize the number of low-level noise signals crossing through zero.

If two consecutive data points are given as X_i and X_{i+1}

Then according to [109], ZC can be incremented if

$$sgn(-x_i * x_{i+1}) \; and \; (|x_i - x_{i+1}|) \geq threshold)$$

Same threshold value was used as in SSC.

8.2.Appendix B: Intramuscular EMG for Myoelectric Control

Intramuscular EMG recording have several advantages over surface EMG. EMG signals from the deep muscles are severely attenuated at the electrode-skin interface while the imEMG contain more information as they are recoded from deep muscles. Further, imEMG has less crosstalk than sEMG [68].

Use of imEMG in myoelectric control started in 1968 [110] and researchers utilized different techniques for control of prosthetic hand with imEMG. Different control strategies for myoelectric control using imEMG are pattern recognition [65, 111], regression[47, 112] and proportional control[68] etc.

In 2013, Smith et al [65]compared the performance of sEMG with imEMG for simultaneous multiple degree of freedom (DOF) motions using pattern recognition technique. In one of their technique, they used the three classifiers to predict each of the 3 DOF motions including wrist rotation, wrist flexion/extention and hand open/close. It was analyzed that imEMG significantly reduce the error (p<0.01) for parallel configurations of classifiers as compared to that of sEMG. Their analysis was performed offline.

The same year, Kamavuako et al [111]performed a study to investigate the performance of imEMG for 2 DOF using Fitts' law approach by combining classification and proportional control to perform a real time task with user feedback. sEMG and imEMG signals were collected from nine healthy subjects and five performance matrices including throughput, path efficiency, average speed, overshoot and completion rate were used in order to compare the performance of both types of data. In their analysis, it was observed that imEMG performed much better than sEMG for path efficiency and overshoot. No significant difference was found for throughput and completion rate. While sEMG average speed was much better than imEMG.

In this study, it was concluded that imEMG has much potential ascontrol source for advance myoelectric prosthetic devices.

In 2014, smith et al compare the performance of two control schemes including parallel dual-site control and pattern recognition control in real time for simultaneous and proportional myoelectric control of multiple DOF. They used the approach of Fitt's law and it was found that parallel dual-site control performed much better than pattern recognition-based control (throughput increased by 25 %). Form their results, they concluded that parallel dual-site control can perform much better than other sequential myoelectric control schemes.

In 2015, Smith et al [112] evaluated the two regression based simultaneous control schemes for myoelectric control using imEMG. Data was recorded from two amputees and 16 healthy subjects and linear vs probability-weighted regression schemes were compared using Fitts' law approach. It was observed that amputee subjects showed much better performance using probability-weighted regression-based control scheme.

Different other studies are performed in order to compare the performance of imEMG with sEMG. From the results of these studies it is noticed that in some performance matrices, imEMG outperform the sEMG and vice versa. Hence these results suggest that imEMG has much potential to be used as control source for prosthetic devices.

8.3.Appendix C: Conference Paper

A Novel Approach for Classification of Hand Movements using Surface EMG Signals

C.1. ABSTRACT

Surface Electromyography (EMG) signals have many applications in different fields such as myoelectric control for prosthetic devices, human computer-interaction and clinical and biomedical applications. EMG signals recorded with the help of surface electrodes contain different kinds of noise such as electrode-skin interface and electromagnetic noise etc. Hence for myoelectric control, EMG signals must be properly preprocessed to achieve the accurate classification results. A novel classifier using Stacked sparse autoencoders (SSAEs) is presented in this paper which gives better myoelectric control. Data of six surface EMG channels is collected from the right or amputated hand of five healthy and two amputee subjects for two days. Performance of the classifier is evaluated using offline classification error and results achieved from SSAEs are compared with standard LDA. For within day analysis, SSAEs ($1.29 \pm 0.83\%$) surpassed LDA ($4.09 \pm 2.15\%$) with p value of 0.0018 for both healthy and amputee subjects. In between days' analysis, SSAEs surpassed ($P < 0.001$) LDA for both able-bodied and amputee subjects. These results clearly indicate that deep features of Autoencoders are helpful control source for refined myoelectric control systems and the performance can be remarkably improved as compared to classical machine learning algorithm.

C.2. BACKGROUND

Electromyographic signals are the electrical signals generated as a result of contraction of muscles which are controlled by nervous system [113]. Previous studies show that the analysis

of these signals is very useful for controlling the robotic hands. Either surface or needle electrodes are used to record these signals, also called surface electromyography (sEMG) and intramuscular (iEMG) respectively. The most widely used sEMG is the non-invasive [67] source helpful in the prosthetic control of upper limb disabilities [65]. Conversly, imEMG is an invasive method [64] which is more advantageous than sEMG because of little crosstalk and stable control signals from deep muscles [62, 64, 68]. But unlike sEMG, the problem with these signals is providing limited information at specific sites, as more detailed information about muscles can be gained using sEMG [69].

Different myoelectric control schemes have been introduced that utilize either surface or intramuscular EMG signals as control source [11, 70]. A control system for robotic hand may be either sequential or simultaneous in nature [11]. Large number of commercially available methods simply use encoded EMG signals recorded from one or few sites [66], but they don't ensure satisfactory control of movements of dexterous prosthetic hands, hence not reliable for wide range of hand positions [1, 71]. Surface EMG based pattern recognition methods [34, 72-74] have attained satisfactory results as good control techniques and related studies [47, 63-66] proved that either sEMG did well as compared to iEMG or both of them gave similar results. In these methods, features are extracted from raw EMG signals and they provide considerable useful information to assist many tasks of prosthetic hand.

 Classification accuracy of hand movements is very determining for the reason that a misclassification may lead to a mishap for the robotic hand's user [114]. Different classifiers including Artificial neural network (ANN), Linear discriminant analysis (ANN), support vector machine (SVM), self-organizing map (SOP) and fuzzy classifiers are doing well in signals classification [113]. Chen and Green [36] introduced LDA classifier which acts as a convention

for other developing algorithms. Autoencoders are being successfully applied in Electroencephalography [115, 116], Electrocardiography [117] and various other fields of biomedical signals processing [118-120] but its application in EMG is limited.

This study introduces two layers stacked sparse autoencoders (SSAEs) to investigate its effectiveness in improving myoelectric control. To reveal this, its performance is compared with LDA. For both the classifiers, sEMG data of five abled and two amputee subjects is used as control source. In sections 2, methodology of the work is explained and results are presented in section 3.

C.3. METHODOLOGY

C.3.1. Data collection and Experimental procedure

Five healthy and two transradial amputee subjects participated for the collection of data in this study. For experimentation, data was recorded using the right hand of all subjects except one amputee subject whose left hand was used. The whole experimentation process was followed in conformity with Declaration of Helsinki and was authorized by the ethical committee of Riphah International University. Six surface EMG channels were recorded from each healthy subject. In case of amputees, one subject had only five surface electrodes. Data was recorded with sampling frequency of 8000 Hz and was filtered with analogue bandpass filter of bandwidth 10-500 Hz. Data for eleven movements were recorded for two successive days and on a single day, four repetitions of each movement were completed with a contraction and relaxation time of five secs each. Movements included hand open, hand close, flex hand, extend hand, pronation, supination, side grip, fine grip, agree, pointer and rest. The total duration for each session was 400 secs and sequence of movements was randomized for each session.

C.3.2. Data Processing

Raw EMG signals are mostly polluted by various sources of noise which worsen the classification performance of classifier if used unprocessed. Therefore, after initial digital bandpass filtering with Butterworth 3rd order filter of bandwidth 20-500 Hz, power spectral density of the data was examined as indicated in figure 1. A noise of 50 Hz and its randomly distributed harmonics were observed in the signals for each subject. This noise was removed using a 3rd order configurable Butterworth bandstop filter to achieve better classification.
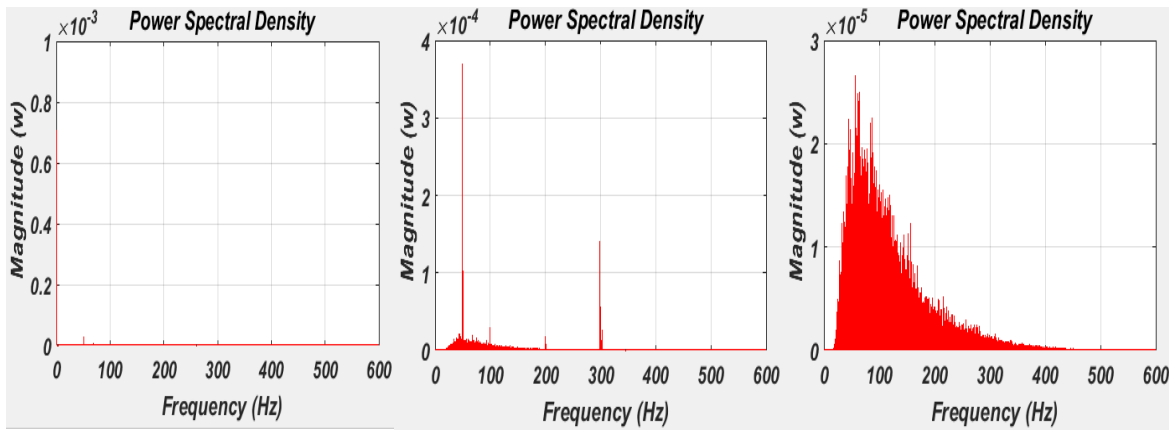
Figure C-1: It shows the application of configurable Butterworth filter to raw EMG data. left figure shows the raw EMG signal with motion artifacts. Central figure shows the result after bandpass filtering while right figure shows the EMG signal after noise removal with configurable Butterworth bandstop filter

After filtering, windows of 200 msec were chosen with window gap of 28.5 msec and four features including, waveform length (WL), zero crossing (ZC), slope sign change (SSC) and moving average value (MAV) were extracted from each window. For classification, both the autoencoders and LDA classifiers are used. Autoencoders used in this study contained two layers each with length of 24 and 12 units respectively. Parameters were tuned for both layers and were stacked with final softmax classifier layer. The network was properly processed before classification and its performance was examined with the standard LDA classifier which was introduced to provide convention for other emerging algorithms. Two types of analysis

including within day and between days' performance of classifiers were evaluated. For within day analysis, five-fold cross validation scheme was used while for between days' analysis, four-fold scheme was used. All these steps were applied in exactly the same way for both healthy and amputee subjects.

In order to evaluate the performance difference of two classifiers, Friedman's statistical test was used and p values less than 0.05 were considered significant.

C.4. Results

C.4.1. Within day Analysis

In this analysis, for an individual subject, data of a single day was randomly divided into five equal folds. Four folds were used for training the classifier and one-fold for testing. This was repeated five times and each time; a new fold was used for testing. Classification errors from each repetition were averaged for a single day and for an individual subject, classification error was calculated as mean of two days. Results are presented as mean of all five healthy and two amputee subjects separately and are shown in figure 2.
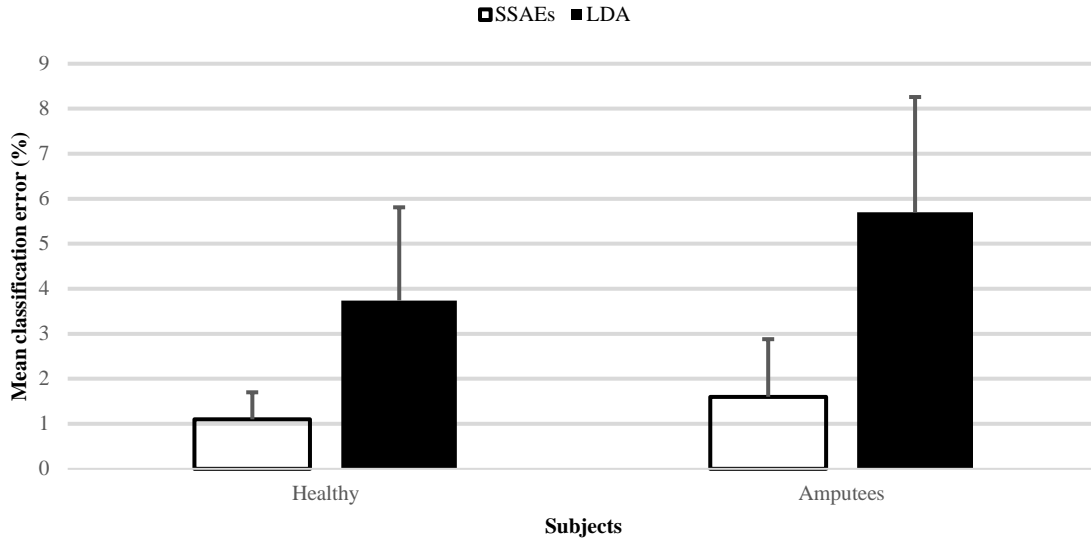
Figure C-2: Mean classification errors of within day analysis for both the healthy and amputee subjects obtained with both SSAEs and LDA. Bars represent the standard deviation between ten healthy and six amputee subjects' data.

To compare the performance of both kinds of data, statistical tests were conducted and P-values are tabulated in table1.

TABLE C-1: Friedman test for within day analysis. p values were calculated to quantify the difference of classifiers for both healthy and amputee subjects

Subjects	Mean accuracy ± standard deviation		P value
	SSAEs	*LDA*	
healthy	98.90 ± 0.60	96.26 ± 2.07	0.0017
amputee	98.40 ± 1.28	94.27 ± 2.56	0.0020

SSAEs achieved comparatively less error rates than LDA and outperformed it for both healthy and amputee subjects. As can be seen from table 1, there was a less error difference between the healthy and amputee subject's data using SSAEs while this difference was quite enough for LDA as compared to SSAEs with percentage points of 2.02. Hence, SSAEs significantly improved the performance for amputee subjects as compared to LDA.

C.4.2. Between days Analysis

In this analysis, data of two days was randomly divided into four equal folds. Three folds were used for training the classifier and one-fold was used for testing. It was repeated four times and each time a new fold was used for testing. Classification error for an individual subject are calculated as mean of four repetitions and overall results are presented as mean of all five healthy and two amputee subjects and are shown in figure 3.
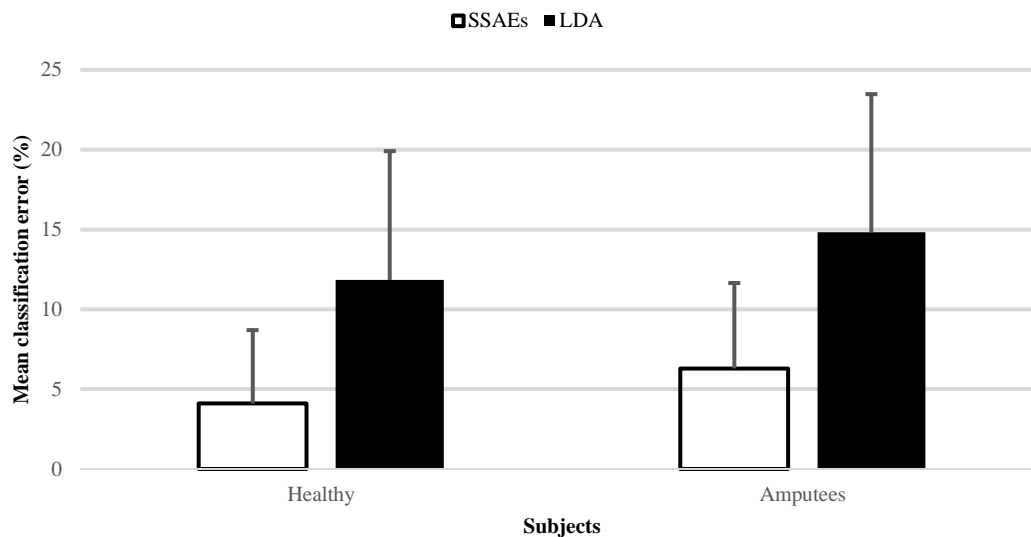
Figure C-3: Mean classification errors of Between days' analysis for both the healthy and amputee subjects obtained with both SSAEs and LDA. Bars represent the standard deviation between ten healthy and six amputee subjects' data.

Table C-2: Friedman test for between days' analysis. p values were calculated to quantify the difference of classifiers for both healthy and amputee subjects.

Subjects	Mean accuracy ± standard deviation		P value
	SSAEs	*LDA*	
healthy	95.90 ± 4.60	88.16 ± 8.07	2.53e-10
amputee	93.70 ± 5.35	85.17 ± 8.65	9.63e-07

As can be seen from table 2, SSAEs outperformed the LDA in between days' analysis for both the healthy and amputee subjects. There was a less variation between the error rates of both healthy and amputee subjects while this variation was almost double with LDA classifier as compared to SSAEs.

C.5. DISCUSSION

With the recent hype of Deep Learning approaches in the domains of natural language processing and computer vision [102], various such techniques have also been evaluated for biomedical signals such as Medical Image Processing, ECG and EEG. The motive of this research was to evaluate the performance of an emerging deep learning approach, SSAEs, for various hand movements' classification. For this purpose, results of SSAEs were compared with standard machine learning algorithm for two different methods of analysis by collecting sEMG data of five able bodied and two disabled subjects for two successive days.

In the within day analysis, the performance of SSAEs surpassed the LDA by showing p values of 0.0017 and 0.0020 for both healthy and disabled subjects respectively. Autoencoders revealed better performance for disabled subjects and acquired error rates close to that of able bodied subjects. On the other hand, LDA attained comparatively a high error rate with a difference of 2.02 percent between healthy and disabled subject's data.

For between day analysis, the results of SSAEs again surpassed the LDA with P<0.001 for the data of both healthy and disabled subjects. Classification with SSAEs and LDA indicated the percentage error difference of 2.20 and 3.0 respectively between the data of both healthy and disabled subjects. SSAEs acquired more accuracy for both within day and between day analysis for healthy subjects with percentage difference of 3.0 as compared to LDA which resulted in percentage difference of 8.10. In the same way, SSAEs and LDA concluded percentage points

difference of 4.70 and 9.08 respectively for disabled subjects. Thus autoencoders attained remarkable better performance in case of both healthy and disabled subjects and obtained more accuracy with decreased error rates for between days analysis as compared to LDA, hence proved to be more robust for advanced evaluation.

C.6. CONCLUSION

This study is based on the comparison of the classification accuracy of SSAEs (an emerging deep learning technique) with the standard machine learning algorithm for eleven hand movements. It was found that SSAEs performed remarkably superb in case of both the healthy and amputee subjects and its results were more satisfactory than LDA in both cases.

8.4.Appendix D: Database of 1st Study

This appendix discusses about the generalized protocol (D.1.), data labeling/ understanding (D.2.) and general preprocessing (D.3.) of data.
NOTE: Data and codes are available upon request.

D.1. GENERALIZED PROTOCOL FOR DATA COLLECTION:

Total Healthy subjects = 10

Total Amputee subjects = 6

Total recording channels = 12

Surface electrodes: Electrodes 1,2 and 3 are placed on extensors and 4,5 ,and 6 are placed on flexors muscles

Intramuscular electrodes: Six pair of wires were inserted. 7, 8 and 9 on extensors and 10,11 and 12 on flexors muscles

BIOPATREC SETTINGS:

Sampling Frequency: 8000

Number of Motions: 10

Number of repetitions: 4

Contraction Time: 5 seconds

Relaxing Time: 5 seconds

Mode of acquisition for surface: mono polar   HP Filter: 10 Hz   Lp Filter: 500Hz Gain: 5k

Mode of acquisition for intramuscular: Refer mono polar HP Filter: 100 Hz   Lp Filter: 4.4 KHz Gain: 5k

Figure D-1: Electrodes placements for healthy subject. Six surfaces and six intramuscular electrodes were placed on extensor and flexor muscles. Three of each electrode were placed in extensor and three in flexor muscles. In healthy subjects, all electrodes were placed on the right arm of subjects.

Figure D-2: Electrodes placements for Amputee subject. Again, the sequence of six surfaces and six intramuscular electrodes placement was same for amputees as for healthy subjects. However due to limit space for few of amputees, number of surface electrodes varied from 5-6 while number of intramuscular electrodes varied from 3-6. In amputee subjects, electrodes were placed on their effected hand.

D.2. DATA UNDERSTANDING AND LABELING:

This section provides the completing information about the data labeling which was performed due to time drifting found in the onset period of contraction

Basic understanding of Data:
- Sampling frequency is **Fs= 8000 Hz**.
- Data is recorded over 12 channels with 1st 6 channels for surface and last 6 channels for intramuscular EMG Data.
- Every subject performed ten different hand movements for 7 days.
- On an individual day, each movement was repeated 4 times with 5 sec contraction and 5 sec relaxation time. So, overall data of 40 secs was recorded for individual movement with 4 active and 4 resting chunks and hence with given sampling rate, a data of 40 sec contain 40*8000=**320000** samples. (active data chunks are highlighted in table)

Table D-1: 40 sec time distribution for a single movement with 4 contraction and 4 resting periods		
Time period	Samples range	8 chunks of 5 secs
0-5	1-40000	1st Contracting data chunk
5-10	40001-80000	1st resting chunk
10-15	80001-120000	2nd Contracting data chunk
15-20	120001-160000	2nd resting chunk
20-25	160001-200000	3rd Contracting data chunk
25-30	200001-240000	3rd resting chunk
30-35	240001-280000	4th Contracting data chunk
35-40	280001-320000	4th resting chunk

- **.mat** file for individual day of each subject is basically a **320000*12*10** matric
- 1st dimension of matric represent each movement with 4 active and 4 resting chunks
- 2nd dimension represent channel number
- 3rd dimension represent movement number

Data Labeling:
   Our goal is to extract the contraction or active data chunks (highlighted in table). From above table, samples range is clear for active data chunks but there was time drifting found in the onset of active period of data as shown in figure D-3. Therefore, labels are marked for individual chunks of all movements over all days and are presented in tables below (Healthy subject's tables and Amputee subject's tables).
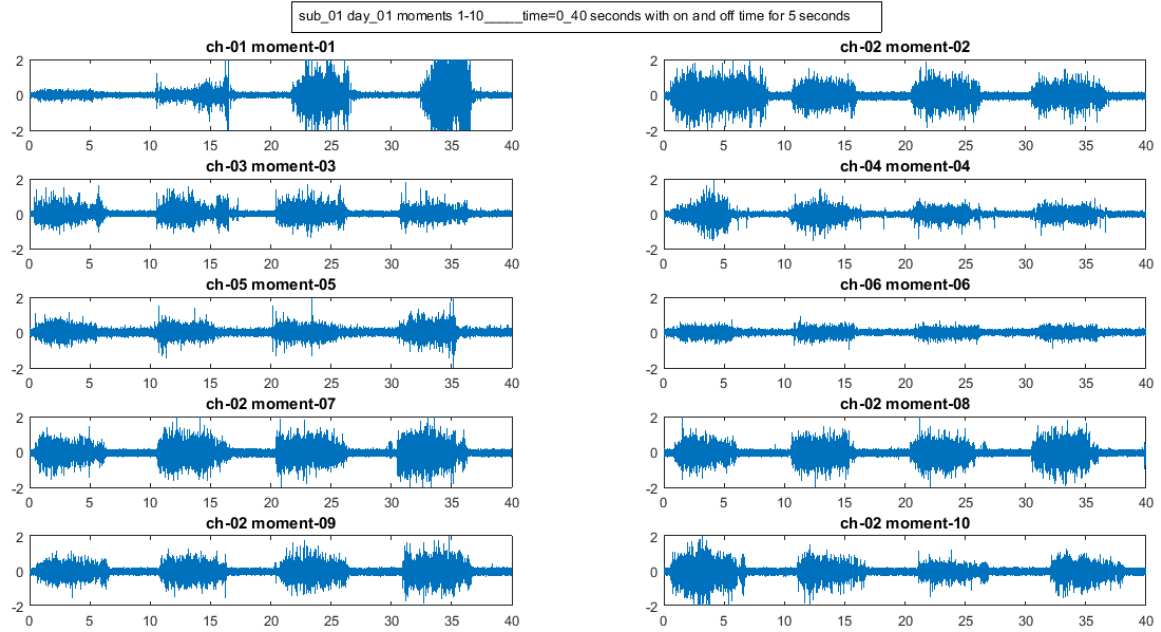
Figure D-3: Visualization of time drifting found in onset and offset of EMG signals.

Table notations are abbreviated as

M_ represent Movement no

C_ represent Chunk no

The number in individual cell represent the 1st active sample in data chunk (length of a chunk is 5*8000= 40000 samples)

Corresponding start time of each chunk can be calculated using formula

$$time(sec) = sample\ no \times \left(\frac{40}{320000}\right)$$

Healthy Subject's tables

Subject_01	Starting 'sample no' for all four chunks of each movement						
Movement		Day_1	Day_2	Day_3	Day_4	Day_5	Day_6	Day_7
M_1	C_1	3461	4854	10155	4309	4969	4130	4389
	C_2	83229	83961	85246	84208	95138	85801	83257
	C_3	165404	173323	165635	164303	192329	164816	163143
	C_4	246295	259458	243643	245007	279960	245851	252082
M_2	C_1	4971	8941	3405	7936	4389	7049	4337
	C_2	83424	85644	84348	85034	83457	87748	87630
	C_3	164663	165349	166875	167543	163617	167954	176469
	C_4	244651	244328	244588	245088	251720	249194	267059
M_3	C_1	5593	3077	4304	6002	2935	3796	4080
	C_2	83448	84860	87090	85466	84029	92933	83514
	C_3	166162	163848	169117	165736	164696	173505	172544
	C_4	244511	246422	251099	244586	248021	255112	250210
M_4	C_1	4399	4725	4100	6261	4240	5271	2425
	C_2	84484	83617	90981	84591	86409	83857	83158
	C_3	165013	163723	172428	163892	166399	164679	164311
	C_4	245240	244994	251443	243355	249626	244486	243120
M_5	C_1	3184	4109	4292	5332	5430	6294	4849
	C_2	88241	84090	84072	87602	86260	83734	92431
	C_3	167772	164202	167474	167011	166671	164225	170635
	C_4	250015	244292	243909	245202	246005	246606	255320
M_6	C_1	5084	6949	5212	5448	3863	4773	4259
	C_2	84407	87811	83485	86534	86582	83625	83959
	C_3	163870	167398	163858	163964	164745	163721	162995
	C_4	244912	248237	247218	243692	244408	245416	246313
M_7	C_1	4030	3920	3918	4679	3563	4215	5657
	C_2	83515	85538	84644	83913	84122	83366	83542
	C_3	164924	163600	163831	163776	164242	164902	163380
	C_4	243988	244473	250669	243705	244639	253969	243956
M_8	C_1	5151	7343	6415	3137	3309	6239	3076
	C_2	83772	84866	92562	85640	83549	84111	83388
	C_3	172794	163930	176237	170014	163540	163802	163578
	C_4	256689	244408	265364	250150	253975	244397	244102
M_9	C_1	4871	4968	4225	3700	3641	4135	4203
	C_2	84245	86796	83591	85056	83545	85393	83280
	C_3	163150	166981	173211	165725	163948	167395	171850
	C_4	244730	247409	251033	244253	245770	247062	255139
M_10	C_1	3815	4683	5893	4171	3828	5419	6076
	C_2	92352	89286	84868	83750	82715	87880	83168
	C_3	174199	169409	164606	165173	163540	168023	174197
	C_4	253945	257330	254976	246854	244476	245240	264498

Subject_02	Starting 'sample no' for all four chunks of each movement							
Movement		Day_1	Day_2	Day_3	Day_4	Day_5	Day_6	Day_7
M_1	C_1	4841	4809	9684	3642	5497	4396	3621
	C_2	84184	84570	90127	85199	84195	83854	85474
	C_3	166190	163087	170323	172745	165648	175252	165498
	C_4	247631	248754	254780	254376	244390	264720	244976
M_2	C_1	9075	6271	6707	5083	7101	8174	6842
	C_2	84150	90144	83211	83152	83215	83631	83129
	C_3	170452	169751	163547	163244	163415	164059	162837
	C_4	248400	253323	250873	244333	255931	243172	252250
M_3	C_1	6181	8648	3081	8358	4254	4076	3455
	C_2	83534	83345	81929	84815	84061	84680	83079
	C_3	167227	172757	163076	172312	162918	175609	173938
	C_4	248679	253014	246231	259190	244262	254886	256642
M_4	C_1	10179	4239	8622	7201	5903	4309	7061
	C_2	84395	84120	84179	83701	83363	83423	82979
	C_3	165173	165897	162983	163386	162961	163966	171710
	C_4	246121	247166	243772	243628	242487	245939	255121
M_5	C_1	3419	4200	6560	6961	4834	8272	11521
	C_2	92275	84178	85426	83770	83621	84094	83846
	C_3	169129	165211	169340	173923	164637	163868	172909
	C_4	251155	247250	260539	266051	243852	244807	257511
M_6	C_1	4140	8738	5687	3934	6169	5075	17608
	C_2	83709	84173	83104	84987	83829	89961	83818
	C_3	163878	170583	164718	165346	162936	169634	163676
	C_4	245809	244174	243288	254502	243356	250059	243403
M_7	C_1	4401	3743	3774	3643	5571	3058	2947
	C_2	86227	84490	83741	83268	82959	82749	83426
	C_3	168740	163580	164266	163847	165760	162811	162932
	C_4	243861	243773	235957	249409	245854	244288	243498
M_8	C_1	5536	4169	4575	4223	3493	4143	3658
	C_2	83806	88917	83934	88639	83578	83550	83299
	C_3	173618	168834	164208	169160	168826	163100	163012
	C_4	255584	257711	244002	248818	251012	243343	243209
M_9	C_1	5659	3101	3715	2633	4489	7959	4805
	C_2	82916	82952	83364	83170	83093	83252	82908
	C_3	167564	179603	163737	163236	163206	163178	173764
	C_4	248989	259446	251492	249495	244434	243494	260080
M_10	C_1	8111	4024	3157	5026	4559	4202	3446
	C_2	83973	82873	83367	91910	82999	83017	83123
	C_3	169526	163239	163529	171828	163136	164126	163715
	C_4	249370	242799	253233	250895	243097	243359	245733

Subject_03	Starting 'sample no' for all four chunks of each movement							
Movement		Day_1	Day_2	Day_3	Day_4	Day_5	Day_6	Day_7
M_1	**C_1**	4435	6065	6067	4857	8779	5788	13518
	C_2	86274	84372	84461	87315	92957	88142	95489
	C_3	163916	168428	169023	175589	175745	167832	173235
	C_4	245736	248125	249672	269906	255792	258403	255102
M_2	**C_1**	5706	6021	5812	3440	8915	7139	4742
	C_2	91777	83127	82833	90286	84767	82719	84162
	C_3	173946	164945	164897	172543	164413	163742	163249
	C_4	254118	254242	255711	252807	247559	243090	244159
M_3	**C_1**	6009	3710	3301	9302	6974	4105	3535
	C_2	88140	82744	83637	84026	85484	88705	96221
	C_3	165878	164175	165264	171930	163814	163265	169157
	C_4	248480	244410	244729	253608	245736	244623	249481
M_4	**C_1**	4641	3198	3541	8445	4520	4301	4232
	C_2	85571	84957	84710	85988	83811	85248	90798
	C_3	165111	164342	164329	176404	164803	171418	171952
	C_4	248874	251696	251872	257679	245249	250573	251817
M_5	**C_1**	6380	11772	13869	5826	6001	6368	7681
	C_2	85140	84349	84524	85319	84661	83213	86307
	C_3	165053	164131	164159	163811	165561	169995	172230
	C_4	246239	245007	245970	254492	247459	249220	252053
M_6	**C_1**	5190	4681	4996	3189	4853	4605	3695
	C_2	93107	81259	82523	84511	88376	84662	97974
	C_3	174267	162233	164480	162740	170187	164464	176017
	C_4	254806	243876	244671	246239	250452	243333	256750
M_7	**C_1**	5764	5191	5145	2804	5121	3155	5031
	C_2	85039	84812	84521	84011	84875	82485	85763
	C_3	165811	163268	163550	163112	165423	166358	165183
	C_4	245586	246642	248021	256393	244296	245156	251784
M_8	**C_1**	7568	5345	5957	1926	5640	26343	2915
	C_2	83775	89274	89310	91244	84513	84492	84405
	C_3	169703	178192	178531	172504	164188	174739	163795
	C_4	246018	267494	267803	266398	245646	262391	256957
M_9	**C_1**	5387	5910	5310	5231	4853	6404	5823
	C_2	85096	82952	83658	88568	84788	91444	84382
	C_3	165238	161427	163528	167172	165312	182569	163656
	C_4	245161	251314	251135	258959	251841	251786	243249
M_10	**C_1**	6282	6339	6617	4829	5249	4372	4635
	C_2	85380	82716	83097	91660	86627	84247	87488
	C_3	165352	163844	164008	163787	166112	163504	169064
	C_4	248191	248151	246680	250769	245166	244368	248867

Subject_04	Starting 'sample no' for all four chunks of each movement							
Movement		Day_1	Day_2	Day_3	Day_4	Day_5	Day_6	Day_7
M_1	C_1	3639	2976	3149	5207	2955	2434	1977
	C_2	88565	83096	85627	83570	84703	81743	83968
	C_3	168705	167659	166119	162862	178653	162054	163519
	C_4	258901	248441	256050	243648	247807	242619	244952
M_2	C_1	5373	4800	6496	3358	5093	3714	2720
	C_2	83837	82699	90846	86973	85904	83311	87974
	C_3	170095	163083	171613	166131	163047	163530	162589
	C_4	251404	248296	251369	247148	245988	246494	243598
M_3	C_1	4872	5557	5841	6083	6550	2576	2775
	C_2	83121	84920	84903	95441	90385	83599	83683
	C_3	170571	165638	161471	169215	165908	171522	163506
	C_4	248658	261878	246184	260440	250447	255687	242968
M_4	C_1	5915	2377	2440	4907	2561	3183	3124
	C_2	83080	81823	83539	83735	83505	83941	111160
	C_3	162245	174194	170242	163534	161756	163963	164008
	C_4	245291	254506	252463	244914	244027	243783	242748
M_5	C_1	2544	3414	10645	8093	4372	2492	2342
	C_2	82367	83510	82844	86210	86919	85140	81972
	C_3	164005	163560	162909	162981	165041	163174	181160
	C_4	243881	242477	246207	243683	250985	256423	261096
M_6	C_1	5307	2514	5213	4243	3169	2399	2834
	C_2	83422	91582	83346	91565	82447	87476	81001
	C_3	167831	182228	162911	173314	166243	162836	162270
	C_4	248481	263189	246792	250382	246152	248991	241568
M_7	C_1	4014	2496	2909	6943	4353	3841	3150
	C_2	83216	88598	83644	85694	86069	84108	82465
	C_3	163351	168072	163152	166590	168175	166842	163217
	C_4	243485	251099	242655	247645	249421	245309	251995
M_8	C_1	5192	2987	3733	3461	4974	2417	4608
	C_2	92388	91219	82981	85838	84541	82748	84100
	C_3	181850	176780	164785	162670	167764	163637	163344
	C_4	263126	257186	256204	243776	263042	244211	245441
M_9	C_1	2632	4127	2987	3929	3871	3600	2454
	C_2	88035	83399	83580	86620	84730	83246	84905
	C_3	167258	173124	162775	169220	163818	164253	162063
	C_4	248658	252428	248459	256388	272806	256737	245733
M_10	C_1	4403	19885	3851	3997	3279	6033	3371
	C_2	86436	92614	92781	83300	83174	90129	82833
	C_3	166925	174943	171645	165576	163688	170275	165594
	C_4	246999	253511	250554	244000	244498	250629	243611

Subject_05		Starting 'sample no' for all four chunks of each movement						
Movement		Day_1	Day_2	Day_3	Day_4	Day_5	Day_6	Day_7
M_1	C_1	4192	4287	4140	3441	5558	4306	5139
	C_2	83815	82949	82937	83961	85698	85447	85544
	C_3	165226	165566	164999	162209	167366	165689	168529
	C_4	244155	248552	248552	243321	244178	243722	249435
M_2	C_1	2577	5450	5740	3797	5218	5364	7574
	C_2	83787	84841	84848	86402	84935	86185	82740
	C_3	172237	166412	164559	163847	163936	163941	165875
	C_4	249936	245005	244985	250628	246319	244199	245644
M_3	C_1	2348	4808	4808	2954	3728	3500	6524
	C_2	83562	84695	83798	83380	84402	81821	83827
	C_3	163107	168293	168932	170915	165769	164603	167784
	C_4	244707	246359	246067	250855	244969	242494	250566
M_4	C_1	1726	2903	3149	3366	5031	8001	6792
	C_2	83396	81046	82098	85248	86047	85588	88817
	C_3	168312	162812	164587	168447	164375	168262	170172
	C_4	243509	244517	244517	251167	243845	252341	251791
M_5	C_1	2440	3658	3640	4300	7651	5143	5858
	C_2	81307	81811	80794	83565	83948	87297	85387
	C_3	164090	163882	163416	164628	164496	166571	169545
	C_4	243335	244421	244403	249788	248030	244147	252077
M_6	C_1	5428	5335	5653	4610	4610	6679	7474
	C_2	86372	89763	89763	85226	94062	90366	88311
	C_3	165183	167270	166946	164117	175546	168034	169655
	C_4	245065	249150	248081	250668	254597	250284	252450
M_7	C_1	5886	3716	2689	4651	6068	5666	4227
	C_2	82931	81340	80119	84636	85932	85826	87296
	C_3	165577	160534	160534	169029	164986	172910	164798
	C_4	246515	243259	240966	248262	245149	253516	248812
M_8	C_1	4881	4360	4309	5124	5701	5585	7999
	C_2	84350	84629	84631	82896	85980	87961	88800
	C_3	163291	169855	170092	166787	165859	170679	170218
	C_4	243653	245436	245089	244096	247458	254456	250928
M_9	C_1	4136	4509	4864	4715	4813	4838	8001
	C_2	83446	81080	81516	88934	83437	87185	93287
	C_3	165203	163105	163133	170497	177800	164443	164432
	C_4	244933	241378	241981	262366	256704	243401	249907
M_10	C_1	3133	2640	2886	3487	6388	5162	3790
	C_2	83278	81867	83006	84896	84428	85796	84899
	C_3	174329	161615	163870	165042	163668	165568	162717
	C_4	253547	252860	252863	245434	245282	247945	245112

Subject_06	Starting 'sample no' for all four chunks of each movement						
Movement		Day_1	Day_2	Day_3	Day_4	Day_5	Day_6	Day_7
M_1	C_1	3499	2297	2609	3074	3427	1969	3198
	C_2	99102	83348	83461	81754	83514	83062	88075
	C_3	177428	164664	183409	163016	168072	171256	169211
	C_4	271256	247651	253833	243179	243190	253146	251230
M_2	C_1	2412	1600	2274	2765	3492	3664	3833
	C_2	83092	80686	81268	83332	83235	91803	85285
	C_3	161177	163205	162420	168286	164147	169106	163228
	C_4	255155	242025	241664	255159	259258	263550	242534
M_3	C_1	3420	2432	3101	2769	3541	4227	3100
	C_2	84199	83108	82995	82937	83450	87284	83213
	C_3	165562	162109	162937	163364	162901	165163	162625
	C_4	244439	244387	244578	243587	242919	249926	243605
M_4	C_1	3300	1878	2680	2178	2822	2040	1973
	C_2	80121	82463	82508	80813	81546	82642	79973
	C_3	163654	161992	163017	163358	161771	161903	162419
	C_4	254800	251456	258955	242901	240907	249689	253460
M_5	C_1	3100	2517	3074	4565	2518	4822	3085
	C_2	83614	80413	83019	83688	83275	82836	82709
	C_3	163790	163365	160920	163238	164412	162524	163722
	C_4	243726	245926	248230	241377	241291	258106	243092
M_6	C_1	3399	2253	2875	3976	2496	2550	2041
	C_2	88788	82992	88027	82344	82641	83740	84467
	C_3	169935	168061	168692	170374	164393	165275	164954
	C_4	250084	258724	256845	262509	244504	244244	245687
M_7	C_1	3646	2982	3999	3794	4566	3215	4285
	C_2	83402	84223	91237	82678	83111	89169	85699
	C_3	164020	161165	171308	163232	164071	170708	174462
	C_4	243550	262097	251032	245138	245691	252818	247240
M_8	C_1	3188	2812	5235	2457	2669	2988	2468
	C_2	84025	80685	84524	83626	83931	86773	84606
	C_3	164065	169996	162740	164094	163643	175039	162515
	C_4	244541	254402	244085	245795	245486	263903	245487
M_9	C_1	3660	2794	2824	4570	3362	2592	5024
	C_2	85725	91479	82971	83589	83766	86102	84557
	C_3	170371	169176	168469	165556	163798	164349	163419
	C_4	247817	251791	258819	256530	245381	245475	243034
M_10	C_1	2638	2361	2589	3204	3362	5595	3771
	C_2	83744	82554	90136	86124	83581	89647	83558
	C_3	162903	162880	164164	167236	162366	164707	173473
	C_4	245666	240886	243264	246072	242670	245056	256480

Subject_07		Starting 'sample no' for all four chunks of each movement						
Movement		Day_1	Day_2	Day_3	Day_4	Day_5	Day_6	Day_7
M_1	C_1	9086	4420	4043	3335	3964	3028	6515
	C_2	88571	88466	85811	90056	81552	84767	83612
	C_3	169637	164663	163347	182748	161810	161326	163652
	C_4	258933	243507	250127	269905	241244	242297	243854
M_2	C_1	12188	8705	2490	5866	5927	3296	6267
	C_2	87986	91034	83542	86980	83533	95892	83911
	C_3	168649	165635	169745	164989	164344	176858	169661
	C_4	250100	248324	257673	243673	248722	257085	252242
M_3	C_1	4918	3452	2533	7092	3589	10375	5989
	C_2	88797	83272	91979	86469	91335	81966	85228
	C_3	168493	173685	179940	164269	176337	174095	163582
	C_4	257252	255027	260065	245770	259373	255030	249010
M_4	C_1	2620	2470	4750	1961	1614	1007	1606
	C_2	83589	90449	82994	84707	80437	93650	82336
	C_3	163395	162073	161388	164138	162321	175560	162574
	C_4	243920	243062	253181	252387	242985	259416	246622
M_5	C_1	3089	2429	3263	2174	6490	2451	2646
	C_2	83025	81950	82933	83222	82975	85736	81968
	C_3	163387	160861	168897	164171	162835	161740	162698
	C_4	247283	254068	251233	244787	240878	247948	243247
M_6	C_1	1603	3386	3349	4120	9939	4512	1779
	C_2	82442	84935	89922	85997	89767	90637	83138
	C_3	160976	162821	168755	162349	164869	172375	162131
	C_4	242820	243490	254407	244937	258724	250912	243083
M_7	C_1	2260	7482	3686	2765	2422	3552	2055
	C_2	84902	83919	88460	85682	84327	91639	83697
	C_3	163155	161797	176275	164585	165355	170616	163354
	C_4	244539	244017	255769	254082	248892	264273	242634
M_8	C_1	3129	4072	2892	3520	1982	3880	2156
	C_2	83615	83907	83953	83493	84531	84020	82709
	C_3	164167	161220	172954	160733	162586	163563	164822
	C_4	258097	244769	255706	255683	247870	243726	242533
M_9	C_1	2689	5910	6556	6942	4213	3280	1604
	C_2	85473	85069	84995	82992	83769	83321	82635
	C_3	165055	164165	165086	163789	163263	163143	164252
	C_4	250813	242451	245103	246005	242997	255075	243821
M_10	C_1	3804	4481	8271	2808	3193	4851	2784
	C_2	84725	85302	83948	83525	94788	86802	104646
	C_3	161480	171263	163692	164194	173706	165806	174078
	C_4	244105	252472	244184	244908	264159	243223	254683

Subject_08	Starting 'sample no' for all four chunks of each movement							
Movement		Day_1	Day_2	Day_3	Day_4	Day_5	Day_6	Day_7
M_1	C_1	3209	2960	2554	3285	2355	3320	3491
	C_2	84567	84285	89102	89132	83423	81897	82623
	C_3	163633	162283	177915	176635	163503	162814	163075
	C_4	257861	245126	256771	256382	243119	244059	245086
M_2	C_1	2910	2694	2866	3386	3254	2825	4612
	C_2	82908	84827	84749	86671	84976	86051	86104
	C_3	167816	178954	176008	179668	164323	163667	163264
	C_4	244490	259915	266622	272476	244977	247305	247847
M_3	C_1	5049	3421	5865	6953	4142	2253	4496
	C_2	85922	83341	86424	87362	81815	83305	80586
	C_3	165706	164227	170875	171955	163861	161649	175136
	C_4	247242	252559	257319	256785	243960	244424	250965
M_4	C_1	5650	2636	3989	4658	5559	2489	4546
	C_2	87169	87131	86073	80620	83023	97701	92719
	C_3	163743	167056	171089	164355	163951	171397	172467
	C_4	244898	260770	253145	243429	247214	257223	255593
M_5	C_1	3423	5848	4440	5045	3605	3553	10457
	C_2	84466	82973	87999	87893	85429	86107	82655
	C_3	165410	163915	167360	181883	167344	162913	164080
	C_4	245043	243715	250000	267249	243279	243507	248092
M_6	C_1	2989	2971	3237	5830	3745	6338	3390
	C_2	83676	84279	88749	83695	83353	84231	83369
	C_3	171774	163112	172437	167162	164276	163624	163538
	C_4	263644	243324	252710	251852	252506	247105	247744
M_7	C_1	5007	4349	4519	2996	2956	5588	4200
	C_2	85187	84877	92107	81693	86704	85536	83719
	C_3	164239	165707	173054	163419	164370	163610	164537
	C_4	246573	258288	250911	248590	246060	244915	244286
M_8	C_1	4319	4116	3158	8680	7072	6293	3757
	C_2	85592	84154	85007	86001	83973	89258	83688
	C_3	164537	167679	165721	161345	164355	171378	166664
	C_4	244698	263311	245416	244069	243519	252793	250527
M_9	C_1	3789	4382	8239	4595	5412	4105	2427
	C_2	94217	89055	95347	86483	83514	84366	85778
	C_3	175698	170018	172466	163228	164276	163295	163950
	C_4	257645	251261	255074	257013	246465	256522	246162
M_10	C_1	4428	4754	4634	4107	4065	6698	4734
	C_2	83633	89301	85278	85060	86510	87501	85189
	C_3	164100	170704	175461	161557	164813	171794	162838
	C_4	242991	250017	248218	253391	248137	262887	241520

Subject_09	Starting 'sample no' for all four chunks of each movement							
Movement		Day_1	Day_2	Day_3	Day_4	Day_5	Day_6	Day_7
M_1	**C_1**	3931	5068	4808	3840	4639	2903	3552
	C_2	81890	83702	83691	82873	81580	83148	84450
	C_3	163465	164400	163866	163590	163774	162598	166844
	C_4	244359	246242	245916	250355	244103	243560	252828
M_2	**C_1**	5455	3115	4401	3502	4399	3688	4923
	C_2	84468	93499	84287	84715	82209	86186	84701
	C_3	164293	170856	179347	164222	164624	161845	164351
	C_4	246217	249785	243387	244743	244274	246747	244885
M_3	**C_1**	4893	4553	4428	8894	5054	5939	5584
	C_2	83037	87713	83670	92294	83548	81276	84722
	C_3	163077	166046	163552	180544	164998	165160	164906
	C_4	243820	245372	258466	261125	243534	253528	250075
M_4	**C_1**	4806	3618	3877	4687	3401	3072	4052
	C_2	83227	83820	83780	92977	87934	82378	87730
	C_3	163175	162137	163888	181276	174920	163500	169097
	C_4	243438	255292	246130	262141	255956	243656	261957
M_5	**C_1**	2813	3536	4081	4437	7785	5024	4878
	C_2	89904	92048	82035	93259	83216	80931	81687
	C_3	161856	177979	174168	171892	170903	161042	161714
	C_4	244626	258299	260865	252646	254275	242563	243059
M_6	**C_1**	3187	1536	6745	4343	6967	3664	4257
	C_2	80212	91105	92886	83487	82449	81911	83022
	C_3	167104	172929	172103	164226	162809	161836	163064
	C_4	255178	249452	253457	245428	244990	249539	244359
M_7	**C_1**	6570	4043	3128	7143	4930	5139	4667
	C_2	91175	83258	88296	84642	83093	89641	84604
	C_3	179875	163749	167395	164139	163399	165271	164338
	C_4	261940	255492	248895	243010	244688	245654	242450
M_8	**C_1**	5239	3115	3693	3924	2888	3866	5464
	C_2	87095	85483	87686	85848	86271	80999	82679
	C_3	170136	163443	163344	175462	167789	161170	164094
	C_4	252281	245527	243680	257639	246596	242236	254687
M_9	**C_1**	4891	4690	4122	3674	10550	7590	4145
	C_2	89576	83186	83475	84019	83780	85219	82038
	C_3	164799	164581	166487	163779	164334	166746	163441
	C_4	243969	246911	244247	244231	245572	250353	244624
M_10	**C_1**	5838	5415	4728	4841	2623	4900	4990
	C_2	85573	84992	83589	92202	83053	86992	84642
	C_3	164765	162948	166413	173768	171584	166743	165245
	C_4	245995	241158	243381	256962	265721	246643	244587

Subject_10	Starting 'sample no' for all four chunks of each movement							
Movement		Day_1	Day_2	Day_3	Day_4	Day_5	Day_6	Day_7
M_1	C_1	5578	3602	4384	4005	3977	3298	3697
	C_2	99682	83312	83912	83719	83900	92806	84612
	C_3	182117	163250	163193	163420	164158	181688	163049
	C_4	270121	255778	244254	244229	244813	274689	250723
M_2	C_1	4247	3166	2850	3353	6534	3000	2928
	C_2	84490	85047	83677	83939	85274	85825	84142
	C_3	164256	165548	170536	172933	163580	163009	163769
	C_4	244868	251881	249610	253547	243354	243422	252625
M_3	C_1	7159	3588	5524	3976	5488	6115	4172
	C_2	87269	84629	84743	85108	84435	86387	82923
	C_3	171301	163322	164243	162243	166936	164925	164730
	C_4	251613	244601	247901	249425	245936	250380	245922
M_4	C_1	4554	4640	2845	3910	3305	2807	3646
	C_2	82492	81961	83909	84235	83519	83655	82513
	C_3	164776	162921	164280	170935	162987	163500	174213
	C_4	244302	245257	246933	252150	243372	243559	254200
M_5	C_1	4885	4380	5770	5190	4408	2811	6442
	C_2	83286	82898	89715	83337	93540	83771	88347
	C_3	162706	169682	169229	164600	172587	163172	168864
	C_4	244738	254143	256563	251931	251783	244791	248494
M_6	C_1	4030	5003	2817	3376	3303	4158	6740
	C_2	85861	84246	82900	84684	90116	83341	83078
	C_3	164203	163034	162941	163199	173822	162282	162899
	C_4	256994	243501	242930	243770	254530	255836	244944
M_7	C_1	4127	3543	2315	3400	2929	5236	2279
	C_2	83902	84852	82973	92064	82850	85975	83168
	C_3	163521	175940	162980	175550	163783	163173	162571
	C_4	244680	255279	243386	254930	243807	244459	247624
M_8	C_1	3821	2914	3287	3046	2964	3812	3359
	C_2	83387	88146	83197	83600	91340	83195	82893
	C_3	165249	170340	162385	164228	172180	173495	163591
	C_4	244186	259492	243626	244708	263254	257584	245870
M_9	C_1	4331	3315	3973	2706	4487	3767	2186
	C_2	96834	90792	83921	84011	83605	87392	83333
	C_3	164180	170616	163664	167542	162773	166989	162637
	C_4	244487	252264	246879	250747	243738	248270	243403
M_10	C_1	3825	3454	4165	3196	4085	3000	3204
	C_2	83539	90697	91349	82570	80849	87417	93418
	C_3	165649	172659	171301	164385	170740	168410	171097
	C_4	243958	258756	251370	242934	252790	252310	263855

Amputee Subject's Tables

Subject_01		Starting 'sample no' for all four chunks of each movement						
Movement		Day_1	Day_2	Day_3	Day_4	Day_5	Day_6	Day_7
M_1	C_1	4837	3083	2793	4301	3965	3137	3076
	C_2	83492	83747	83870	83672	83195	83713	83840
	C_3	164024	168828	168670	163619	169943	162903	162529
	C_4	244467	249965	248949	243977	259548	243994	243591
M_2	C_1	6791	3538	3660	4334	5341	3015	3526
	C_2	86906	82911	86508	83746	85167	83671	85171
	C_3	166218	165021	173849	170766	173119	165447	164739
	C_4	245455	245078	255273	258536	261516	243278	244112
M_3	C_1	5200	4639	4716	3231	5933	3678	3885
	C_2	87379	84645	84044	83129	84392	89253	82989
	C_3	165883	165533	179112	165852	163958	168911	163584
	C_4	246701	251358	258594	255543	243973	251980	244209
M_4	C_1	3350	3155	3126	2542	3469	4272	3647
	C_2	83632	84232	84169	82651	84936	82833	83809
	C_3	164287	163645	175997	164597	180717	163005	162956
	C_4	242921	244539	273887	247028	269888	242582	254759
M_5	C_1	11039	5957	6235	6359	3171	3350	3471
	C_2	92074	87682	83446	89090	83378	83341	83800
	C_3	172657	173074	165144	169942	170309	163254	163646
	C_4	254211	251609	249752	249106	257040	244482	243134
M_6	C_1	6618	3785	6411	5972	4225	4378	5813
	C_2	84083	87437	85421	87765	83905	91818	86558
	C_3	163758	167578	169405	167977	163743	172547	167013
	C_4	245996	247984	249543	248231	244718	253518	260474
M_7	C_1	5111	4698	5204	8403	4387	3416	3175
	C_2	84654	85112	84424	90410	83745	83580	83161
	C_3	164348	171413	165302	172174	176898	163714	164048
	C_4	253425	249246	252439	262497	278201	243939	243220
M_8	C_1	3319	4304	4345	3665	6177	3080	8239
	C_2	83588	85437	85051	83261	87088	82843	90830
	C_3	162409	172328	164385	164097	167018	162995	172486
	C_4	242900	252289	265932	244748	252670	247703	253209
M_9	C_1	4340	2954	3312	3142	4755	3457	3302
	C_2	83834	84157	84527	83801	85016	83732	83653
	C_3	163959	166131	173166	164514	163736	163067	164073
	C_4	246540	250508	267258	244535	244561	247850	244838
M_10	C_1	6456	4346	4695	5399	3008	3640	6429
	C_2	87674	91164	87406	84856	82731	82761	91821
	C_3	167137	184887	172437	173715	173543	163326	173956
	C_4	247224	276495	263042	256005	254060	245160	252290

Subject_02	Starting 'sample no' for all four chunks of each movement						
Movement		Day_1	Day_2	Day_3	Day_4	Day_5	Day_6	Day_7
M_1	C_1	4530	3689	3745	3660	3832	3812	4608
	C_2	85240	92789	83474	92819	85221	81753	85125
	C_3	165492	182405	163991	172019	169630	166736	164339
	C_4	245901	275604	245377	252579	246141	248004	245813
M_2	C_1	3981	2916	3682	3145	4185	2869	4858
	C_2	85698	84547	94146	85781	84731	86693	87846
	C_3	171226	165719	172880	170007	169178	167538	169364
	C_4	244419	252977	253218	247168	255736	258344	264917
M_3	C_1	4269	5844	3305	3935	3385	3123	4495
	C_2	86362	86086	92663	91555	86677	83017	90235
	C_3	164252	165330	176821	178546	168304	162937	170157
	C_4	243993	262987	259205	262195	258379	244410	250621
M_4	C_1	6531	3782	4345	3665	3559	4923	5390
	C_2	85918	88295	88313	121952	85574	84099	87351
	C_3	172249	164685	163984	173388	166847	164320	175075
	C_4	247960	245979	245162	252232	251524	246296	265031
M_5	C_1	3901	8115	9930	5601	4558	4546	7587
	C_2	85595	84914	85503	86232	88327	90037	95975
	C_3	166802	167332	165450	166717	167677	166152	177425
	C_4	247388	245072	246129	248082	247269	259810	269272
M_6	C_1	4010	4023	5151	5627	6241	7347	4572
	C_2	84802	94968	83811	85650	84770	88193	86502
	C_3	166479	180649	165488	163978	175603	175301	163604
	C_4	246072	268717	250252	247722	271164	257610	244805
M_7	C_1	5391	4872	4120	4478	4715	3222	4034
	C_2	90194	90920	86971	93052	88444	84012	85125
	C_3	166209	181495	166677	170310	165774	163946	165147
	C_4	252245	272695	257518	252202	258738	245696	254600
M_8	C_1	4668	3673	3125	3477	6309	3926	3606
	C_2	85410	86781	86557	93526	86922	84163	84455
	C_3	169094	166010	165173	172460	176225	162153	165166
	C_4	245570	257999	245483	252999	263480	246269	246713
M_9	C_1	4304	4212	3969	5679	4227	3813	4955
	C_2	97282	84089	84849	89670	84904	93360	85792
	C_3	165124	165260	164646	179816	166271	175143	163992
	C_4	245679	248925	244857	260646	257082	267680	245648
M_10	C_1	12957	3880	3976	2997	3551	3689	4906
	C_2	91581	92749	91001	84756	83303	85702	85090
	C_3	165064	176704	170174	168027	163512	166265	165923
	C_4	245514	271817	250550	253083	246605	244801	246202

Subject_03		Starting 'sample no' for all four chunks of each movement						
Movement		Day_1	Day_2	Day_3	Day_4	Day_5	Day_6	Day_7
M_1	C_1	2424	5163	4253	3691	4085	2480	4483
	C_2	82089	90789	85018	84104	84706	83730	91473
	C_3	162602	186006	174626	163668	164365	170568	179425
	C_4	241494	267995	255438	244563	249646	250516	270744
M_2	C_1	3286	4821	4390	4567	4760	3409	4189
	C_2	83650	84142	93031	83268	87559	85065	84388
	C_3	166015	163568	177951	164514	168860	165482	173176
	C_4	245596	253247	259734	253602	249855	243867	253708
M_3	C_1	3003	4726	3878	3353	4233	2339	5354
	C_2	84735	85071	85924	81903	89105	85265	89081
	C_3	164034	172340	166904	163786	170879	164775	170214
	C_4	246082	255738	247736	246838	250515	246958	254707
M_4	C_1	4074	5370	3880	2806	3579	3648	4330
	C_2	83487	83825	84200	83424	89189	88520	84835
	C_3	173018	166732	164414	169806	168388	167876	164909
	C_4	250673	243529	246615	260973	248712	248067	243813
M_5	C_1	4279	4607	4744	1385	4128	3825	5322
	C_2	84032	88301	84926	91320	87878	83804	86406
	C_3	167419	169729	167834	175223	168243	164290	170928
	C_4	263212	257850	246227	265270	247035	254028	257282
M_6	C_1	4883	3668	3808	3624	3091	3879	3393
	C_2	85068	85092	85368	88001	86760	83260	84234
	C_3	164916	171195	164947	167439	172024	166688	166833
	C_4	247279	253722	260233	253721	252701	244373	258078
M_7	C_1	2957	5225	5711	3693	4277	4106	5391
	C_2	84354	86242	91176	88384	92134	84934	83513
	C_3	165312	165369	172663	171503	171435	163942	164268
	C_4	247731	246243	251440	260580	254702	243902	243366
M_8	C_1	3917	2315	5404	4186	2963	5232	4370
	C_2	90471	85620	87169	86165	83880	84730	90871
	C_3	178427	166404	176012	164210	172672	164006	171294
	C_4	259869	249257	243803	248475	254581	250196	250502
M_9	C_1	4329	4693	3201	4316	3568	2730	2577
	C_2	87960	97542	86872	93313	87707	85020	84308
	C_3	164827	180368	164217	176759	167819	164227	164979
	C_4	257216	264913	246978	263840	253657	244473	252941
M_10	C_1	2762	8875	6566	8405	6099	4878	4409
	C_2	86890	99848	85065	86084	90046	83158	84743
	C_3	172271	188933	168714	178423	165386	161644	164819
	C_4	253453	273864	248850	258290	248965	244875	260528

Subject_04	Starting 'sample no' for all four chunks of each movement						
Movement		Day_1	Day_2	Day_3	Day_4	Day_5	Day_6	Day_7
M_1	C_1	6399	4592	4061	6351	2777	7141	4596
	C_2	90717	79077	84245	91795	88951	89283	81994
	C_3	170917	182188	165076	168553	166512	173762	171821
	C_4	248762	260260	247151	259731	247784	263578	254653
M_2	C_1	2374	7591	8387	5006	6622	3914	7749
	C_2	84394	89250	89999	90005	84210	85064	81463
	C_3	170322	163484	165610	168830	165283	175791	165728
	C_4	244291	279939	246265	263774	244994	267851	246882
M_3	C_1	1739	11402	5542	4525	11489	3169	7240
	C_2	88444	86517	87633	86297	86435	82677	96008
	C_3	165058	167218	162495	165636	167199	168195	171169
	C_4	255840	247715	246093	244465	247623	255455	259702
M_4	C_1	3525	2903	6395	6691	5279	1844	6833
	C_2	85802	86300	83862	89339	95092	88655	99336
	C_3	163328	167568	167038	169574	171703	169690	167905
	C_4	258119	245293	244458	251219	251415	249352	258971
M_5	C_1	5034	5858	5636	10067	6778	3971	4856
	C_2	83474	83473	87885	96624	85271	85272	85664
	C_3	170617	165646	165454	176329	166360	163367	165423
	C_4	256805	251798	255195	262958	246303	264668	244679
M_6	C_1	4845	4167	6691	7693	7077	4543	6726
	C_2	81439	83366	86673	88316	92293	87832	91465
	C_3	165972	165065	166739	165741	171216	173402	170539
	C_4	252756	258108	246912	257555	250839	253717	244807
M_7	C_1	3108	7998	11027	5993	8142	3613	10697
	C_2	90913	87566	106864	90369	84822	84527	84880
	C_3	170234	171334	185393	165567	164692	163748	171104
	C_4	246982	255323	264049	243685	244154	243724	259561
M_8	C_1	7886	7477	8639	3949	7227	5573	5461
	C_2	93009	85170	88443	84327	91908	95365	86665
	C_3	173461	173809	167222	165349	173643	176913	163179
	C_4	244030	248666	247516	246836	250669	252628	253580
M_9	C_1	3037	6757	6374	6049	5020	4667	4980
	C_2	87551	85948	89118	85969	83339	85552	88642
	C_3	167473	170425	167737	174727	164304	165323	165478
	C_4	245814	257075	247656	255874	244285	258630	255322
M_10	C_1	3668	7739	6145	8437	6148	3362	6312
	C_2	84788	86331	89941	83131	83575	84082	85992
	C_3	168517	168450	177825	170573	160851	166282	164566
	C_4	254927	257565	260182	257639	248549	258007	257740

Subject_05		Starting 'sample no' for all four chunks of each movement						
Movement		Day_1	Day_2	Day_3	Day_4	Day_5	Day_6	Day_7
M_1	C_1	4676	4479	3528	6446	5482	2999	5750
	C_2	82287	84933	82119	84509	87888	89718	83404
	C_3	160910	164242	163233	163455	166834	170574	161291
	C_4	242290	247833	244238	242618	251019	249574	248888
M_2	C_1	3573	5928	4606	4402	2098	4589	4546
	C_2	82652	85431	83057	84622	80821	83322	82510
	C_3	162817	164105	174557	163779	164439	164951	162803
	C_4	244219	243730	256588	243727	243101	243889	240707
M_3	C_1	5304	4816	5093	3400	4157	6002	6613
	C_2	84600	85000	84815	83859	86032	83873	90926
	C_3	165563	162736	172832	164056	168934	164237	171989
	C_4	245228	252915	259721	249671	249268	255742	252308
M_4	C_1	3319	6849	4700	4214	4830	4756	5199
	C_2	84013	83875	83581	81235	84497	89461	87227
	C_3	163691	172624	163395	163550	162794	170285	178297
	C_4	247937	259552	244124	249958	243191	258427	258655
M_5	C_1	3079	7270	3070	4977	4571	4658	5700
	C_2	85766	84347	87199	89885	83723	92273	91154
	C_3	166153	164450	170799	171922	165950	173310	169962
	C_4	246320	246820	263122	263195	247901	258777	250123
M_6	C_1	3845	2440	2287	5055	4437	3148	4995
	C_2	85048	85515	83363	83565	86504	94833	85500
	C_3	162532	164187	163808	161511	172953	188065	174287
	C_4	243571	245179	245623	250382	246880	254583	254601
M_7	C_1	5383	5385	4645	5837	4511	3507	4295
	C_2	87980	86926	83019	93557	83969	87254	82404
	C_3	168359	164184	163225	174424	164617	168610	163014
	C_4	248940	245414	243144	273276	244270	251189	243715
M_8	C_1	2791	5735	5326	4693	4100	4689	14850
	C_2	86154	83530	90788	89856	84426	86810	94012
	C_3	163868	164568	172901	175759	164053	161792	173779
	C_4	242240	243531	253796	252345	245156	250148	250472
M_9	C_1	5048	3564	3826	5624	5554	1897	4683
	C_2	87157	85075	96530	84195	83927	90322	82380
	C_3	164053	165739	189050	165014	163897	171266	162670
	C_4	244893	245414	278295	250384	247674	257735	255291
M_10	C_1	3982	4638	6279	6284	3630	6359	5476
	C_2	84740	87833	81929	89960	83127	92700	83646
	C_3	165159	166096	165665	163519	163317	173489	162486
	C_4	240558	251995	261736	254538	242733	263965	243231

Subject_06	Starting 'sample no' for all four chunks of each movement						
Movement		Day_1	Day_2	Day_3	Day_4	Day_5	Day_6	Day_7
M_1	C_1	3212	2923	4682	3716	6462	2949	5943
	C_2	82530	83488	84781	83833	84121	89740	87339
	C_3	163326	163210	166598	164459	163240	172729	166487
	C_4	243697	244883	247081	249278	243711	258256	247180
M_2	C_1	2582	5721	5561	3914	4878	6110	5944
	C_2	83535	81440	82629	83360	84773	98340	83294
	C_3	163840	162455	163015	162741	163086	181681	162713
	C_4	249910	243327	242535	243365	242973	263814	241538
M_3	C_1	5081	5850	6839	7259	7904	5592	5013
	C_2	84049	83504	85281	83007	83509	88469	86879
	C_3	162283	167808	162928	174962	163599	167613	167429
	C_4	245055	243084	247680	260918	243208	250088	255230
M_4	C_1	4015	4074	6334	3306	5250	3971	3423
	C_2	83339	82840	83180	83210	84212	83496	87987
	C_3	163255	161147	163008	163247	162931	162898	169714
	C_4	246996	255450	249554	243274	249621	242859	249607
M_5	C_1	3438	3273	6825	9492	4195	7871	3795
	C_2	82192	83937	82831	85338	83645	83443	85359
	C_3	163102	163534	163704	163485	163846	162840	175325
	C_4	244795	253172	254223	243326	244124	244611	274820
M_6	C_1	5168	3671	3657	3827	5022	6151	4183
	C_2	82850	84618	83250	83330	83072	88749	83224
	C_3	170624	165992	162966	166730	163435	168423	162728
	C_4	254803	247476	243324	250674	243646	250473	243118
M_7	C_1	4582	3589	6355	5281	8886	2902	4248
	C_2	83154	82223	83308	84337	83085	83182	82809
	C_3	163154	163445	163439	163295	169404	163954	171340
	C_4	243818	251050	245196	250284	264356	244522	257979
M_8	C_1	2287	7525	4849	4442	4421	6263	3957
	C_2	84417	84248	82962	84012	84343	88621	82644
	C_3	163412	187720	162846	167330	163675	169138	167593
	C_4	243061	245889	243160	252346	245140	248067	260606
M_9	C_1	4440	4617	13686	5860	5157	4483	5336
	C_2	83247	83655	84021	83418	83271	88343	88431
	C_3	163252	165111	162624	165303	165046	176257	171492
	C_4	243678	244116	245541	246117	244046	259583	256628
M_10	C_1	3996	6835	7195	5987	7513	7179	6460
	C_2	83297	85105	83506	85727	83470	83451	85874
	C_3	162679	163509	164648	171959	163033	163792	168066
	C_4	243073	242795	244442	253302	243883	245821	246925

D.3. PREPROCESSING OF DATA:

Both the magnitude and frequency spectrum was analyzed for all the four datasets (healthy_surface, healthy_intramuscular, amputee_surface and amputee_intramuscular). A sample figures of both the raw data magnitude (figure D-4, D-5, D-6 and D-7) and raw data frequency spectrums (D-8, D-9, D-12(a) and D-13(a)) from each dataset are shown.

To reduce the unwanted 50 Hz noise and its harmonics, 3rd order configurable Butterworth filter was used and resultant frequency and power spectral density (PSD) spectrums are shown in figure D-10, D-11, D-12(b) and D-13(b).
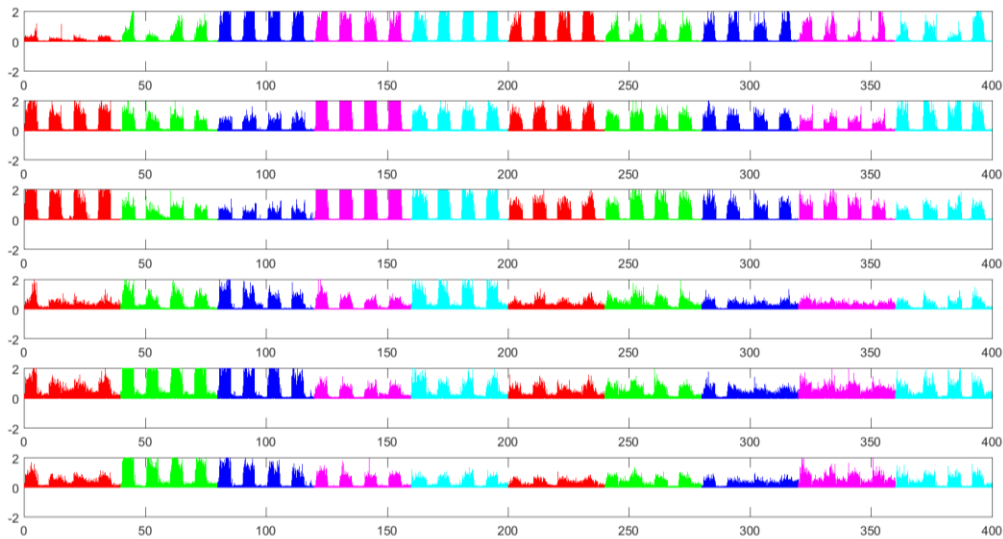
Figure D-4: Healthy subject 01 surface EMG amplitude spectrum of a complete session (it includes the four repetitions of ten movements over all six channels).
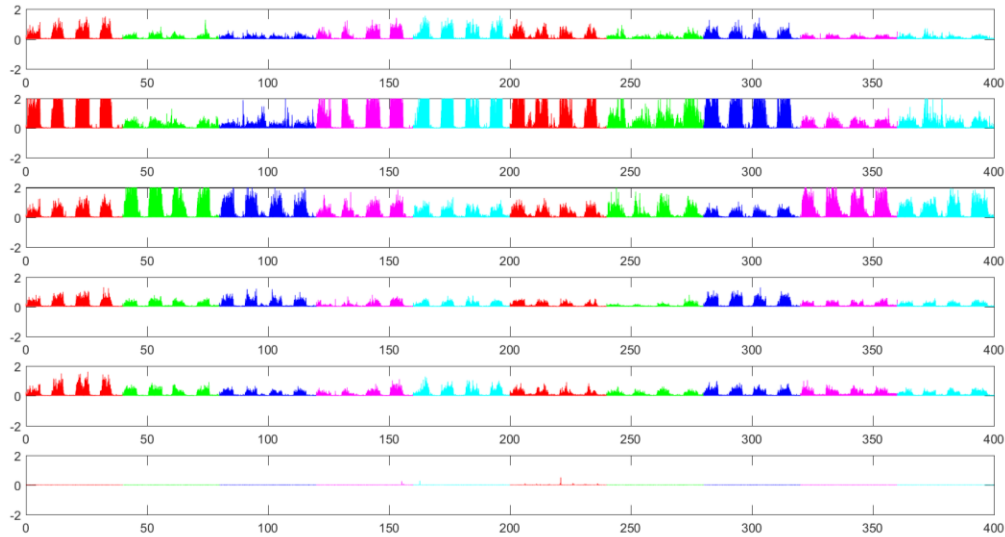
Figure D-5: Amputee subject 01 surface EMG amplitude spectrum of a complete session (it includes the four repetitions of ten movements over all six channels). As mentioned in chapter 02, only five surface electrodes were placed due to limited available space.
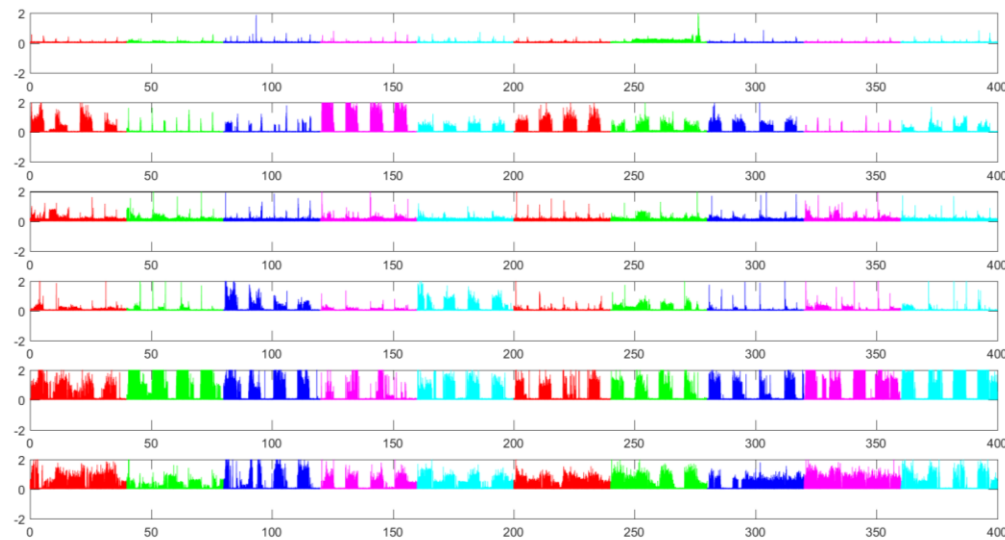
Figure D-6: Healthy subject 01 intramuscular EMG amplitude spectrum of a complete session (it includes the four repetitions of ten movements over all six channels). In this session, channel 1, 3 and 4 are not responding very well.
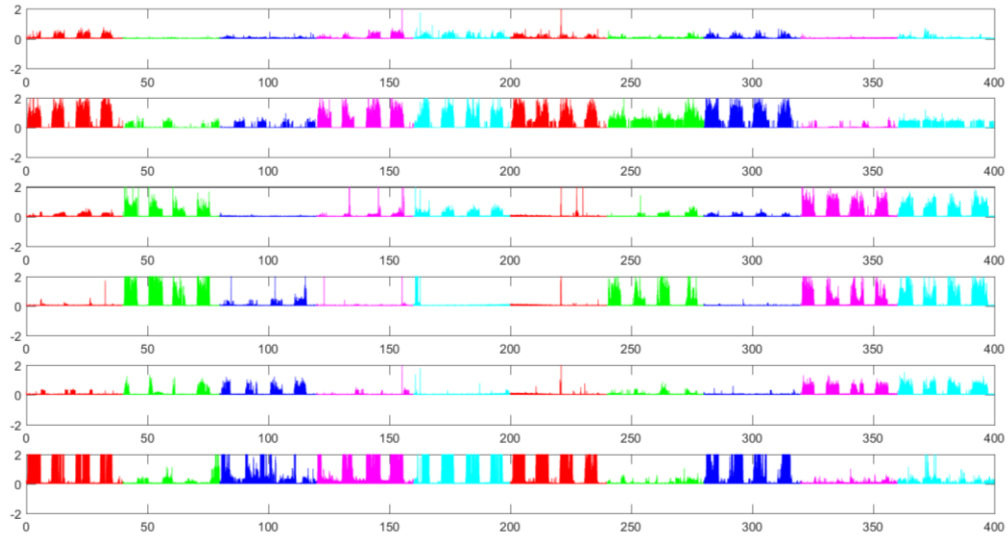
Figure D-7: Amputee subject 01 Intramuscular EMG amplitude spectrum of a complete session recorded on day 01 (it includes the four repetitions of ten movements over all six channels). In this session, electrodes over some channels did not respond very well to few movements.
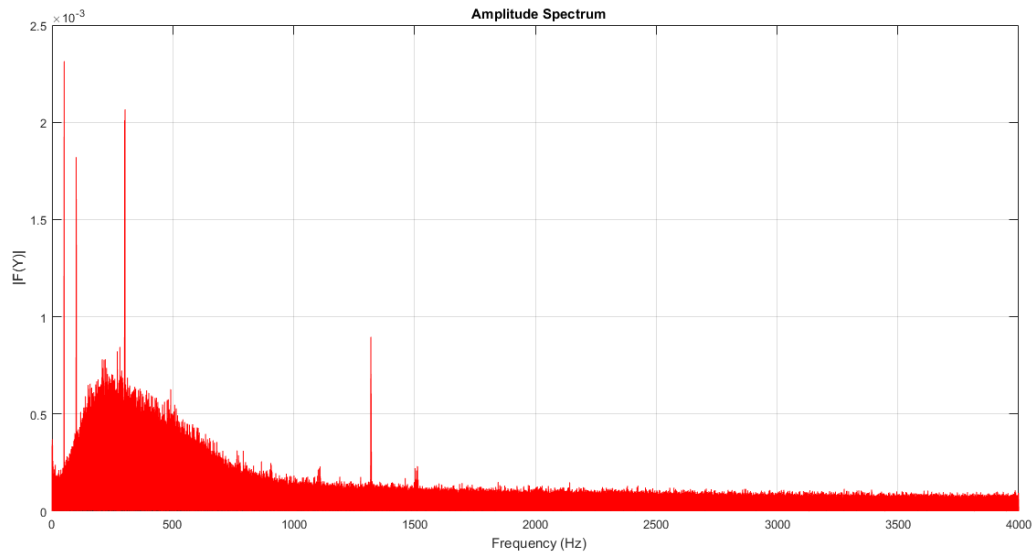
Figure D-8: Healthy subject 01 intramuscular EMG Frequency spectrum of day 01. Its corresponding magnitude spectrum in time domain is shown in figure B-6.
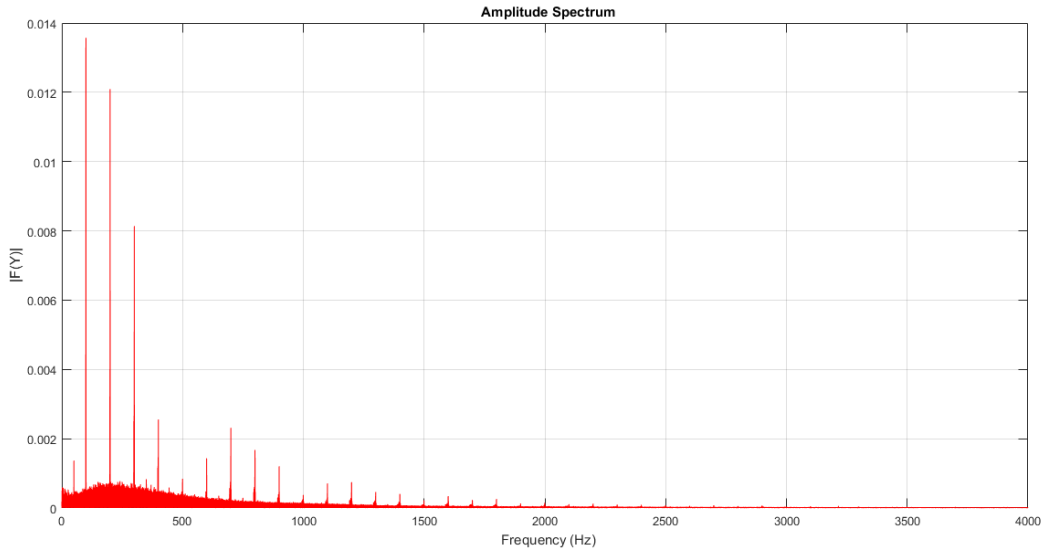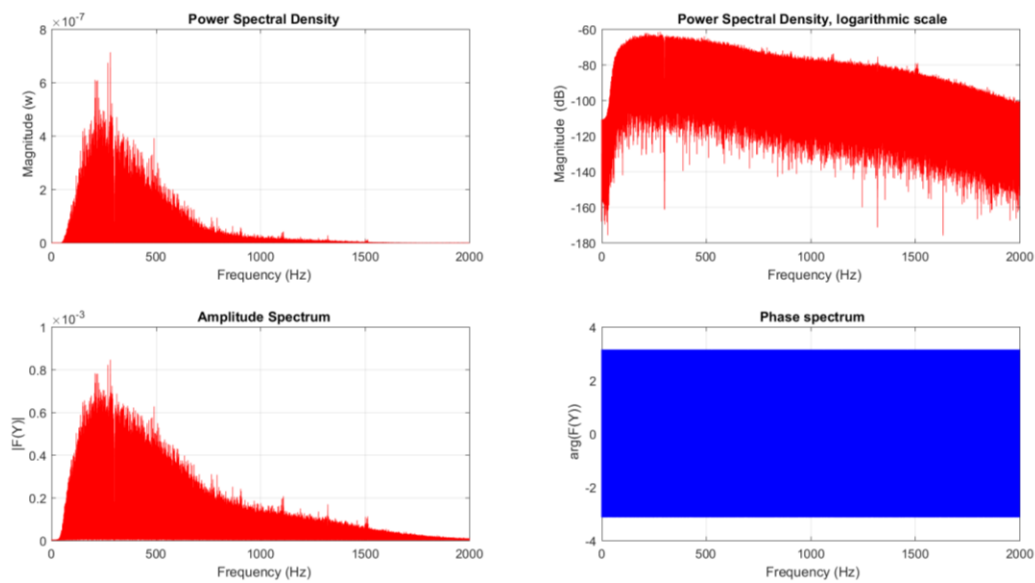
Figure D-9: Amputee subject 01 intramuscular EMG Frequency spectrum of day 01. Its corresponding magnitude spectrum in time domain is shown in figure B-7.

Figure D-10: Application of configurable Butterworth filtering to intramuscular data of healthy subject 01 days 01. Its corresponding time domain and frequency spectrum of raw data are shown in figure B-6 and B-8 respectively.
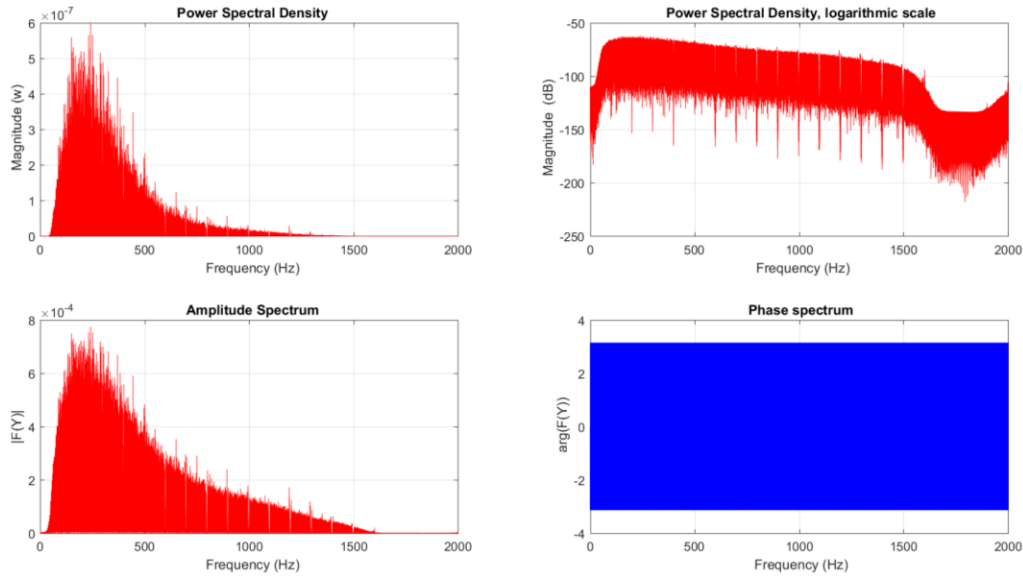
Figure D-11: Application of configurable Butterworth filtering to intramuscular data of amputee subject 01 days 01. Its corresponding time domain and frequency spectrum of raw data are shown in figure B-7 and B-9 respectively.
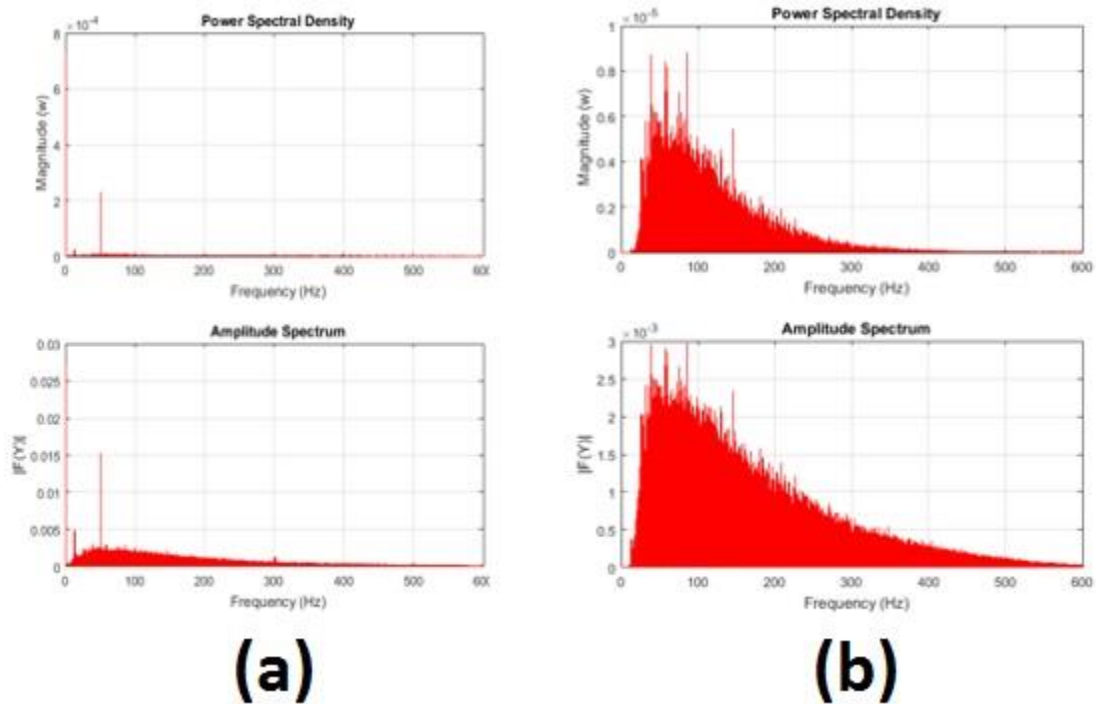

Figure D-12: Healthy subject 01 surface EMG frequency (and PSD) spectrums (a) raw EMG frequency spectrum (b) application of configurable Butterworth filtering. Its corresponding time domain spectrum of raw data is shown in figure B-4.
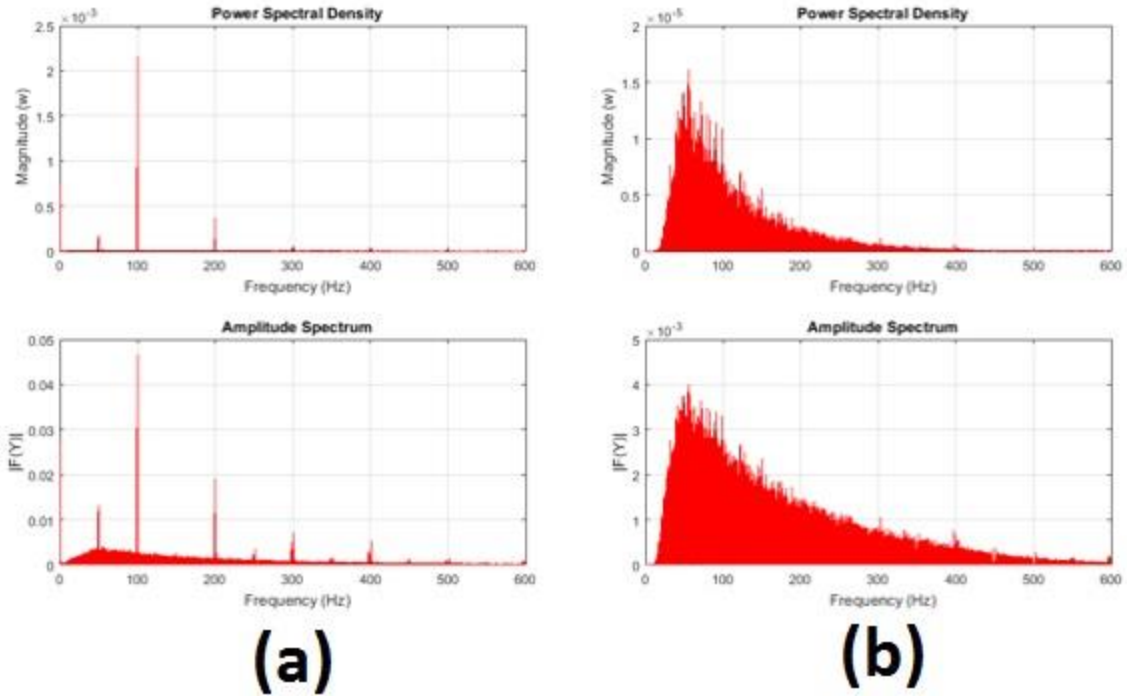
Figure D-13: Amputee subject 01 surface EMG frequency (and PSD) spectrums (a) raw EMG frequency spectrum (b) application of configurable Butterworth filtering. Its corresponding time domain spectrum of raw data is shown in figure B-5.

8.5.Appendix E: Question/Answers Report

This appendix addresses the answers to the few questions raised during Final Defense Presentation.

E.1. GENDER SPECIFIC STUDY:

In our 2nd study, four male and three female subjects participated. Table E-1 shows the mean classification errors of each subjects obtained in all four-analysis using all four classifiers.

Table E-1: Mean classification errors of each subject in all four analyses

Analysis type	Classifier	Sub 01	Sub 02	Sub 03	Sub 04	Sub 05	Sub 06	Sub 07
Within session	LDA	2.24	5.83	1.73	4.32	10.07	13.5	10.9
	SSAE-f	1.08	2.9	1.05	0.7	2.61	1.36	3.4
	SSAE-r	18.25	28.69	16.83	19.38	23.42	21.56	27.08
	CNN	1.39	4.72	0.68	0.1	2.69	1.83	5.38
Between sessions	LDA	6.28	10.57	4.43	9.4	13.82	16.61	20.54
	SSAE-f	3.69	10.56	1.78	4.05	7.02	7.08	16.16
	SSAE-r	20.63	30.67	17.06	23.91	24.13	23.95	35.06
	CNN	3.39	8.93	1.53	3.52	5.17	6.28	14.52
Between pair of days	LDA	8.06	14.66	7.63	11.27	16.5	20.33	24.65
	SSAE-f	5.43	15.59	6.54	6.8	10.06	12.02	20.39
	SSAE-r	20.62	29.21	21.12	24.15	24.39	25.39	31.32
	CNN	5.06	14.05	6.24	6.82	8.45	10.23	17.63
Leave-one-out between days	LDA	5.35	10.3	3.8	8.92	14.58	16.55	19.76
	SSAE-f	2.19	6.5	1.56	2.34	5.78	5.7	14.34
	SSAE-r	19.95	22.5	24.38	26.15	22.69	19.14	23.64
	CNN	2.62	6.96	1.46	2.79	4.48	3.89	10.02

In table E-1, first four subjects are all male and last three subjects are females. It was found that mean classification errors of females were comparatively higher than male subjects.

So next study will focus on Gender-specific flexor and extensor muscle's EMG analysis and if same results repeat, i.e. classification errors of females were found higher than male subjects, then intelligent classification approaches will be explored that can significantly reduce the classification errors of female subjects.

E.2. AMPUTEES AND HEALTHY SUBJECTS' EMG (BOTH SURFACE AND INTRAMUSCULAR) CORRELATION AND PERFORMANCE OVER TIME:

The correlation of EMG signals for both amputee and healthy subjects over days for performing different hand motions, was performed on this dataset in a separate study titled "The effect of time on EMG classification of hand motions in able-bodied and transradial amputees" [121].

The demographic data of amputee subjects in shown in Table E-2.

Table E-2: Demographic data of amputee subjects

Subject	Age	Affected arm	Time since amputation	Residual forearm length
Amp1	23	Left	2 years	22 cm
Amp2	56	Right	18 years	19 cm
Amp3	31	Right	5 years	09 cm
Amp4	35	Right	2 years	11 cm
Amp5	20	Left	2 years	07 cm
Amp6	22	Right	3 years	24 cm

A regression analysis was performed on all datasets of both able-bodied and amputee subjects for both the within day classification errors (WCE) and between days classification errors (BCE).

BCE was computed from time difference over days (DF) Df = 0 (training and testing of classifier on the same day) to Df = 6 (training on day one and testing on day 7) i.e. difference between training and testing day was increased from 0 days to 6 days. Figure E-1 shows the regression fit between BCE and Df (0–6) for EMG (surface and intramuscular) in amputee and able-bodied. The slopes with amputees were 3.6, 95% CI [0.42, 1.04] and 4.6, 95% CI [0.69, 1.16] for sEMG and iEMG respectively. The slopes for able-bodied were 1.55, 95% CI [−0.02, 0.64] and 4.3, 95% CI [0.26, 1.45] for sEMG and iEMG respectively. The slopes for cEMG were 1.91, 95% CI [−0.06, 0.82] and 1.59, 95% CI [0.14, 0.48] for amputees and able- bodied respectively. Results indicated that performance continuously degraded as time difference between training and testing day increased
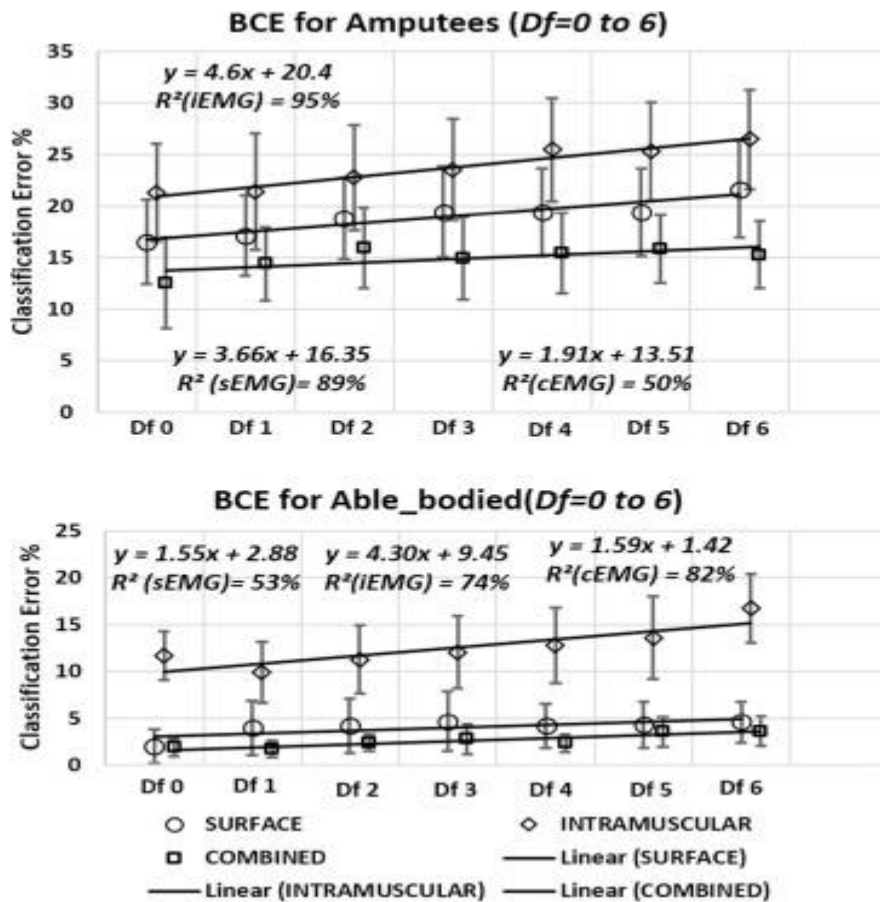

Figure E-1: Polynomial fit between BCE and Df = 0 to 6 for surface and iEMG. Results are given as mean across subjects ± standard deviation (bars)

BCE was computed for all possible combinations between the days. For all subjects, surface sEMG $(7.2 \pm 7.6\%)$, iEMG $(11.9 \pm 9.1\%)$ and cEMG $(4.6 \pm 4.8\%)$ were significantly different $(P < 0.001)$ from each other. A regression between WCE and days $(1–7)$ was on average not significant implying that performance may be considered similar within each day. Regression between BCE and time difference (Df) in days was significant. The slope between BCE and Df $(0–6)$ was significantly different from zero for sEMG $(R2 = 89\%)$ and iEMG $(R2 = 95\%)$ in amputees. Results indicate that performance continuously degrades as the time difference between training and testing day increases. Furthermore, for iEMG, performance in amputees was directly proportional to the size of the residual limb.

E.3. DATA ANNOTATION:

Appendix D discusses about the protocol of data collection and subject's information. Appendix D.2 briefly explain about the data understanding and labeling. Tables of active chunks duration for all ten healthy and six amputee subjects are given appendix D.

Chapter 9.   Bibliography

1.   Atzori, M., M. Cognolato, and H. Müller, *Deep learning with convolutional neural networks: a resource for the control of robotic prosthetic hands via electromyography.* Frontiers in Neurorobotics, 2016. **10**: p. 9.
2.   Goodfellow, I., et al., *Deep learning*. Vol. 1. 2016: MIT press Cambridge.
3.   Chorowski, J.K., et al. *Attention-based models for speech recognition*. in *Advances in Neural Information Processing Systems*. 2015.
4.   Liu, N., et al. *Predicting eye fixations using convolutional neural networks*. in *Proceedings of the IEEE Conference on Computer Vision and Pattern Recognition*. 2015.
5.   Min, S., B. Lee, and S. Yoon, *Deep learning in bioinformatics.* Briefings in bioinformatics, 2017. **18**(5): p. 851-869.
6.   Goen, A. and D. Tiwari, *Review of surface electromyogram signals: its analysis and applications.* World Academy of Science, Engineering and Technology, International Journal of Electrical, Computer, Energetic, Electronic and Communication Engineering, 2013. **7**(11): p. 1429-1437.
7.   Putnam, W. and R.B. Knapp. *Real-time computer control using pattern recognition of the electromyogram*. in *Engineering in Medicine and Biology Society, 1993. Proceedings of the 15th Annual International Conference of the IEEE*. 1993. IEEE.
8.   Kobrinskiy, A., *Bioelectrical control of prosthetic devices.* Her Acad Sci, 1960. **30**: p. 58-61.
9.   Popov, B., *The bio-electrically controlled prosthesis.* J Bone Joint Surg Br, 1965. **47**: p. 421-424.
10.   McKenzie, D., *The Russian myoelectric arm.* The Journal of Bone and Joint Surgery, 1965. **47**: p. 418-420.
11.   Geethanjali, P., *Myoelectric control of prosthetic hands: state-of-the-art review.* Medical Devices (Auckland, NZ), 2016. **9**: p. 247.
12.   Segil, J.L., *Design and validation of a morphing myoelectric hand posture controller based on principal component analysis of human grasping.* IEEE Transactions on Neural Systems and Rehabilitation Engineering, 2014. **22**(2): p. 249-257.
13.   Roche, A.D., et al., *Prosthetic myoelectric control strategies: a clinical perspective.* Current Surgery Reports, 2014. **2**(3): p. 44.
14.   Muceli, S. and D. Farina, *Simultaneous and proportional estimation of hand kinematics from EMG during mirrored movements at multiple degrees-of-freedom.* IEEE transactions on neural systems and rehabilitation engineering, 2012. **20**(3): p. 371-378.
15.   Muceli, S., N. Jiang, and D. Farina, *Extracting signals robust to electrode number and shift for online simultaneous and proportional myoelectric control by factorization algorithms.* IEEE Transactions on Neural Systems and Rehabilitation Engineering, 2014. **22**(3): p. 623-633.
16.   Nielsen, J.L., et al. *Enhanced EMG signal processing for simultaneous and proportional myoelectric control*. in *Engineering in Medicine and Biology Society, 2009. EMBC 2009. Annual International Conference of the IEEE*. 2009. IEEE.
17.   Boostani, R. and M.H. Moradi, *Evaluation of the forearm EMG signal features for the control of a prosthetic hand.* Physiological measurement, 2003. **24**(2): p. 309.
18.   Rosenberg, R. *The biofeedback pointer: EMG control of a two dimensional pointer*. in *Wearable Computers, 1998. Digest of Papers. Second International Symposium on*. 1998. IEEE.

19.   Tsenov, G., et al. *Neural networks for online classification of hand and finger movements using surface EMG signals*. in *Neural Network Applications in Electrical Engineering, 2006. NEUREL 2006. 8th Seminar on*. 2006. IEEE.

20.   Jung, K.K., et al. *EMG pattern classification using spectral estimation and neural network*. in *SICE, 2007 Annual Conference*. 2007. IEEE.

21.   El-Daydamony, E.M., M. El-Gayar, and F. Abou-Chadi. *A computerized system for SEMG signals analysis and classifieation*. in *Radio Science Conference, 2008. NRSC 2008. National*. 2008. IEEE.

22.   Tsuji, T., et al., *An EMG controlled pointing device using a neural network.* Transactions of the Society of Instrument and Control Engineers, 2001. **37**(5): p. 425-431.

23.   Bu, N., et al. *FPGA implementation of a probabilistic neural network for a bioelectric human interface*. in *Circuits and Systems, 2004. MWSCAS'04. The 2004 47th Midwest Symposium on*. 2004. IEEE.

24.   Kim, J., S. Mastnik, and E. André. *EMG-based hand gesture recognition for realtime biosignal interfacing*. in *Proceedings of the 13th international conference on Intelligent user interfaces*. 2008. ACM.

25.   Mobasser, F. and K. Hashtrudi-Zaad. *A method for online estimation of human arm dynamics*. in *Engineering in Medicine and Biology Society, 2006. EMBS'06. 28th Annual International Conference of the IEEE*. 2006. IEEE.

26.   Chen, X., et al. *Hand gesture recognition research based on surface EMG sensors and 2D-accelerometers*. in *Wearable Computers, 2007 11th IEEE International Symposium on*. 2007. IEEE.

27.   Ahsan, M.R., M.I. Ibrahimy, and O.O. Khalifa, *EMG signal classification for human computer interaction: a review.* European Journal of Scientific Research, 2009. **33**(3): p. 480-501.

28.   Park, K.-H. and S.-W. Lee. *Movement intention decoding based on deep learning for multiuser myoelectric interfaces*. in *Brain-Computer Interface (BCI), 2016 4th International Winter Conference on*. 2016. IEEE.

29.   Atzori, M. and H. Müller. *The ninapro database: a resource for semg naturally controlled robotic hand prosthetics*. in *Engineering in Medicine and Biology Society (EMBC), 2015 37th Annual International Conference of the IEEE*. 2015. IEEE.

30.   Cun, L., et al. *Comparison of learning algorithms for handwritten digit recognition [Z]*. in *Proc 1st Int Conf on Artificial Neural Networks, Sofia, Bulgaria*. 1995.

31.   Zia ur Rehman, M., et al., *Stacked sparse autoencoders for EMG-based classification of hand motions: A comparative multi day analyses between surface and intramuscular EMG.* Applied Sciences, 2018. **8**(7): p. 1126.

32.   ur Rehman, M.Z., et al. *Performance of combined surface and intramuscular EMG for classification of hand movements*. in *2018 40th Annual International Conference of the IEEE Engineering in Medicine and Biology Society (EMBC)*. 2018. IEEE.

33.   Zia ur Rehman, M., et al., *Multiday EMG-based classification of hand motions with deep learning techniques.* Sensors, 2018. **18**(8): p. 2497.

34.   Hudgins, B., P. Parker, and R.N. Scott, *A new strategy for multifunction myoelectric control.* IEEE Transactions on Biomedical Engineering, 1993. **40**(1): p. 82-94.

35.   Beale, M.H., M.T. Hagan, and H.B. Demuth, *Neural Network Toolbox™ Reference*. 1992, MATLAB R2015b, The MathWorks, Natick, MA.

36.   Chan, A.D. and G.C. Green. *Myoelectric control development toolbox*. in *Proceedings of 30th conference of the Canadian medical & biological engineering society*. 2007.

37.   Zhuang, F., et al. *Transfer learning with multiple sources via consensus regularized autoencoders*. in *Joint European Conference on Machine Learning and Knowledge Discovery in Databases*. 2014. Springer.

38.   Bengio, Y., *Learning deep architectures for AI.* Foundations and trends® in Machine Learning, 2009. **2**(1): p. 1-127.

39.   Said, A.B., et al., *Multimodal deep learning approach for joint EEG-EMG data compression and classification.* arXiv preprint arXiv:1703.08970, 2017.

40.   Olshausen, B.A. and D.J. Field, *Sparse coding with an overcomplete basis set: A strategy employed by V1?* Vision research, 1997. **37**(23): p. 3311-3325.

41.   Kullback, S., *Information theory and statistics*. 1997: Courier Corporation.

42.   Ngiam, J., et al. *On optimization methods for deep learning*. in *Proceedings of the 28th International Conference on Machine Learning (ICML-11)*. 2011.

43.   Tsinalis, O., P.M. Matthews, and Y. Guo, *Automatic sleep stage scoring using time-frequency analysis and stacked sparse autoencoders.* Annals of biomedical engineering, 2016. **44**(5): p. 1587-1597.

44.   Møller, M.F., *A scaled conjugate gradient algorithm for fast supervised learning.* Neural networks, 1993. **6**(4): p. 525-533.

45.   Bengio, Y., et al., *Greedy layer-wise training of deep networks.* Advances in neural information processing systems, 2007. **19**: p. 153.

46.   Ison, M. and P. Artemiadis, *Proportional myoelectric control of robots: muscle synergy development drives performance enhancement, retainment, and generalization.* IEEE Transactions on Robotics, 2015. **31**(2): p. 259-268.

47.   Ameri, A., et al., *Support vector regression for improved real-time, simultaneous myoelectric control.* IEEE Transactions on Neural Systems and Rehabilitation Engineering, 2014. **22**(6): p. 1198-1209.

48.   Herberts, P., et al., *Hand prosthesis control via myoelectric patterns.* Acta Orthopaedica Scandinavica, 1973. **44**(4-5): p. 389-409.

49.   Graupe, D. and W.K. Cline, *Functional separation of EMG signals via ARMA identification methods for prosthesis control purposes.* IEEE Transactions on Systems, Man, and Cybernetics, 1975(2): p. 252-259.

50.   Fukuda, O., T. Tsuji, and M. Kaneko. *An EMG controlled pointing device using a neural network*. in *Systems, Man, and Cybernetics, 1999. IEEE SMC'99 Conference Proceedings. 1999 IEEE International Conference on*. 1999. IEEE.

51.   Fukuda, O., J. Arita, and T. Tsuji. *An EMG-controlled omnidirectional pointing device using a HMM-based neural network*. in *Neural Networks, 2003. Proceedings of the International Joint Conference on*. 2003. IEEE.

52.   Selami, K., *Classification Of Emg Signals Using Decision Tree Methods.* 2012.

53.   Geethanjali, P. and K. Ray, *Identification of motion from multi-channel EMG signals for control of prosthetic hand.* Australasian physical & engineering sciences in medicine, 2011. **34**(3): p. 419-427.

54.   Alkan, A. and M. Günay, *Identification of EMG signals using discriminant analysis and SVM classifier.* Expert Systems with Applications, 2012. **39**(1): p. 44-47.

55.   Phinyomark, A., P. Phukpattaranont, and C. Limsakul, *Feature reduction and selection for EMG signal classification.* Expert Systems with Applications, 2012. **39**(8): p. 7420-7431.

56.   Min, S., B. Lee, and S. Yoon, *Deep learning in bioinformatics.* Briefings in Bioinformatics, 2016: p. bbw068.

57.   Lin, Q., et al. *Classification of Epileptic EEG Signals with Stacked Sparse Autoencoder Based on Deep Learning*. in *International Conference on Intelligent Computing*. 2016. Springer.

58.   Yang, J., et al., *A novel electrocardiogram arrhythmia classification method based on stacked sparse auto-encoders and softmax regression.* International Journal of Machine Learning and Cybernetics, 2017: p. 1-8.

59.   Yuan, C., et al. *Automated atrial fibrillation detection based on deep learning network*. in *Information and Automation (ICIA), 2016 IEEE International Conference on*. 2016. IEEE.

60.   Najdi, S., A.A. Gharbali, and J.M. Fonseca. *Feature Transformation Based on Stacked Sparse Autoencoders for Sleep Stage Classification*. in *Doctoral Conference on Computing, Electrical and Industrial Systems*. 2017. Springer.

61.   Spüler, M., et al. *Extracting Muscle Synergy Patterns from EMG Data Using Autoencoders*. in *International Conference on Artificial Neural Networks*. 2016. Springer.

62.   Kamavuako, E.N., et al., *Relationship between grasping force and features of single-channel intramuscular EMG signals.* Journal of neuroscience methods, 2009. **185**(1): p. 143-150.

63.   Farrell, T.R., *A comparison of the effects of electrode implantation and targeting on pattern classification accuracy for prosthesis control.* IEEE Transactions on Biomedical Engineering, 2008. **55**(9): p. 2198-2211.

64.   Kamavuako, E.N., et al., *Influence of the feature space on the estimation of hand grasping force from intramuscular EMG.* Biomedical Signal Processing and Control, 2013. **8**(1): p. 1-5.

65.   Smith, L.H. and L.J. Hargrove. *Comparison of surface and intramuscular EMG pattern recognition for simultaneous wrist/hand motion classification*. in *Engineering in Medicine and Biology Society (EMBC), 2013 35th Annual International Conference of the IEEE*. 2013. IEEE.

66.   Hargrove, L.J., K. Englehart, and B. Hudgins, *A comparison of surface and intramuscular myoelectric signal classification.* IEEE Transactions on Biomedical Engineering, 2007. **54**(5): p. 847-853.

67.   Winter, D., A. Fuglevand, and S. Archer, *Crosstalk in surface electromyography: theoretical and practical estimates.* Journal of Electromyography and Kinesiology, 1994. **4**(1): p. 15-26.

68.   Smith, L.H., T.A. Kuiken, and L.J. Hargrove, *Real-time simultaneous and proportional myoelectric control using intramuscular EMG.* Journal of neural engineering, 2014. **11**(6): p. 066013.

69.   Merletti, R. and D. Farina, *Analysis of intramuscular electromyogram signals.* Philosophical Transactions of the Royal Society of London A: Mathematical, Physical and Engineering Sciences, 2009. **367**(1887): p. 357-368.

70.   Madusanka, D., et al. *A review on hybrid myoelectric control systems for upper limb prosthesis*. in *Moratuwa Engineering Research Conference (MERCon), 2015*. 2015. IEEE.

71.   Vodovnik, L., et al., *Some topics on myoelectric control of orthotic/prosthetic systems, Rep*. 1967, EDC 4-67-17, Case Western Reserve University, Cleveland, OH.

72.   Chan, A.D. and K.B. Englehart, *Continuous myoelectric control for powered prostheses using hidden Markov models.* IEEE Transactions on Biomedical Engineering, 2005. **52**(1): p. 121-124.

73.   Englehart, K., et al., *Classification of the myoelectric signal using time-frequency based representations.* Medical engineering & physics, 1999. **21**(6): p. 431-438.

74.   Chu, J.-U., I. Moon, and M.-S. Mun, *A real-time EMG pattern recognition system based on linear-nonlinear feature projection for a multifunction myoelectric hand.* IEEE Transactions on biomedical engineering, 2006. **53**(11): p. 2232-2239.

75.   Iqbal, N.V. and K. Subramaniam, *A Review on Upper-Limb Myoelectric Prosthetic Control.* IETE Journal of Research, 2017: p. 1-13.

76.   Oskoei, M.A. and H. Hu, *Myoelectric control systems—A survey.* Biomedical Signal Processing and Control, 2007. **2**(4): p. 275-294.

77.   Scott, R. *Myoelectric control of prostheses: A brief history*. 1992. Myoelectric Symposium.

78.   Hahne, J.M., M. Markovic, and D. Farina, *User adaptation in Myoelectric Man-Machine Interfaces.* Scientific reports, 2017. **7**(1): p. 4437.

79.   Erik Scheme MSc, P. and P. Kevin Englehart PhD, *Electromyogram pattern recognition for control of powered upper-limb prostheses: State of the art and challenges for clinical use.* Journal of rehabilitation research and development, 2011. **48**(6): p. 643.

80. Li, G., A.E. Schultz, and T.A. Kuiken, *Quantifying pattern recognition—based myoelectric control of multifunctional transradial prostheses.* IEEE transactions on neural systems and rehabilitation engineering: a publication of the IEEE Engineering in Medicine and Biology Society, 2010. **18**(2): p. 185.

81. Purushothaman, G. and K. Ray, *EMG based man–machine interaction—A pattern recognition research platform.* Robotics and Autonomous Systems, 2014. **62**(6): p. 864-870.

82. Ortiz-Catalan, M., *Cardinality as a highly descriptive feature in myoelectric pattern recognition for decoding motor volition.* Frontiers in neuroscience, 2015. **9**.

83. Phinyomark, A., C. Limsakul, and P. Phukpattaranont, *A novel feature extraction for robust EMG pattern recognition.* arXiv preprint arXiv:0912.3973, 2009.

84. Adewuyi, A.A., L.J. Hargrove, and T.A. Kuiken, *evaluating eMg Feature and classifier selection for application to Partial-hand Prosthesis control.* Frontiers in neurorobotics, 2016. **10**.

85. Phinyomark, A., et al., *EMG feature evaluation for improving myoelectric pattern recognition robustness.* Expert Systems with Applications, 2013. **40**(12): p. 4832-4840.

86. Phinyomark, A., et al., *Navigating features: a topologically informed chart of electromyographic features space.* Journal of The Royal Society Interface, 2017. **14**(137): p. 20170734.

87. Chan, A.D. and G.C. Green, *Myoelectric control development toolbox.* CMBES Proceedings, 2017. **30**(1).

88. Sebelius, F.C., B.N. Rosen, and G.N. Lundborg, *Refined myoelectric control in below-elbow amputees using artificial neural networks and a data glove.* The Journal of hand surgery, 2005. **30**(4): p. 780-789.

89. Oskoei, M.A. and H. Hu, *Support vector machine-based classification scheme for myoelectric control applied to upper limb.* IEEE transactions on biomedical engineering, 2008. **55**(8): p. 1956-1965.

90. Wolczowski, A. and M. Kurzynski, *Control of dexterous hand via recognition of EMG signals using combination of decision-tree and sequential classifier.* Computer Recognition Systems 2, 2007: p. 687-694.

91. Atzori, M., et al., *Electromyography data for non-invasive naturally-controlled robotic hand prostheses.* Scientific data, 2014. **1**: p. 140053.

92. Zhai, X., et al., *Self-recalibrating surface EMG pattern recognition for neuroprosthesis control based on convolutional neural network.* Frontiers in neuroscience, 2017. **11**: p. 379.

93. Collobert, R. and J. Weston. *A unified architecture for natural language processing: Deep neural networks with multitask learning*. in *Proceedings of the 25th international conference on Machine learning*. 2008. ACM.

94. Nurse, E., et al. *Decoding EEG and LFP signals using deep learning: heading TrueNorth*. in *Proceedings of the ACM International Conference on Computing Frontiers*. 2016. ACM.

95. Acharya, U.R., et al., *Application of deep convolutional neural network for automated detection of myocardial infarction using ECG signals.* Information Sciences, 2017. **415**: p. 190-198.

96. Narejo, S., E. Pasero, and F. Kulsoom, *EEG Based Eye State Classification using Deep Belief Network and Stacked AutoEncoder.* International Journal of Electrical and Computer Engineering, 2016. **6**(6): p. 3131.

97. Atzori, M., et al. *Building the Ninapro database: A resource for the biorobotics community*. in *Biomedical Robotics and Biomechatronics (BioRob), 2012 4th IEEE RAS & EMBS International Conference on*. 2012. IEEE.

98. Geng, W., et al., *Gesture recognition by instantaneous surface EMG images.* Scientific reports, 2016. **6**: p. 36571.

99. Du, Y., et al., *Surface EMG-Based Inter-Session Gesture Recognition Enhanced by Deep Domain Adaptation.* Sensors, 2017. **17**(3): p. 458.

100. Xia, P., J. Hu, and Y. Peng, *EMG-Based Estimation of Limb Movement Using Deep Learning With Recurrent Convolutional Neural Networks.* Artificial organs, 2017.
101. Côté-Allard, U., et al. *Transfer Learning for sEMG Hand Gestures Recognition Using Convolutional Neural Networks*. in *International Conference On Systems, Man and Cybernetics*. 2017. IEEE.
102. Day, S., *Important factors in surface EMG measurement.* Bortec Biomedical Ltd publishers, 2002: p. 1-17.
103. Lee, S. and J. Kruse, *Biopotential electrode sensors in ECG/EEG/EMG systems.* Analog Devices, 2008. **200**: p. 1-2.
104. Mendez, I., et al. *Evaluation of the Myo armband for the classification of hand motions*. in *Rehabilitation Robotics (ICORR), 2017 International Conference on*. 2017. IEEE.
105. Kamavuako, E.N., E.J. Scheme, and K.B. Englehart, *Determination of optimum threshold values for EMG time domain features; a multi-dataset investigation.* J. Neural Eng, 2016. **13**(4): p. 1-10.
106. Dean, J., et al. *Large scale distributed deep networks*. in *Advances in neural information processing systems*. 2012.
107. Linderman, M., M.A. Lebedev, and J.S. Erlichman, *Recognition of handwriting from electromyography.* PLoS One, 2009. **4**(8): p. e6791.
108. Atzori, M., M. Cognolato, and H. Müller, *Deep learning with convolutional neural networks applied to electromyography data: A resource for the classification of movements for prosthetic hands.* Frontiers in neurorobotics, 2016. **10**.
109. Adewuyi, A.A., *Pattern Recognition-Based Myoelectric Control of Partial-Hand Prostheses*, in *Depatment of Biomedical Engineering*. 2016, NORTHWESTERN UNIVERSITY: EVANSTON, ILLINOIS.
110. Herberts, P., et al., *Implantation of micro-circuits for myo-electric control of prostheses.* J Bone Jt Surg Br, 1968. **50**(4): p. 780-91.
111. Kamavuako, E.N., E.J. Scheme, and K.B. Englehart, *On the usability of intramuscular EMG for prosthetic control: A Fitts' Law approach.* Journal of Electromyography and Kinesiology, 2014. **24**(5): p. 770-777.
112. Smith, L.H., T.A. Kuiken, and L.J. Hargrove. *Real-time simultaneous myoelectric control by transradial amputees using linear and probability-weighted regression*. in *Engineering in Medicine and Biology Society (EMBC), 2015 37th Annual International Conference of the IEEE*. 2015. IEEE.
113. Chowdhury, R.H., et al., *Surface electromyography signal processing and classification techniques.* Sensors, 2013. **13**(9): p. 12431-12466.
114. Wang, G., et al., *Classification of surface EMG signals using harmonic wavelet packet transform.* Physiological measurement, 2006. **27**(12): p. 1255.
115. Stober, S., et al., *Deep feature learning for EEG recordings.* arXiv preprint arXiv:1511.04306, 2015.
116. Tabar, Y.R. and U. Halici, *A novel deep learning approach for classification of EEG motor imagery signals.* Journal of neural engineering, 2016. **14**(1): p. 016003.
117. Xiong, P., et al., *Denoising autoencoder for eletrocardiogram signal enhancement.* Journal of Medical Imaging and Health Informatics, 2015. **5**(8): p. 1804-1810.
118. Shin, H.-C., et al., *Stacked autoencoders for unsupervised feature learning and multiple organ detection in a pilot study using 4D patient data.* IEEE transactions on pattern analysis and machine intelligence, 2013. **35**(8): p. 1930-1943.
119. Shin, H.-C., et al. *Autoencoder in time-series analysis for unsupervised tissues characterisation in a large unlabelled medical image dataset*. in *Machine Learning and Applications and Workshops (ICMLA), 2011 10th International Conference on*. 2011. IEEE.
120. Kumar, D., A. Wong, and D.A. Clausi. *Lung nodule classification using deep features in CT images*. in *Computer and Robot Vision (CRV), 2015 12th Conference on*. 2015. IEEE.
121. Waris, A., et al., *The effect of time on EMG classification of hand motions in able-bodied and transradial amputees.* Journal of Electromyography and Kinesiology, 2018. **40**: p. 72-80.